STUDIES ON HYDRAZINE SYNTHESIS

Technical Report No. 3

FUNDAMENTAL STUDIES ON THE SYNTHESIS OF HYDRAZINE
BY THE PHOTOLYSIS OF AMMONIA AT 1849 Å AND BY THE
DECOMPOSITION OF AMMONIA WITH MERCURY-6($^3P_1$) ATOMS

by

C. C. McDonald and H. E. Gunning

January 1954

Department of Chemistry
Illinois Institute of Technology
3300 South Federal Street
Chicago 16, Illinois

STUDIES ON HYDRAZINE SYNTHESIS

Technical Report No. 3

FUNDAMENTAL STUDIES ON THE SYNTHESIS OF HYDRAZINE
BY THE PHOTOLYSIS OF AMMONIA AT 1849 Å AND BY THE
DECOMPOSITION OF AMMONIA WITH MERCURY-6($^3P_1$) ATOMS

by

C. C. McDonald and H. E. Gunning

January 1954

Department of Chemistry
Illinois Institute of Technology
3300 South Federal Street
Chicago 16, Illinois

TABLE OF CONTENTS

TABLE OF CONTENTS (Continued)

INTRODUCTION

The present report, comprising the doctoral thesis of one of us (C.C.M.), represents the results of a three-year study on two photodecompositions wherein hydrazine is an important product of the reaction. These reactions are

(a) the photolysis of gaseous ammonia by radiation of wavelength 1849 $\overset{\circ}{A}$, under flow conditions, and

(b) the mercury-6($^3P_1$)-photosensitized decomposition of ammonia under flow conditions using 2537 $\overset{\circ}{A}$ radiation.

The objective of these fundamental studies has been to elucidate the basic mechanism of the reactions, and evaluate the factors which determine the conversion of ammonia into hydrazine. It is hoped that the results of our investigation will provide basic kinetic data on the synthesis of hydrazine from amino radical recombination.

For a commentary on the functional aspects of the photochemical synthesis of hydrazine from ammonia, reference should be made to our status report dated December 15, 1953.

ABSTRACT

The mercury-photosensitized decomposition of flowing ammonia was studied at room temperature. The products of the decomposition were hydrazine, hydrogen, and nitrogen. The quantum yield for ammonia decomposition did not depend on the linear flow rate of the ammonia through the irradiated zone but increased in an exponential manner, as the ammonia reaction pressure was decreased, from a value of 0.09 at 650 mm. pressure toward unity at very low pressures. The percentage of the decomposed ammonia which was recovered as hydrazine increased from zero at low ammonia linear flow rates to 95 per cent at high flow rates. At a particular flow rate the hydrazine-to-nitrogen ratio increased, as the reaction pressure was increased, from zero to a maximum value which was pressure independent at high ammonia pressures. The hydrazine-to-nitrogen ratio increased and the quantum yield decreased as the incident light intensity was decreased. When ethylene was added to the reaction, the hydrazine-to-nitrogen ratio was greatly increased, the amount of hydrogen produced was decreased, and ethylamine was qualitatively detected. The reaction was not changed when platinum wire was introduced into the irradiated zone.

The products of the static mercury-photosensitized decomposition of ammonia were hydrogen and nitrogen. The quantum yield of ammonia decomposition decreased when the exposure time was increased or when hydrogen was added to the reaction. At very short exposure times and high ammonia pressures the quantum yield had about the same value as in the flow experiments at comparable pressures. When the exposure time was kept constant, the quantum yield was constant at ammonia pressures from 650 mm. to 150 mm.; at lower pressures the quantum yield

vi

decreased. At an ammonia pressure of 200 mm. the quantum yield did not depend on the intensity of the incident radiation.

The photolysis of flowing ammonia by 1849 Å radiation was also investigated at room temperature. The products of the reaction were hydrazine, hydrogen, and nitrogen. The percentage of the decomposed ammonia which was recovered as hydrazine did not depend on the ammonia pressure in the irradiated zone but it increased from 34 per cent to 85 per cent as the ammonia linear flow rate through the irradiated zone was increased from 7 to 1700 cm. per second. The rate of the decomposition of ammonia did not depend on the ammonia flow rate and was almost constant at ammonia pressures from 100 to 560 mm. At lower ammonia pressures the rate increased until at 10 mm. pressure it was twice as great as the rate at 100 mm. The reaction was not changed when the surface-to-volume ratio in the zone immediately following the irradiated zone was increased by a factor of ten.

The products of the static photolysis of ammonia were hydrogen and nitrogen. At ammonia pressures from 10 to 264 mm. the rate of ammonia decomposition was about one-half as great as the rate in the flow experiments at comparable pressures.

The following mechanism was proposed for the photodecomposition of ammonia to interpret the experimental results:

$$NH_3 + h\nu_{1849} \longrightarrow NH_2 + H \qquad (1)$$

$$\text{or } NH_3 + Hg\ 6(^3P_1) \longrightarrow NH_2 + H + Hg\ 6(^1S_0) \qquad (2)$$

$$NH_2 + H \longrightarrow NH_3^* \qquad (3)$$

$$NH_3^* \longrightarrow NH_2 + H \qquad (4)$$

$$NH_3^* + NH_3 \longrightarrow 2NH_3 \qquad (5)$$

$$NH_2 + NH_2 \longrightarrow N_2H_4 \tag{6}$$

$$H + N_2H_4 \longrightarrow H_2 + N_2H_3 \tag{7}$$

$$H + N_2H_3 \longrightarrow H_2 + N_2H_2 \tag{8}$$

$$N_2H_2 \longrightarrow N_2 + H_2 \tag{9}$$

$$H + wall \longrightarrow 1/2\ H_2 \tag{10}$$

$$NH_2 + H_2 \longrightarrow NH_3 + H \tag{11}$$
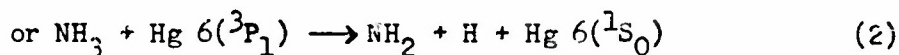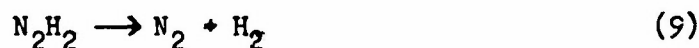
The extinction coefficient of ammonia for 1849 Å radiation was found to be 1.21×10^3 liters moles^{-1} cm.$^{-1}$ at ammonia pressures from 0.45 to 202 mm.

Hydrazine at 14 mm. pressure was photolytically decomposed in a static system by 2537 Å radiation. The reaction obeyed the stoichiometrical equation

$$2\ N_2H_4 = 2\ NH_3 + N_2 + H_2$$

LIST OF TABLES

LIST OF ILLUSTRATIONS

CHAPTER I

INTRODUCTION

General

For many years, a large part of chemical endeavor has been devoted to the characterization of the fundamental particles involved in elementary chemical reactions and to the elucidation of the mechanism of these primitive reactions. The importance of free radicals in such reactions has long been recognized.

Chemical reactions which proceed by a mechanism involving free radicals may be initiated in a number of ways. One of the most successful methods for the initiation of free radical reactions in the gas phase is the irradiation of the reactant with light. This technique has resulted in the branch of chemical investigation known as photochemistry.

Two conditions must be fulfilled for a useful photochemical gas phase reaction to occur. An appreciable fraction of the incident radiation must be absorbed by the reactant material. Furthermore, the energy of the absorbed photons must be great enough to raise the energy of the absorbing molecule to an excited level such that chemical reaction is highly probable. Fortunately, most molecules absorb light in some part of the ultraviolet region of the electromagnetic spectrum. These photons usually have sufficient energy to cause the rupture of one of the chemical bonds of the absorbing molecule. In many reactions, as a result of such a rupture, free radicals are produced. This process is referred to as photolysis.

The photolytic method of initiation of chemical reactions has several advantages of which the following are perhaps the most important:

1

1. Absorption of light of a given wavelength usually ruptures a specific bond of the absorbing molecule. This bond frequently is not the weakest bond in the molecule, as is the case in thermally-induced molecular dissociation.

2. The primary act of photolysis is usually as efficient at or below room temperature as it is at elevated temperatures. Thus, the radicals formed are often thermally stable and do not complicate the reaction by decomposing into other particles.

Only light from the long wavelength region of the ultraviolet spectrum is convenient for use in photochemical investigations. In the far ultraviolet, the optical techniques required to handle the radiation become very difficult. Many molecules, however, do not absorb radiation which has a convenient wavelength from the experimental viewpoint. This difficulty has been obviated in many cases by the use of a "sensitizing" agent, a technique which was introduced by Cario and Franck.[4]* These authors irradiated a mixture of hydrogen and mercury vapor with light containing the resonance frequencies of mercury. This radiation was capable of being absorbed only by the mercury atoms but evidence was obtained to show that some of the hydrogen was dissociated into hydrogen atoms. Since that time, this phenomenon, known as photosensitized decomposition, has been amply elucidated. Mercury in its $6(^1S_0)$ ground state can absorb only two frequencies of ultraviolet light. These frequencies, the so-called resonance frequencies of mercury, correspond to wavelengths of 2537 $\overset{o}{A}$ and 1849 $\overset{o}{A}$. The former wavelength excites mercury to a $6(^3P_1)$ state, the latter to a $6(^1P_1)$ state. The excited mercury atoms normally

---

*For all numbered references, see the bibliography.

return to the ground state by losing their excitation energy by fluorescence. If, however, they collide with another molecule, the excitation energy may be transferred to this molecule. Since the energy above the ground state of mercury atoms in the $6(^3P_1)$ and $6(^1P_1)$ states is 112.2 kcal. per mole and 154 kcal. per mole respectively, the transferred energy is often sufficient to cause bond rupture in the energy acceptor. The mercury is said to sensitize the decomposition of the molecule which is not capable of absorbing the ultraviolet radiation directly.

Many substances, particularly metal atoms, have been used as sensitizers but in most photosensitized decompositions the sensitizing agent has been mercury. Mercury is convenient to use since it has a relatively high vapor pressure and a large absorption coefficient for its own resonance radiation. Consequently, the resonance radiation is absorbed in a few centimeters path length by mercury vapor at room temperature. Moreover, the energy of mercury $6(^3P_1)$ atoms is sufficient to rupture the single bonds of most molecules. Radiation of 2537 Å wavelength is easily obtained with sufficient intensity for photochemical studies from low pressure mercury-rare gas discharge lamps. As in photolytic decompositions, mercury-photosensitized decompositions usually result in the rupture of a specific bond of the molecule which accepts the energy from the excited mercury atom. If the molecule contains hydrogen atoms, a hydrogen bond is usually broken. There is some evidence that this specificity is due to the transient formation of a mercury hydride, but this hypothesis has not been convincingly established.[33]

The Photochemistry of Ammonia

The decomposition of ammonia was one of the first reactions to be studied in which the photochemical method was used. In 1904, Regener[31] decomposed ammonia with ultraviolet light and found the products of the reaction to be nitrogen and hydrogen. Since that time, the ammonia molecule has been the subject of many intensive photochemical investigations. Ammonia decomposition has been found to be a very complex reaction so that, in spite of the large amount of work that has been done on it, only certain features of the reaction are well understood. The nature of most of the primitive reactions involved in the decomposition is still the subject of considerable controversy. Since the body of experimental data and conjecture which has accumulated in the chemical literature is so large, only the important features of the most thorough investigations will be summarized here. For more extensive information on previous photochemical studies of the decomposition of ammonia, the reader is referred to the excellent reviews by H. S. Taylor,[36] W. A. Noyes, Jr. and P. A. Leighton,[26] and by A. G. Parts.[28]

The detailed structure of the absorption spectrum of ammonia in the ultraviolet region has been thoroughly examined.[9,10] The absorption threshold is at a wavelength of about 2400 $\overset{o}{A}$. Between this limit and a low wavelength limit of 1665 $\overset{o}{A}$, lies a series of diffuse double-headed absorption bands which have an intense maximum between 1850 $\overset{o}{A}$ and 1900 $\overset{o}{A}$. The ammonia absorption coefficient is so large around 1850 $\overset{o}{A}$ that the ammonia absorption appears to be continuous even at ammonia pressures of only a few centimeters of mercury. Other series of absorption bands exist at shorter wavelengths.

The diffuse absorption lines of ammonia were interpreted by

Bonhoeffer and Farkas[2] to be a result of predissociation. That is, when ammonia absorbs radiation from the near ultraviolet region of the spectrum, it is raised to an excited state and proceeds through a radiationless transition to an unstable state before it has time to lose its excitation energy by fluorescence or by collision. The only fate of the unstable state is dissociation. To prove that predissociation occurred, the following experimental facts were adduced:

1. The ammonia absorption bands remain diffuse even at high dispersion.

2. There is no fluorescence from the irradiated ammonia even at very low pressures.

3. The diffuse bands could not be obtained as emission lines when ammonia was excited by electron bombardment.

Energetically, the primary dissociation of ammonia may occur in two ways. These modes are shown in the following reactions:

$$NH_3 + h\nu \quad NH_2 + H \quad E = 110 \pm 10 \text{ kcal. per mole} \tag{1}$$

$$NH_3 + h\nu \quad NH + H_2 \quad E = 50 \pm 10 \text{ kcal. per mole} \tag{2}$$
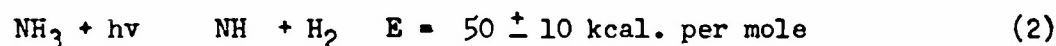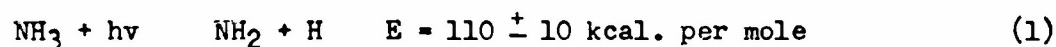
In these reactions, E represents the energy required for the reaction to occur and $h\nu$ represents an absorbed photon of radiation. Since an ultraviolet photon with a wavelength of 2400 Å has an energy of 118 kcal. per mole, any photon capable of being absorbed by ammonia has sufficient energy to cause the ammonia to dissociate by either reaction (1) or reaction (2).

Considerable evidence has been presented to show that the primary dissociation occurs according to reaction (1). Noyes[26] found that liquid ammonia was not affected by radiation which decomposed gaseous ammonia. The reverse of reaction (1) in liquid ammonia would explain

this observation. If reaction (2) was operative, hydrogen should have been formed in liquid as well as in gaseous ammonia. When ammonia containing oxygen was irradiated, the products included water, nitrite ions, and nitrate ions; but no hydrogen. Irradiation of liquid ammonia containing dissolved metals produced hydrogen and amido (NH_2^-) ions. All these products may be explained most readily on the basis of reaction (1).

Geib and Harteck[13] observed that the rate of conversion of ortho-hydrogen to para-hydrogen was increased in the presence of ammonia which was being photochemically decomposed. The increase in rate was attributed to hydrogen atoms produced by the decomposing ammonia.

Taylor and Eméleus[38] observed a rapid pressure decrease when ethylene was added to ammonia which was undergoing photolysis. This pressure decrease was not obtained when ethylene or a mixture of ethylene and hydrogen were irradiated. The rate of the reaction did not depend on the ethylene pressure but increased with the ammonia pressure until the absorption of the radiation was complete. These results were attributed to the polymerization of the ethylene initiated by hydrogen atoms and amino radicals from the photolysis of the ammonia. Taylor and Bates[37] found that yellow tungstic oxide turned blue when present during the photolysis of ammonia. They ascribed this color change to the reduction of the oxide by hydrogen atoms.

Perhaps the most convincing evidence for reaction (1) is to be found in the recent work of Herzberg and Ramsay.[14] By exposing ammonia to very high intensities of radiation for a fraction of a second, they found that the concentration of the primary decomposition products was high enough to permit their absorption spectra to be measured. This technique, called flash photolysis, showed that amino radicals (NH_2)

existed in the decomposition products but there was no evidence for imino radicals (NH).

The rate of a photochemical reaction usually depends on the intensity of the absorbed radiation. This dependence is expressed by the quantum yield which is the ratio of the number of moles of observed chemical reaction to the number of einsteins (moles of photons) of radiation absorbed. Warburg[42] found the average quantum yield for ammonia decomposition in the ammonia photolysis to be 0.25. The reaction was studied at ammonia pressures from 45 to 900 mm.[*] The photolysis of ammonia was also studied by Kuhn[17,18] using radiation of 2025 $\overset{\text{o}}{\text{A}}$ to 2140 $\overset{\text{o}}{\text{A}}$ wavelength. The quantum yield was 0.45 and did not depend on the temperature or pressure of the ammonia. The addition of nitrogen had no influence on the reaction but the quantum yield at high temperatures was decreased when hydrogen was added to the ammonia.

The mercury-photosensitized decomposition of ammonia by mercury $6(^3P_1)$ atoms was reported in 1926 by Bates and Taylor.[39] A mixture of ammonia and mercury vapor was distilled past a lamp emitting 2537 $\overset{\text{o}}{\text{A}}$ wavelength radiation and was condensed in a trap immersed in liquid air. Hydrogen and nitrogen were the only products which were detected but the hydrogen-to-nitrogen ratio was greater than three to one as required by the stoichiometric reaction

$$2 \text{ NH}_3 \longrightarrow \text{N}_2 + 3 \text{ H}_2 \tag{3}$$

This equation had been obeyed in all the previous studies. Bates and Taylor suggested that the decomposition went through several elementary

---

[*]All gas pressures in this thesis will be reported in terms of millimeters of mercury unless otherwise specified.

reactions, in some of which hydrazine was involved. If hydrazine was a product of the reaction, the hydrogen-to-nitrogen ratio would be greater than three to one since the additional stoichiometric reaction

$$2 NH_3 \longrightarrow N_2H_4 + H_2 \tag{4}$$

would be operative. The same investigators[39] reported that the hydrogen-to-nitrogen ratio was also greater than three to one in the photolysis of ammonia. Hydrazine was again proposed as a reaction product and the photolysis of pure hydrazine was examined. Ammonia was a major product in the initial stages of the hydrazine photolysis but as the reaction continued the ammonia produced in the reaction was photolytically decomposed. The decomposition of hydrazine was unimolecular, and did not depend on the temperature or the pressure of nitrogen, hydrogen, or ammonia. The thermal decomposition of hydrazine did not begin until the temperature had been raised to 250°C. In the mercury-photosensitized decomposition of hydrazine, the reaction rate was proportional to the light intensity but again was not influenced by added nitrogen, hydrogen, or ammonia. The quantum yield was at least 13. The quantum yield of the hydrazine photolysis was measured by Wenner and Beckman.[44] It increased from 1.0 to 1.7 as the hydrazine pressure was increased from 2.0 to 14 mm. Koenig and Brings[16] were able to show that hydrazine was a product of the photolytic decomposition of ammonia but only trace quantities were obtained.

The mercury-photosensitized decomposition of ammonia was also studied by Dickinson and Mitchell.[6,7] At very low pressures of ammonia the decomposition was accompanied by a green and ultraviolet fluorescence. The reaction rate increased with increasing ammonia pressure. The only reaction products were nitrogen and hydrogen. When argon or

nitrogen at 0.3 mm. pressure was added, the reaction was unchanged but the addition of even lower pressures of hydrogen caused the reaction rate to decrease greatly.

The photolysis of ammonia in the presence of carbon monoxide was examined by Emeléus.[11] Formamide was a product of the reaction. The quantum yield for ammonia decomposition was double that for the photolysis of pure ammonia, but only 5 per cent of the decomposed ammonia was recovered as nitrogen.

The quantum yield for the ammonia photolysis was reinvestigated by Wiig and Kistiakowsky in 1932.[45] A value of 0.25 was obtained at 25°C. This value did not depend on the wavelength or the intensity of the radiation and was not changed when the ammonia pressure or the exposure time to the radiation was varied. At 500°C., the quantum yield rose to 0.5. In all cases the hydrogen-to-nitrogen ratio was three to one. The following primitive reactions were considered to be important secondary steps in the ammonia decomposition:

$$H + H + M \longrightarrow H_2 + M \tag{5}$$

$$NH_2 + H + M \longrightarrow NH_3 + M \tag{6}$$

$$NH_2 + H_2 \longrightarrow NH_3 + H \tag{7}$$

$$H + NH_3 \longrightarrow NH_2 + H_2 \tag{8}$$

$$NH_2 + NH_2 + M \longrightarrow N_2H_4 + M \tag{9}$$

$$NH_2 + NH_2 \longrightarrow N_2 + 2 H_2 \tag{10}$$

$$N_2H_4 + H \longrightarrow N_2H_3 + H_2 \tag{11}$$

$$N_2H_3 + N_2H_3 \longrightarrow 2 NH_3 + N_2 \tag{12}$$
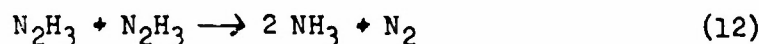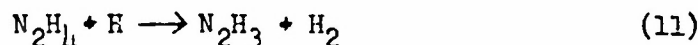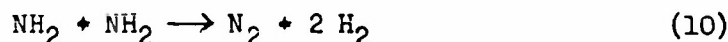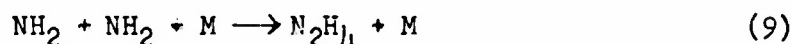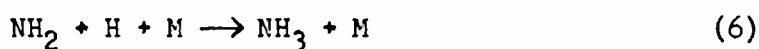
In these reactions, M represented any molecule capable of carrying off part of the radical recombination energy. Reactions (7) and (8) were important only at high temperatures. The low quantum yield was

accounted for by reactions (6), (11) and (12). Nitrogen, hydrogen, and hydrazine appeared by way of reactions (9), (10), and (12) but part of the hydrazine was consumed by reactions (11) and (12).

The role of hydrazine as a reaction product in the ammonia photolysis was firmly established by Gedye and Rideal.[12] In their experiments, ammonia flowed past the full radiation of a mercury arc and was condensed in a trap. Up to 50 per cent of the decomposed ammonia was recovered as hydrazine. The hydrazine yield was favored by lowering the temperature of the reaction vessel and by rapid cooling of the gaseous products of the decomposition. The mercury-photosensitized decomposition of ammonia under the same conditions produced only trace amounts of hydrazine.

Dixon[8] used a flow technique to study the reaction of hydrogen atoms with hydrazine and with ammonia. With hydrazine, the hydrogen atoms reacted rapidly to produce ammonia, nitrogen, and hydrogen. Ammonia appeared to be inert to attack by hydrogen atoms. This work substantiated reaction (11) proposed by Wiig and Kistiakowsky.

In 1932, Melville[19] reported the results of an examination of the photolysis of ammonia in which the hydrogen atom concentration was increased above the normal value. A zinc spark was used to provide radiation for the photolysis of ammonia in a mixture of ammonia, hydrogen, and mercury vapor. Mercury $6(^3P_1)$ atoms were then produced in the reaction by irradiating it with a mercury arc. The excited mercury atoms were quenched by hydrogen which dissociated into hydrogen atoms. The increase in the hydrogen atom concentration caused a large decrease in the quantum yield of ammonia decomposition. This work was presented as evidence that the low quantum yield was due to the reaction

$$NH_2 + H + M \longrightarrow NH_3 + M \qquad (6)$$

In a later investigation, Melville and Birse[20] measured the hydrogen atom concentration in the photolysis of ammonia by measuring the rate of conversion of ortho-hydrogen to para-hydrogen. They considered that the hypothesis of Wiig and others, whereby amino radicals combined to form hydrazine which in turn was decomposed by hydrogen atoms, was untenable since sufficient hydrazine could not be formed to lower the hydrogen atom concentration to the value which they obtained in their experiments. These authors felt that the only secondary reactions of importance were the following:

$$H + H \longrightarrow H_2 \qquad (13)$$

$$NH_2 + NH_2 \longrightarrow 2 H_2 + N_2 \qquad (10)$$

$$H + NH_2 \longrightarrow NH_3 \qquad (14)$$
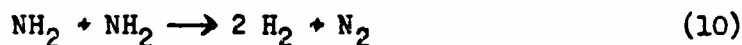
In their opinion only a fraction of the excited ammonia molecules dissociated into hydrogen atoms and amino radicals while the remainder were deactivated without reaction.

The regeneration of ammonia in the secondary processes of the ammonia decomposition was shown by Taylor and Jungers.[40] Deutero-ammonias were formed when a mixture of ammonia and deuterium underwent mercury-photosensitized decomposition. Since no exchange occurred except when the ammonia was decomposed, they concluded that the low quantum yield in the ammonia decomposition was due to reaction (14) and that the reaction of hydrogen atoms with ammonia was negligible at room temperature.

In 1935, Wiig[46] reported a very careful study of the quantum yield of the ammonia photolysis. As the ammonia pressure was increased from

about 10 mm. to about 100 mm., the quantum yield increased from 0.10 to 0.30. At higher pressures, the quantum yield decreased until at one atmosphere pressure the value was 0.18. Ogg, Leighton and Bergstrom[27] found the quantum yield to be 0.14 from one to eight atmospheres pressure. These authors found that the quantum yield did not depend on the wavelength of the absorbed radiation but, as the ammonia temperature was increased to 400°C., the quantum yield increased to 0.5. When the ammonia contained 0.3 per cent hydrazine, an ammonia-sensitized decomposition of hydrazine occurred with a quantum yield of 1.28. From these results and the knowledge that the decomposition of hydrazine produces ammonia, Ogg and his coworkers deduced that the low quantum yield in the ammonia reaction was due to an ammonia-reforming step in the decomposition of hydrazine. They proposed that nitrogen was formed by the reaction

$$N_2H_4 + 2 NH_2 \longrightarrow 2 NH_3 + N_2 + H_2 \tag{15}$$
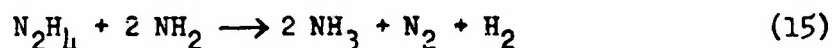
Except for a minor change in reaction (15), this mechanism was supported by Mund.[24] A kinetic analysis based on the following reactions and reaction coefficients agreed with the experimental results of Wiig and Ogg:

$$20(NH_3 + h\nu \longrightarrow NH_2 + H) \tag{1}$$

$$17(2 NH_2 + M \longrightarrow N_2H_4) \tag{9}$$

$$16(N_2H_4 + H \longrightarrow NH_3 + NH_2) \tag{11}$$

$$1(N_2H_4 + 2 NH_2 \longrightarrow 2 N_2 + 4 H_2) \tag{16}$$

$$2(H + H + M \longrightarrow H_2 + M) \tag{5}$$
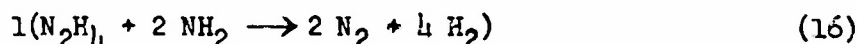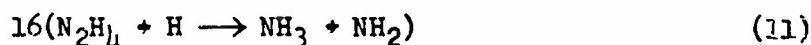
The above mechanism predicted an increase in the quantum yield with increased light intensity. This effect was later shown to exist.[25]

The reaction coefficients were obtained by fitting the mechanism to Wiig's data. Ogg showed that an equally satisfactory fit could be obtained if other coefficients were used and if reaction (15) was substituted for reaction (16). Ogg preferred reaction (15) because ammonia had been shown to be a product of the decomposition of hydrazine.[39]

An interesting investigation of the photolysis of ammonia was reported by Welge and Beckman.[43] Radiation of 1990 $\overset{o}{A}$ wavelength was used, and the photolysis was studied at ammonia pressures from 2 to 128 mm. The ammonia was exposed to the radiation for very short time intervals so that the pressure of the products was only from 3×10^{-4} to 8×10^{-4} mm. Hydrogen accounted for over 90 per cent of the gaseous product in the experiments with the shortest exposure times. When the extent of decomposition was greater, the hydrogen-to-nitrogen ratio decreased to three to one. The quantum yield for ammonia decomposition approached unity when the ammonia pressure was low and the extent of the decomposition was small. At higher ammonia pressures, the quantum yield was 0.8. Hydrazine was found adsorbed on the walls of the reaction vessel. In the mercury-photosensitized decomposition of ammonia under similar conditions, fluorescence was observed and the quantum yield was 0.12. The following reactions were considered to be the most important;

$$NH_3 + hv \longrightarrow NH_2 + H \tag{1}$$

$$H + H + M \longrightarrow H_2 + M \tag{5}$$

$$NH_2 + NH_2 + M \longrightarrow N_2H_4 + M \tag{9}$$
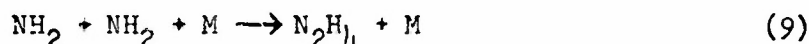
It was suggested that the low quantum yield at the higher extents of decomposition resulted from ammonia reforming steps involved in the

decomposition of ammonia. Since the experiments were done at very low ammonia pressures, reactions (5) and (9) were considered to occur mainly at the walls of the reaction vessel.

Wiig[47] was unable to reproduce the work of Welge and Beckman. He found no increase in the quantum yield even when the pressure of the products was only 4×10^{-3} mm. The quantum yield did increase, however, when the cell diameter was decreased. The reaction appeared to be heterogeneous at ammonia pressures below 300 mm.

The Budde effect (expansion due to irradiation) was used by Shida[32] to measure the rate of the ammonia photolysis. His quantum yield values were similar to those of Wiig except at low ammonia pressures. Shida found the quantum yield continued to increase as the ammonia pressure was decreased. Wiig had reported that the quantum yield decreased when the ammonia pressure fell below 150 mm. In Shida's experiments, the reaction appeared to be heterogeneous and the quantum yield increased when the wall area was enlarged or when the size of the illuminated zone was increased.

A recent investigation of the ammonia photolysis by Vanpée[41] showed a maximum in the quantum yield at 150 mm. ammonia pressure, but the values obtained at higher pressures were only slightly smaller. When the ammonia pressure was less than 300 mm., the quantum yield decreased when the light intensity was decreased, especially if hydrogen was present in the reaction. The reaction rate was not changed by the addition of nitrogen or argon but was considerably decreased by hydrogen. When an equimolar mixture of hydrogen and ammonia was irradiated, the quantum yield decreased as the temperature increased but the quantum yield increased with increasing temperature in the photolysis of pure ammonia.

The ammonia photolysis was studied in this laboratory by Kahn.[15]
The ammonia flowed rapidly past a lamp emitting radiation at a wave-
length of 1849 $\overset{o}{A}$ and was condensed in a trap immersed in liquid nitro-
gen. At the end of an experiment, the non-condensable gas was analysed
and the condensed material was analysed for hydrazine. Under the most
favorable conditions, 85 per cent of the ammonia decomposed was
recovered as hydrazine.

The major findings of all these investigations may be summed up
in the following statements:

1. Ammonia decomposes both by photolysis and by mercury-photo-
sensitization into hydrogen atoms and amino radicals.

2. The radicals produced in the dissociation of ammonia undergo
secondary reactions which produce only hydrogen and nitrogen when the
decomposition is examined under static conditions. In the ammonia
photolysis, if the ammonia flows through the irradiated zone and is
then condensed, hydrazine also appears as a product. Hydrazine is,
therefore, probably an intermediate in the static decomposition.
Hydrazine is rapidly decomposed to ammonia, nitrogen and hydrogen in
the presence of hydrogen atoms. The role of hydrazine in the secondary
reactions of the mercury-photosensitized decomposition of ammonia is
not well established.

3. The quantum yield of ammonia decomposition in the photolysis
of ammonia is 0.2 to 0.3 at 150 mm. ammonia pressure. There is con-
siderable evidence that the quantum yield decreases slowly as the
ammonia pressure is increased. The behavior at low pressures depends
on the experimental conditions. In the mercury-photosensitized
decomposition the quantum yield is much lower than in the photolysis.

4. In the ammonia photolysis, the decomposition rate is not changed by the addition of argon or nitrogen. Hydrogen, however, inhibits the rate. In the mercury-photosensitized decomposition, inhibition of the rate of decomposition by hydrogen is well established.

5. The quantum yield in the photolysis of ammonia does not depend on the wavelength of the radiation but increases when the intensity of the radiation is increased.

6. Several investigators have pointed out that the ammonia decomposition becomes heterogeneous at low pressures.

7. The low quantum yield in the photodecomposition of ammonia has been attributed to the recombination of hydrogen atoms with amino radicals and also to the reformation of ammonia by the decomposition of hydrazine produced in the reaction. The mechanism of ammonia reformation and the mechanism by which nitrogen is formed is not well established.

The research reported in this thesis was undertaken to establish the importance of hydrazine in the photodecomposition of ammonia. Since the role of hydrazine in the mercury-photosensitized decomposition seemed particularly to require detailed study, this photochemical technique was emphasized in the investigation. An examination was also made of the photolysis of ammonia so that a comparison of the two modes of photochemical dissociation could be made.

Since hydrazine was previously observed as an important product only when the ammonia flowed through the radiation, a flow system was used in most of this work. However, both the photolysis and the mercury-photosensitized decomposition of ammonia were also studied under static conditions.

It was hoped that a study of the reaction rate and the reaction

products, using a wide variation of the experimental parameters, would permit a further elucidation of the nature of the secondary processes involved in the photodecomposition of ammonia.

CHAPTER II

EXPERIMENTAL METHODS

Apparatus

Separate systems, shown in Fig. 2 and in Fig. 3, were used for the photolysis and for the mercury-photosensitized decomposition of ammonia because the photolysis apparatus had to be free from mercury vapor. The apparatus used to analyse the hydrogen-nitrogen mixtures produced in all the experiments is also included in Fig. 2. An apparatus was constructed for a brief examination of the photolysis of hydrazine. Equipment for the measurement of the extinction coefficient of ammonia is shown in Fig. 1.

Apparatus for Extinction Coefficient Measurements. Radiation of 1849 $\overset{\circ}{A}$ wavelength was used in the photolysis of ammonia. Since no accurate value was available for the ability of ammonia to absorb light of this wavelength, an apparatus was designed to measure the extinction coefficient at 1849 $\overset{\circ}{A}$. The extinction coefficient was required to calculate the minimum ammonia pressure necessary in the reaction vessel for complete absorption of the incident 1849 $\overset{\circ}{A}$ radiation.

The apparatus for the absorption measurements, shown in Fig. 1, incorporated a mercury-free, high-vacuum system to manipulate the ammonia and an optical assembly designed to produce a beam of 1849 $\overset{\circ}{A}$ radiation and to measure fractional changes in the beam due to absorption of the radiation by ammonia.

The light source, L, was a Hanovia Biosteritron, a low pressure mercury-rare gas discharge, with a quartz envelope. The power required to operate the lamp was supplied by the 3000 volt secondary of a Sola neon sign transformer which was coupled to a 110 volt a.c. power outlet through a Sola constant voltage transformer.

18

The apparatus was designed so that either of two quartz absorption cells could be attached to the vacuum system in position C of Fig. 1. The one was a Hanovia cell with a path length of 0.020 ± 0.003 cm. in the light beam; the other was an Aminco precision cell (style F, class 3) with a path length of 1.0002 ± 0.0005 cm. A Westinghouse WL789 platinum cathode phototube (P in Fig. 1) was used to measure the intensity of the radiation transmitted through the absorption cell. Since the lamp emitted radiation only at the wavelengths of 1849 $\overset{o}{A}$ and 2537 $\overset{o}{A}$ in the ultraviolet region and since the platinum cathode was not sensitive to wavelengths greater than 2100 $\overset{o}{A}$, the phototube responded only to the 1849 $\overset{o}{A}$ radiation. A potential of 90 volts was maintained across the terminals of the phototube when it was in operation by three dry batteries. The current output from the phototube (about 1×10^{-10} amperes) was measured with a Beckman Ultrohmeter. Extensive shielding of the electrical circuits was required to obtain stable meter readings.

The radiation from the lamp was collimated by three brass apertures A_1, A_2, and A_3. The collimated beam passed through the absorption cell and impinged on the platinum cathode of the phototube. The lamp-cell-phototube assembly was rigidly mounted in a brass box blackened on the inside with Kodacoat. To minimize the influence of stray light, the lamp compartment was separated from the absorption cell-phototube compartment except for the aperture A_2. Nitrogen was passed through the brass box, while measurements were made, to eliminate absorption of the 1849 $\overset{o}{A}$ radiation by oxygen in the optical path.

The absorption cell was attached to the Pyrex high-vacuum system by means of a quartz-to-Pyrex graded seal. High vacua were obtained in the manifold by means of an Eitel-McCullough HV-1 oil diffusion pump backed by a Welsh Duoseal two-stage mechanical pump. The vacuum system

consisted of a gas inlet, two traps (T) for distilling ammonia and a gas reservoir (R). The ammonia pressure in the absorption cell was measured with an Alphatron ionization gauge (I) at low pressures and with a mercury manometer (M) at high pressures. The mercury in each limb of the manometer was covered with a 10 cm. layer of Octoil, a hydrocarbon oil which has a vapor pressure of less than 1×10^{-6} mm. at room temperature. Vacuum stopcocks (S), lubricated with Dow Corning Silicone high-vacuum grease, were used throughout the vacuum system.

Apparatus for the Photolysis of Ammonia. The flow and static photolyses of ammonia were done in the apparatus shown in Fig. 2. Except for the quartz lamp, the system was constructed of Pyrex glass. Vacuum stopcocks (S) were used to isolate various sections of the apparatus. The stopcocks were lubricated with Dow Corning Silicone vacuum grease or with Apiezon N stopcock lubricant.

The apparatus was evacuated through S_3 by a two-stage mercury diffusion pump backed up with a Welsh Duoseal mechanical pump. The pumping system was able to reduce the pressure, measured by a McLeod gauge near S_3, to less than 5×10^{-6} mm. Stopcock S_2 separated the reaction system from the pumping system and the apparatus for analysing hydrogen-nitrogen mixtures. The latter systems contained mercury vapor and, therefore, the traps T_1 and T_2 were immersed in liquid nitrogen before S_2 was opened to prevent mercury from diffusing into the reaction system.

A tank of ammonia was connected to the reaction system by a short rubber tube, coated with Glyptal cement. The gas entered the reaction system through a Hoke flow meter (F) calibrated from 4.0 to 35 cu. ft. per hour for ammonia at one atmosphere pressure and at a temperature of
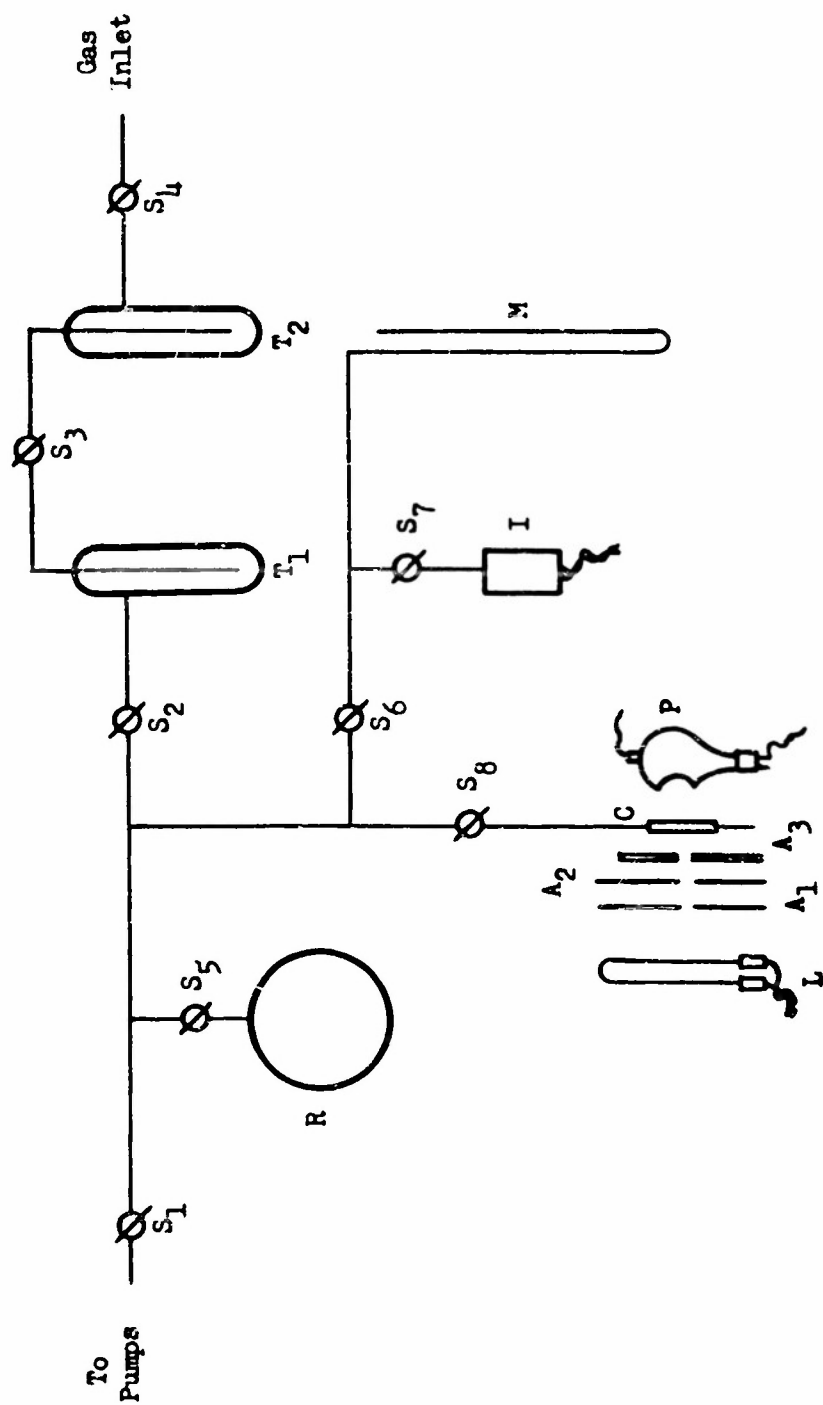
Fig. 1. Apparatus for Absorption Measurements

$0^{o}C$. The mass flow rate of ammonia into the system, measured by this meter, was controlled by a Hoke needle valve, N. The ammonia passed through the lamp zone (L) and the orifice (O) and was condensed in the flask, C.

The lamp was a low pressure mercury-rare gas discharge and was used as an internal source of radiation. This type of lamp is the most convenient source of ultraviolet light with photochemically useful intensities at discrete wavelengths. Moreover, the lamp temperature did not rise higher than $50^{o}C$. even when operated for long periods of time in a static pressure of ammonia. In a stream of flowing ammonia, the lamp temperature was only slightly above room temperature. The lamp consisted of a U-tube fabricated from 10 mm. I.D. Hanovia S.R. grade optical quartz with walls 1 mm. thick. The electrode arms were ring-sealed into the tubing where it was attached to a male quartz 45/50 standard taper joint. This large male joint was fitted into the Pyrex reaction tube by means of a female 45/50 Pyrex standard taper joint. The other end of the quartz tubing into which the lamp was sealed was joined to the Pyrex inlet tubing by a quartz-to-Pyrex graded seal. The lamp contained a drop of mercury and 4 mm. pressure of argon. Only the two resonance lines, at 1849 Å and 2537 Å were emitted by the lamp in the ultraviolet. Since ammonia is transparent at 2537 Å[9,10] the discharge can be regarded as a monochromatic source of 1849 Å radiation with respect to ammonia. The lamp was designed as an internal source since 1849 Å radiation is strongly absorbed by oxygen and is absorbed to some extent by quartz. To utilize the full intensity of the discharge, the quartz envelope of the lamp was made very thin and the lamp was immersed directly into the ammonia stream. Such an arrangement is not as flexible as an external source nor can the radiation be collimated. The density pattern of the

radiation about the lamp was too complicated to express by a simple mathematical expression.

The lamp discharge was maintained by the 5000 volt secondary of a General Electric luminous tube transformer. The voltage input to the primary of this transformer was stabilized by a Sola constant voltage transformer which operated off a 110 volt a.c. power outlet. The lamp intensity could be regulated by varying the primary voltage with a Variac transformer. The lamp current was measured by an ammeter, in series with the lamp, which was calibrated from zero to one hundred milliamperes.

The orifice (O) between the lamp and the condenser flask was adjusted so that various ammonia pressures were obtainable in the reaction zone at a given mass flow rate of ammonia. The pressure in the reaction zone was determined by an Alphatron ionization gauge and by the oil-mercury manometer described in the section dealing with the apparatus for absorption measurements. These pressure measuring devices were connected to the system through stopcock S_8.

Apparatus for the Mercury-photosensitized Decomposition of Ammonia. The flow and static mercury-photosensitized decomposition of ammonia was performed in the apparatus shown in Fig. 3. This system, constructed mainly of Pyrex glass, was similar in most respects to the apparatus used for the photolysis experiments. The ammonia inlet system through the needle valve N, the flow meter F, and the stopcock S_1, was similar to that described in the previous section; as was the pumping equipment used to evacuate the system through S_3. In the flow experiments, the linear flow rate of the ammonia through the reaction vessel (V) into the condenser flask (C) was controlled by the orifice, O.

The ammonia from the inlet passed through a reservoir, R, containing

mercury. This reservoir was wrapped with resistance wire and was then wrapped with asbestos paper. In some experiments, the mercury reservoir was heated by causing an a.c. current to flow in the resistance wire. The temperature of the mercury was measured by a thermometer placed in a well which dipped into the mercury.

The ammonia was irradiated in a quartz tube, V, which was 15 cm. long and 4.0 cm. in diameter. This tube was connected to the Pyrex apparatus by quartz-to-Pyrex graded seals.

The lamp (X) used for the mercury-photosensitized decomposition of ammonia was a low pressure mercury-rare gas discharge. The discharge was contained in an envelope of Vycor 7910 glass, 14 mm. in diameter, which was shaped into a helix, 10 cm. long, of six coils. The helix fitted around the quartz tube, V, with about 1 cm. clearance. Of the ultraviolet radiation produced by the discharge, only that of 2537 $\overset{o}{A}$ wavelength was transmitted by the Vycor glass. The discharge was maintained and measured by the same arrangement of meters and transformers which operated the lamp used for the photolysis of ammonia.

The pressure of ammonia in the irradiated tube was measured by the mercury manometer, M, or by a Martin Glass Co. McLeod gauge, L, calibrated for pressures from 1×10^{-6} to 2.0 mm. of mercury.

The reaction system was connected to the apparatus for analysing hydrogen-nitrogen mixtures through the trap T_1 and the stopcock S_7 as shown in Fig. 3.

Apparatus for the Analysis of Hydrogen-Nitrogen Gas Mixtures. The hydrogen and nitrogen produced in the experiments of this investigation were quantitatively determined in the apparatus shown on the right of stopcock S_7 in Fig. 2. This apparatus, constructed of Pyrex glass, consisted of a Toepler pump (P), a calibrated volume (K), and a series of
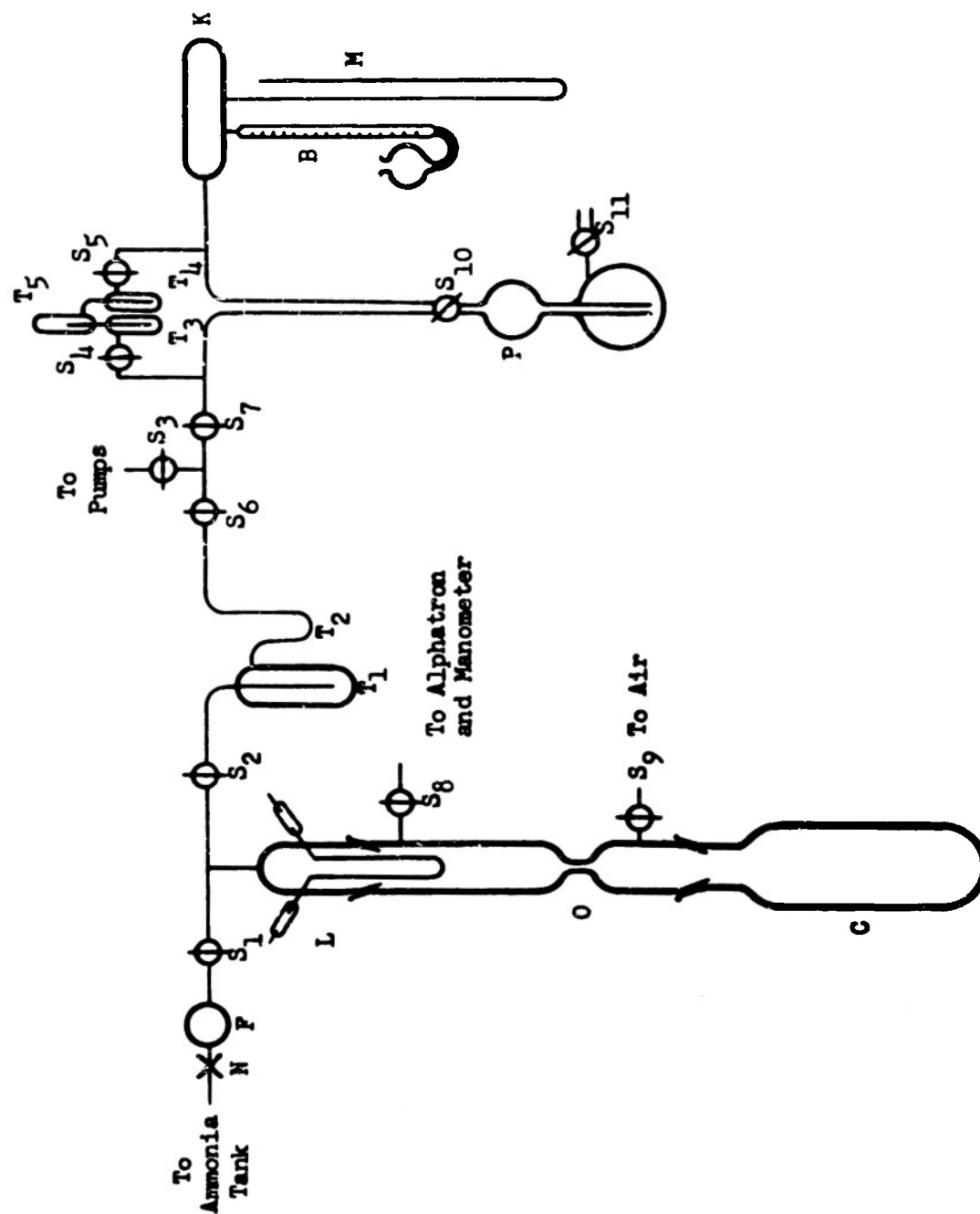
Fig. 2. Apparatus for the Photolysis of Ammonia

traps (T_3, T_4, and T_5) used to convert hydrogen to water.

The lower flask of the Toepler pump was filled with mercury to a level just below the three-way stopcock S_{11} (S_{11} and S_{10} were not vacuum stopcocks). This stopcock permitted air to be admitted to or pumped out of the space above the mercury. The air was pumped out by a Cenco mechanical pump. The three-way stopcock S_{10} opened the upper flask either to the gas inlet at S_7 or to the gas exit which was part of the volume K. After the upper flask and the volume K had been evacuated, gas could be transferred from the gas inlet to the gas outlet by raising and lowering the mercury level in the upper flask together with the proper manipulation of S_{10}. During a large part of the investigation of the mercury-photosensitized decomposition of ammonia, the manual Toepler pump was replaced by a pair of automatic Toepler pumps. These pumps had common gas inlet and gas outlet systems and the air-vacuum arrangement required to raise and lower the mercury level was common to each of them so that they worked in unison with one set of electrical controls. The design and operation of one of the pumps is described in the Appendix.

The capacity of the calibrated volume (K) was variable since it incorporated a gas burette (B). A mercury manometer (M) was used to measure the gas pressure in the calibrated volume. A standard flask, whose exact volume had been established by weighing the amount of mercury required to fill it, was also attached to the volume K. When necessary, the volume K was evacuated and its capacity was calculated from the pressure in it when it was opened to the standard flask which contained a known amount of gas. The calibration of the volume K was reproducible to within 0.1 ml. The capacity of K was about 100 ml. but
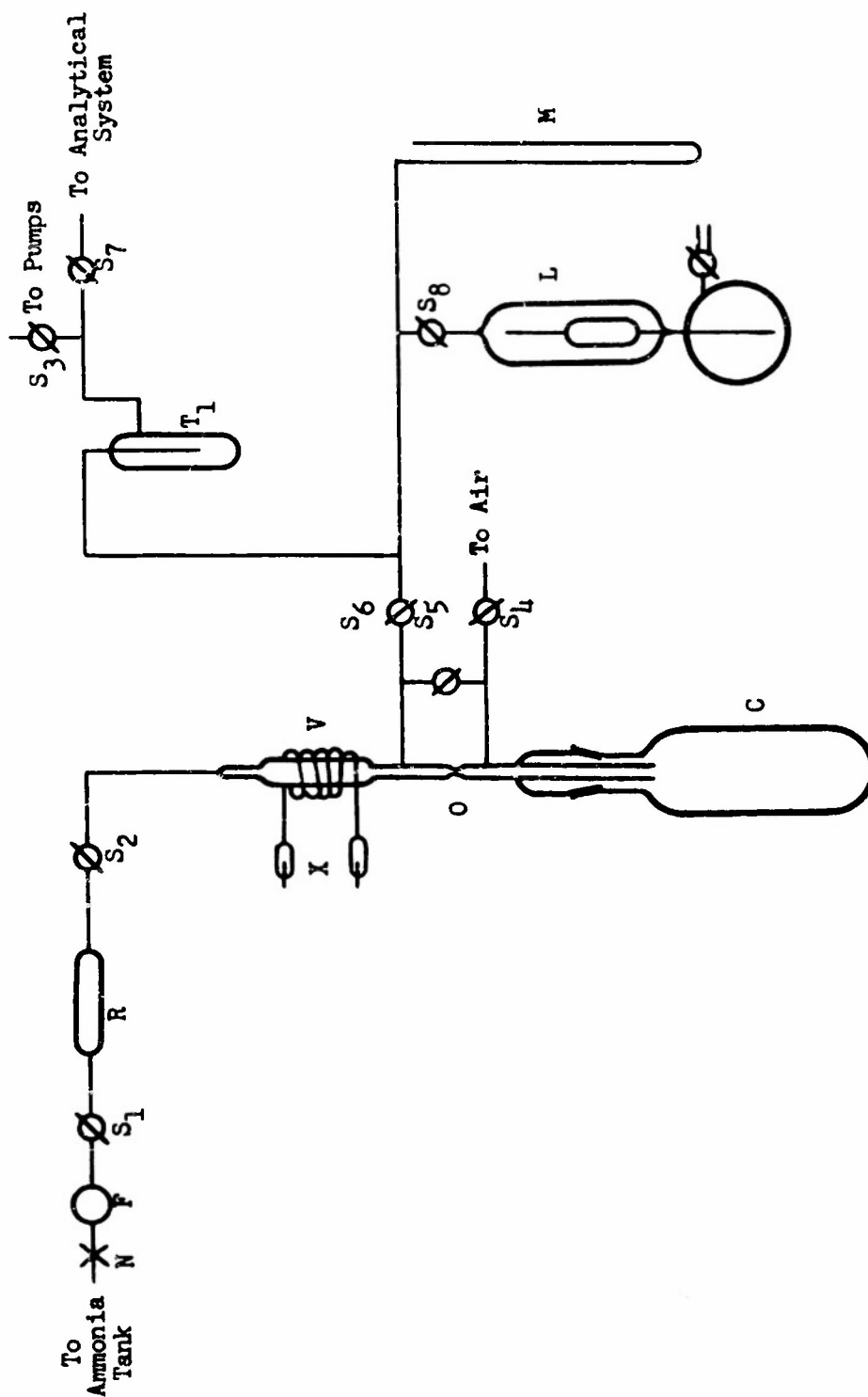
Fig. 3. Apparatus for the Mercury-Photosensitized Decomposition of Ammonia

it could be increased to about 200 ml. by lowering the mercury level in the gas burette.

The trap T_5 contained copper oxide deposited on glass wool and was surrounded by a furnace made of resistance wire and asbestos paper. The furnace temperature was controlled by varying an alternating voltage across the resistance wire with a Variac transformer. The temperature of T_5 was determined from a thermometer whose bulb was inside the furnace. The traps, T_3 and T_4, were used to freeze out the water vapor produced by the oxidation of hydrogen over the hot copper oxide.

Materials

Ammonia. The ammonia used throughout the investigation was obtained from the Matheson Co. and was stated to be 99.5 per cent ammonia. It was also claimed that the non-basic gas did not exceed 0.01 cc. per gm. of liquid ammonia and was less than 0.2 cc. per gm. of ammonia in the overlying gas. The moisture content of the ammonia was rated to be less than fifty parts per million by weight and the oil content was said to be less than three parts per million by weight. Actually the ammonia tanks, when received, contained a considerable quantity of gas which was not condensable at the temperature of liquid nitrogen. The ammonia was allowed to escape rapidly into a fume hood until the non-condensable gas was all swept out. A number of flow runs were done in which the ammonia was not exposed to ultraviolet radiation. The amount of gas collected which was not condensable at the temperature of liquid nitrogen was negligible compared to the amount of hydrogen and nitrogen produced when the flowing ammonia was irradiated. No material which could invalidate the titration analysis for hydrazine in the regular runs was found in the ammonia condensed from the blank runs. An infrared absorption spectrum was obtained from a sample of the tank ammonia

on a Perkin-Elmer Model 21 infrared spectrometer. No absorption peaks were observed except those to be expected for ammonia. Ammonia used directly from the tank and ammonia subjected to fractional distillation decomposed at the same rate within experimental error in the static mercury-photosensitized decomposition of ammonia.

Hydrogen. The hydrogen used in the investigation was obtained from the Air Reduction Sales Co. and was stated to contain 0.09 mole per cent of nitrogen and less than 0.02 mole per cent of other gases.

Ethylene. The ethylene which was added to the ammonia in some of the experiments was the research grade of the Philips Petroleum Co.

Hydrazine. Matheson anhydrous grade hydrazine was used in experiments which required hydrazine. Analysis of this material by titration indicated that it was only about 95 per cent hydrazine. The other 5 per cent was probably water.

n-Propane. Actinometric measurements were made with n-propane. The research grade of the Philips Petroleum Co. and the chemically pure grade of the Matheson Co. gave similar results.

Mercury. The mercury used in any of the apparatus during the investigation was the triply distilled grade obtained from Universal Scientific Industries.

Procedures

The Procedure for Extinction Coefficient Measurements. The high-vacuum system, shown in Fig. 1, was evacuated until the pressure indicated by the Alphatron gauge was less than 1×10^{-4} mm. Ammonia was then admitted to the system through S_4 and was condensed in the trap T_2 which was immersed in liquid nitrogen. Stopcock S_4 was closed and the system was opened to the pumps to remove any non-condensable gas. The ammonia

was distilled from T_2 to T_1, and vice versa, a number of times; a middle fraction was collected at liquid nitrogen temperature from each distillation. The ammonia was then allowed to expand to a pressure of one atmosphere and S_5 was closed to retain ammonia in the reservoir R. The remainder of the system was evacuated and stopcocks S_1 and S_2 were closed.

Before making absorption measurements, the lamp was operated for twenty minutes, with nitrogen passing through the brass box, to insure a constant intensity of radiation. The phototube and the Ultrohmeter were also turned on during this period.

When the apparatus had attained a stable state of operation, the phototube current was recorded. This current represented the intensity of the transmitted 1849 Å radiation when the absorption cell was evacuated. Stopcock S_5 was opened until the desired ammonia pressure was obtained in the absorption cell. The current on the Ultrohmeter was recorded. After some of the ammonia was pumped out through S_1, another current reading was recorded. In this way, the current through the phototube was measured at several ammonia pressures. The ammonia was then completely pumped out of the absorption cell and the phototube current was again recorded. If the initial and final current readings for the evacuated cell did not agree within one per cent due to drift in the instruments, the recorded data was not used. The same procedure was followed over another pressure range with a new sample of ammonia from the gas reservoir. The total exposure time to radiation for each sample of ammonia did not exceed two minutes so that the decomposition of ammonia would not affect the amount of light transmitted through the absorption cell.

The Procedure for the Photolysis of Ammonia. The photolysis in a flowing stream of ammonia was investigated to determine the dependence of the rates of formation of hydrazine, hydrogen, and nitrogen on the ammonia pressure and on the linear flow rate of the ammonia through the irradiated zone. The procedure used for a typical experiment is described below.

The orifice, O, was constricted to the size required to give the desired linear flow rate of ammonia in the irradiated zone and the traps, T_1 and T_2, were immersed in liquid nitrogen to prevent mercury from diffusing into the reaction system. Stopcock S_2 was opened and the system was evacuated until the pressure indicated by the Alphatron gauge was less than 1×10^{-4} mm. The condenser flask was immersed in liquid nitrogen during the remainder of the run. Stopcock S_2 was closed and the system was flushed out with ammonia from the tank so that the walls of the reaction vessel were saturated with ammonia. The system was evacuated again and the lamp was turned on to allow it to warm up to a constant intensity. The Variac transformer, which controlled the voltage supplied to the lamp, was adjusted so that the current through the lamp was ninety milliamperes. When the lamp had been operating for five minutes, the reaction system was isolated by the closing of S_2. Ammonia was allowed to flow from the tank through the irradiated zone into the condenser flask. At the instant that the needle valve, N, was opened to permit ammonia to enter the system, an electric timer calibrated in minutes and hundredths of minutes was turned on. The mass flow rate of ammonia through the reaction system was regulated by the needle valve and was measured by the flow meter. The pressure of ammonia in the irradiated zone was obtained from the Alphatron gauge or the oil-mercury manometer.

When the desired exposure time, usually thirty minutes, had elapsed, the lamp was turned off. The tubing between the lamp and the condenser flask was heated gently for a few minutes to drive any adsorbed hydrazine into the ammonia stream. The stream was then stopped by the closing of the needle valve and S_1. One hour was permitted to elapse so that all the ammonia would condense in the flask immersed in liquid nitrogen. The products of the reaction which were not condensed were then pumped into the gas analysis apparatus through S_2, S_6, and S_7. The traps, T_1 and T_2, served to remove the last traces of ammonia from the non-condensable gases, hydrogen and nitrogen. Stopcock S_2 was closed and S_9 was opened to let air into the reaction system. The condenser flask was removed from the system and the condensate was analysed for hydrazine. When the reaction system was fitted with a clean condenser flask and was evacuated again, it was ready for the next run.

The experiments were grouped into series in which the orifice size remained constant but the mass flow rate and hence the pressure of ammonia in the irradiated zone was varied. When a series of runs had been completed, the orifice size was changed and another group of runs was made in which the ammonia pressure was varied. In two runs, the zone between the lamp and the orifice was filled with Pyrex rods.

The static photolysis of ammonia was also investigated in the apparatus shown in Fig. 2. A sample of ammonia from the tank was subjected to two trap-to-trap distillations in an auxiliary apparatus. A middle fraction was retained from each distillation. The reaction system was evacuated and isolated by S_2 in the usual manner. The desired pressure of the distilled ammonia was admitted to the reaction system. The lamp, which had been operated for five minutes so that it

produced a constant intensity of radiation, was turned off while the ammonia entered the system. The lamp and the electric timer were then turned on. When the lamp was turned off at the end of the run, the condenser flask was immersed in liquid nitrogen for one hour. The reaction products were analysed using the procedure already described for the products of the flow photolysis of ammonia.

The Procedure for the Mercury-Photosensitized Decomposition of Ammonia. The rates of formation of the products of the mercury-photosensitized decomposition of a stream of ammonia were measured in a series of experiments in which the pressure and the linear flow rate of ammonia in the irradiated zone were varied in a systematic manner.

The procedure for a typical mercury-photosensitized experiment was similar to the procedure already described for a typical photolytic experiment. The diameter of the orifice was constricted to the desired size and the reaction system was evacuated until the pressure registered by the McLeod gauge was less than 5×10^{-6} mm. The condenser flask was immersed in liquid nitrogen to a level which was maintained throughout the remainder of the run. The system was flushed with ammonia and then was evacuated again. The stopcock S_5 was opened during evacuation when the orifice was so small that the non-condensable gas was difficult to pump out of the condenser flask. The lamp was turned on and the lamp current was adjusted to ninety milliamperes. The heat radiated from the lamp raised the temperature of the reaction tube only a few degrees above room temperature when the latter had ammonia flowing through it.

When the lamp had operated for five minutes so that it produced a constant intensity of radiation, the reaction system was isolated by the closing of S_6. Ammonia was admitted to the system through S_1 and S_2 at a mass flow rate regulated by the needle valve and measured by

the flow meter. As the ammonia entered the system, an electric timer
was started. After the desired exposure time, usually thirty minutes,
had elapsed, the lamp was turned off and one minute later the needle
valve and S_1 were closed. After fifteen minutes when most of the
ammonia had been condensed in the condenser flask, the non-condensable
gas was transferred into the apparatus for gas analysis through S_6, S_7,
and the trap T_1. This trap was immersed in liquid nitrogen and served
to condense any ammonia which may have remained in the non-condensable
gas. Stopcocks S_2, S_6, and S_7 were closed after the non-condensable
gas was transferred and S_4 was opened to let air into the condenser
flask. The flask was removed from the system and in some of the runs
the condensate was analysed for hydrazine. When the system was fitted
with a clean flask and was evacuated again, it was ready for another
run. Air was not permitted into the section of the system between S_1
and S_2. If air was admitted to this zone, the mercury saturator was
less efficient in the next run probably because a thin film of mercury
oxides was formed on the surface of the mercury which decreased the
rate of evaporation of mercury into the ammonia stream.

As in the photolysis of ammonia, series of experiments were made
in which the orifice size was constant but the ammonia pressure was
varied. When a series of experiments was completed, the orifice size
was changed and again the reaction was studied at various ammonia
pressures.

In a number of experiments the mercury saturator was heated to
$150^{\circ}C$. The temperature of the mercury was not constant, however, since
it was cooled to some extent by the stream of ammonia passing over it.

A series of experiments was done in which the time of exposure of
the ammonia stream to 2537 $\overset{\circ}{A}$ radiation was varied, and in other

experiments the lamp intensity was varied. The reaction zone was packed with fifty feet of platinum wire, 0.0038 inches in diameter, in another group of runs.

Experiments were also made in which ethylene was bled into the ammonia stream before it entered the irradiated zone. Before an experiment of this kind was started, ethylene from a tank was condensed in a reservoir (not shown in Fig. 3) of 2.4 liters volume immersed in liquid nitrogen. The reservoir was then opened to the pumping system to remove any non-condensable gas. The ethylene was allowed to expand so that the pressure in the reservoir, indicated by the mercury manometer, was about seven hundred millimeters. A scratched stopcock allowed the ethylene to be added to the ammonia stream between S_2 and the irradiated zone at a very slow rate. The average rate of addition of ethylene to the stream was calculated from the decrease in pressure in the reservoir during a run. In some of the runs in which ethylene was added, the ammonia stream was irradiated for two or three hours to collect a larger amount of products than was obtained in the usual thirty-minute experiments. At the end of these runs, the condenser flask was removed and the ammonia was allowed to evaporate until only a few milliliters remained. The flask was then refitted to the reaction system, immersed in liquid nitrogen and evacuated. The remaining condensate was allowed to expand into the reaction system and a sample was collected in an infrared absorption cell. The infrared spectrum of the sample was measured from six hundred to four thousand wave numbers on a Model 21 Perkin-Elmer infrared spectrometer. The spectra of tank ammonia, hydrazine, and methylamine were also measured so that they could be compared with the spectrum of the unknown gas.

A few experiments were done in which the ammonia passed through

a Pyrex spiral between the mercury saturator and the reaction vessel.
The spiral was maintained at $360^{\circ}C$. with an electric furnace.

The static mercury-photosensitized decomposition of ammonia was
also investigated in the apparatus shown in Fig. 3. In some of the
experiments the ammonia was taken directly from the tank; in other
experiments the tank ammonia was subjected to several trap-to-trap
distillations and was stored in a reservoir over mercury before it
was admitted to the reaction system. The results obtained from the
decomposition of the distilled ammonia were the same as those obtained
from the untreated ammonia. The procedure for a typical static run is
described below.

The reaction zone was evacuated and isolated by closing S_6.
Ammonia was admitted to the system from the tank or the reservoir (not
shown in Fig. 3). When the ammonia was admitted from the tank, it was
allowed at least one hour to equilibrate with the mercury vapor from a
pool of mercury in the bottom of the condenser flask. If the ammonia
was admitted from the reservoir where it was stored over mercury, it
was equilibrated for a shorter time. While the ammonia was equili-
brating with the mercury vapor, the lamp was turned on so that it would
emit a constant intensity of radiation when the run was started. The
input voltage to the lamp was adjusted so that the lamp current was
ninety milliamperes. The reaction system was shielded from the lamp
radiation until the run began. As the shield was removed, an electric
timer was started to measure the exposure time of the run. After the
lamp was turned off, the condenser flask was immersed in liquid nitro-
gen. When fifteen minutes had elapsed, the trap T_1 was immersed in
liquid nitrogen and the non-condensable gas was transferred through
S_6 and S_7 into the apparatus for gas analysis. In the static mercury-

photosensitized experiments, a wide range of ammonia pressures was investigated. The effect of varying the exposure time was studied and in several runs hydrogen was added to the ammonia from a hydrogen reservoir attached to the system.

The Procedure for the Analysis of the Products of the Photodecomposition of Ammonia. The non-condensable gas which was produced in each experiment on the photodecomposition of ammonia was a mixture of hydrogen and nitrogen. The procedure for the quantitative analysis of the hydrogen-nitrogen mixtures in the apparatus illustrated in Fig. 2 is described below.

Before the gas analysis was started, the analytical system was evacuated. Stopcocks S_4 and S_5 were closed and the hydrogen-nitrogen mixture was admitted to the Toepler pump through S_7. The Toepler pump transferred the gas into the calibrated volume until the pressure in the reaction system was reduced to less than one per cent of its original value. Stopcock S_7 was then closed and the quantity of gas in the calibrated volume was determined from the pressure on the mercury manometer. In this calculation, the temperature of the gas was assumed to be the same as the temperature indicated by a thermometer placed near the calibrated volume. The temperature of the furnace around the trap which contained copper oxide was raised to $300^{\circ}C$. and traps T_3 and T_4 were immersed in liquid nitrogen. The gas from the calibrated volume was admitted to the hot copper oxide. Preliminary experiments, in which hydrogen-nitrogen mixtures were exposed to the hot copper oxide for different time intervals, proved that all the hydrogen in these mixtures was converted to water in less than one hour. The water was condensed in T_3 or T_4. In the routine analyses when the hydrogen-nitrogen mixture had been in contact with the hot copper oxide for one hour, S_5 was

closed and S_4 was opened. The gas from the traps T_3, T_4, and T_5 was transferred into the calibrated volume by the Toepler pump until several cycles of the pump did not increase the pressure of the transferred gas. The amount of this gas, which was assumed to be nitrogen, was calculated from its pressure and temperature in the calibrated volume. The amount of hydrogen produced in a run was assumed to be the difference between the total non-condensable gas and the nitrogen. After a few analyses were made, the copper oxide which had been reduced by hydrogen was reoxidized by allowing air into the analytical system for several hours while the trap T_5 was kept at $300^{o}C$.

In the photolysis experiments and in some of the mercury-photo-sensitized decompositions, the material which was condensed in the flask immersed in liquid nitrogen was analysed for hydrazine. When the flask was removed from the reaction system at the end of a run, the ammonia was allowed to boil away until only a few milliliters of liquid remained. Preliminary analyses showed that as much as ten per cent of the hydrazine produced in a run was swept out of the flask with the evaporating ammonia. Therefore, in the routine analysis that was developed, the evaporating ammonia was bubbled through a trap containing about forty milliliters of distilled water. The hydrazine in the ammonia vapor remained in solution in the water. When almost all of the ammonia had boiled away, the residue in the flask and the contents of the water trap were combined and acidified with concentrated hydrochloric acid. This solution was diluted to a known volume and aliquots were titrated with 0.1 N potassium iodate according to the method of Penneman and Audrieth.[29] Titrations were made with solutions of hydrazine of known purity in which the hydrazine concentrations were similar to the concentrations of hydrazine obtained in the analyses of the

routine experiments. These tests showed that the error in the hydrazine titrations did not exceed two per cent.

Since hydrazine is the only simple hydronitrogen compound known to exist in the free state except ammonia,[1] it was assumed throughout this investigation that the only products of the photodecomposition of ammonia were nitrogen, hydrogen, and hydrazine.

Since the photodecomposition of ammonia was assumed to obey the stoichiometric reaction equations

$$2 \, NH_3 = N_2 + 3 \, H_2 \qquad (3)$$
$$2 \, NH_3 = N_2H_4 + H_2 \qquad (4)$$

the amount of hydrazine produced in a run could also be calculated from the amounts of hydrogen and nitrogen which were produced. This calculation for the hydrazine was more accurate than the determination of the hydrazine directly by titration although both methods gave similar results in the photolysis experiments.

When the condensate of the mercury-photosensitized experiments was analysed for hydrazine by the titration described above, the amount of hydrazine was up to fifty per cent less than the amount of hydrazine which was calculated from the hydrogen and nitrogen produced in the same run. The failure of the titration to account for all the hydrazine was probably due to the decomposition of part of the hydrazine in the condenser flask after it was removed from the reaction system. As the ammonia was evaporated from the condenser flask, the mercury which had been condensed along with the ammonia during the run formed a colloidal film on the surface of the flask. When concentrated hydrochloric acid was added to the residue in the flask, mercuric and mercurous chlorides may have been formed. These chlorides are known

to oxidize hydrazine rapidly to hydrogen and nitrogen.

To test the hypothesis that the missing hydrazine was decomposed by mercury chlorides, a 25 ml. solution of hydrazine of known concentration was mixed with concentrated hydrochloric acid in a flask containing a colloidal mercury film. The concentration of hydrazine in the solution was similar to the concentrations in the experimental runs. When the hydrazine had been shaken with hydrochloric acid in the presence of colloidal mercury for one minute, the solution was titrated in the usual manner. The hydrazine concentration was decreased by 25 per cent. A similar test on a hydrazine solution with hydrochloric acid and a pool of mercury showed no change in the hydrazine concentration. Another technique was used in several mercury-photosensitized flow experiments, to show that the mercury was responsible for the incomplete recovery of the hydrazine which was produced. When the condenser flask was removed from the reaction system, it was immersed in dry ice. When the condensed material in the flask had liquefied, it was decanted into a clean flask containing no mercury. The analysis for hydrazine was then performed in the usual manner. When the hydrazine solution was decanted from the colloidal mercury, the titration indicated that about 85 per cent of the hydrazine produced (calculated from the hydrogen and nitrogen produced) was recovered. Since the hydrazine could not be recovered quantitatively in the presence of colloidal mercury, the amount of the hydrazine produced in the mercury-photosensitized experiments was calculated from the amounts of hydrogen and nitrogen obtained.

In the experiments in which ethylene was added to the ammonia stream, part of the hydrogen produced was removed by reaction with ethylene. The amount of hydrazine produced in these runs was obtained

by the titration procedure since the calculation from the hydrogen-nitrogen analysis was no longer valid. The reported amount of hydrazine formed in these runs was, therefore, at least 15 per cent too small.

The Procedure for the Actinometric Measurements. The static mercury-photosensitized decomposition of n-propane was studied in the apparatus used for the mercury-photosensitized decomposition of ammonia. These experiments were done to determine the intensity of 2537 $\overset{o}{A}$ radiation which was incident on the mercury in the irradiated zone. This incident intensity was used to calculate the quantum yields in experiments in which ammonia was decomposed.

The mercury-photosensitized decomposition of n-propane was chosen as the actinometer since Bywater and Steacie[3] have established the quantum yield for hydrogen production in this reaction. At room temperature and 140 mm. pressure, the only products of the decomposition of n-propane were hydrogen and hexanes. The production of hydrogen was directly proportional to the light intensity and to the exposure time. When 140 mm. pressure of n-propane was used, the quantum yield for hydrogen production was 0.46. Bywater and Steacie used the rate of decomposition of uranyl oxalate as an actinometer to obtain the light intensity used to calculate this quantum yield.

The n-propane used in our investigation was admitted to a series of evacuated traps from a tank. The n-propane was condensed with liquid nitrogen and was subjected to three trap-to-trap distillations. A middle fraction was saved from each distillation. The distilled n-propane was stored over mercury in an evacuated reservoir which was attached to the reaction system. Several milliliters of mercury were placed in flask C shown in Fig. 3 and the reaction system was evacuated

and isolated by closing S_6. The n-propane from the reservoir was
admitted to the reaction system until the propane pressure in the
system was 140 mm. The gas was allowed one hour to equilibrate with
the mercury vapor in the system. Equillibration for a longer time did
not increase the rate of decomposition of the n-propane. While the
equilibration was proceeding the lamp was turned on so that a stable
intensity of radiation would be emitted when the run was started. The
lamp current was adjusted to the desired value. The reaction system
was shielded from the lamp during the equilibration period. When the
lamp shield was removed, an electric timer was started to measure the
exposure time of the run. After the desired time interval, usually
five minutes, the lamp was turned off and the condenser flask was
immersed in liquid nitrogen for one hour. At the end of this time,
the hydrogen was transferred to the apparatus for gas analysis and
measured. The exposure time in these experiments was always less than
five minutes, so that the concentration of the reaction products was
never great enough to influence the rate of formation of hydrogen. The
rate of hydrogen formation was determined for several values of the
lamp current.

The Procedure and Apparatus for the Static Photolysis of Hydrazine.
The static photolysis of hydrazine was investigated to determine
whether it was decomposed by 2537 $\overset{o}{A}$ radiation. A sample of Matheson
Co. anhydrous hydrazine was thoroughly degassed and the hydrazine vapor,
at 14 mm. pressure, was admitted to an evacuated quartz tube attached
to a mercury-free vacuum system. The tube was closed off from the
liquid hydrazine and the hydrazine vapor was exposed to the radiation
from a low pressure mercury-rare gas discharge. The lamp envelope was
fashioned of Vycor 7910 glass so that the hydrazine was exposed only to

ultraviolet radiation of 2537 $\overset{o}{A}$ wavelength. When the lamp was turned
off, a side-arm from the reaction tube was immersed in a mixture of
dry ice and acetone for thirty minutes. The non-condensable gas was
transferred to the apparatus for gas analysis by a Toepler pump and
was measured. The gas was then passed through a trap immersed in
liquid nitrogen to remove ammonia. The residual non-condensable gas
was analysed for hydrogen and nitrogen by the procedure used in the
photodecomposition of ammonia.

CHAPTER III

RESULTS

The Extinction Coefficient of Ammonia at 1849 Å

The extinction coefficient, ε , is defined by the equation

$$I_t = I_0 10^{-\varepsilon c d} \qquad\qquad I$$

where I_0 and I_t are the intensities of the 1849 Å radiation incident
on and transmitted through the ammonia contained in the quartz
absorption cell. The optical path length through the ammonia at a
concentration of c moles per liter is d cm.

The measurements which were made on the absorption of 1849 Å
radiation by ammonia are compiled in Table 1. In this table C_0 and
C_t represent, respectively, the Ultrohmeter current for the evacuated
absorption cell and for the cell containing ammonia.

The quantity, $(\log I_0/I_t)/d$, was calculated for each of the
$(\log C_0/C_t)$ values in Table 1 by assuming that the phototube current
was directly proportional to the intensity of the radiation falling
on it. In Fig. 4, the results of the absorption measurements for the
1.00002 cm. cell are shown as a plot of $(\log I_0/I_t)/d$ versus c, the
concentration of the ammonia. The left hand ordinate figures and the
lower abscissa figures represent the results for this absorption cell.
Within the experimental error, the points fall on a straight line, the
slope of which gives a value for ε of 1.21×10^3 liters moles^{-1}cm.$^{-1}$.
A similar plot was made in Fig. 4 for the measurements obtained with
the Hanovia absorption cell which had a path length of 0.020 cm. The
right hand ordinate figures and the upper abscissa figures of Fig. 4
represent the scale used to plot these results. The value of ε

calculated from the slope of a line through the latter measurements agrees within the experimental error with the value reported for the 1.000 cm. cell. Beer's Law is therefore obeyed by ammonia over the pressure range from 1 to 200 mm.

By using the value, 1.21×10^3 liters moles^{-1} cm.$^{-1}$ for the extinction coefficient and the geometry of the reactor in Eq. I, the minimum ammonia pressure for complete absorption of the 1849 $\overset{\circ}{A}$ radiation in the reaction tube of Fig. 2 was estimated to be 8 to 10 mm.

The Photolysis of Ammonia

Results from the Flow Experiments. The mass flow rate of ammonia was converted to volume flow at the temperature and pressure of the reaction zone. The volume flow divided by the area of the cross-section of the irradiated zone (16.6 cm.^{2}) gave the linear flow rate of the ammonia.

Throughout the range of mass flow rates and ammonia pressures used, the linear flow rate depended essentially on the resistance to flow of the tubing between the lamp and the ammonia condenser. Thus, the linear flow rate was varied by changing the diameter of the orifice in the tubing. With a given orifice size, the pressure rise in the reaction zone when the mass flow was increased was just that required to keep the linear flow rate constant. Fluctuation in the calculated linear flow rate for one orifice size at various mass flow rates was attributed to error in the measurements of the mass flow rates and the ammonia pressures. In several experiments, the mass flow rates were too small to be measured on the flow meter. The linear flow rates for these runs were assumed to be the same as for other runs with the same orifice size and for which the linear flow rates had been calculated.

Table 1. Absorption Measurements on Ammonia at 1849 Å

d = 1.0002 cm.		d = 0.020 cm.	
Ammonia pressure mm.	Log C_o/C_t	Ammonia pressure mm.	Log C_o/C_t
0.45	0.025	33	0.050
0.97	.080	54	.076
1.12	.065	68	.093
2.52	.190	85	.114
3.54	.240	108	.143
4.47	.330	126	.173
4.85	.300	152	.199
6.35	.440	202	.271
7.00	.440		
8.95	.660		
10.4	.650		
12.3	.740		
12.8	.920		
14.0	.830		
14.7	.97		
15.3	1.07		
16.6	1.06		
19	1.25		
20	1.28		
23	1.45		
26	1.67		
29	1.82		
31	2.00		
34	2.22		
37	2.34		
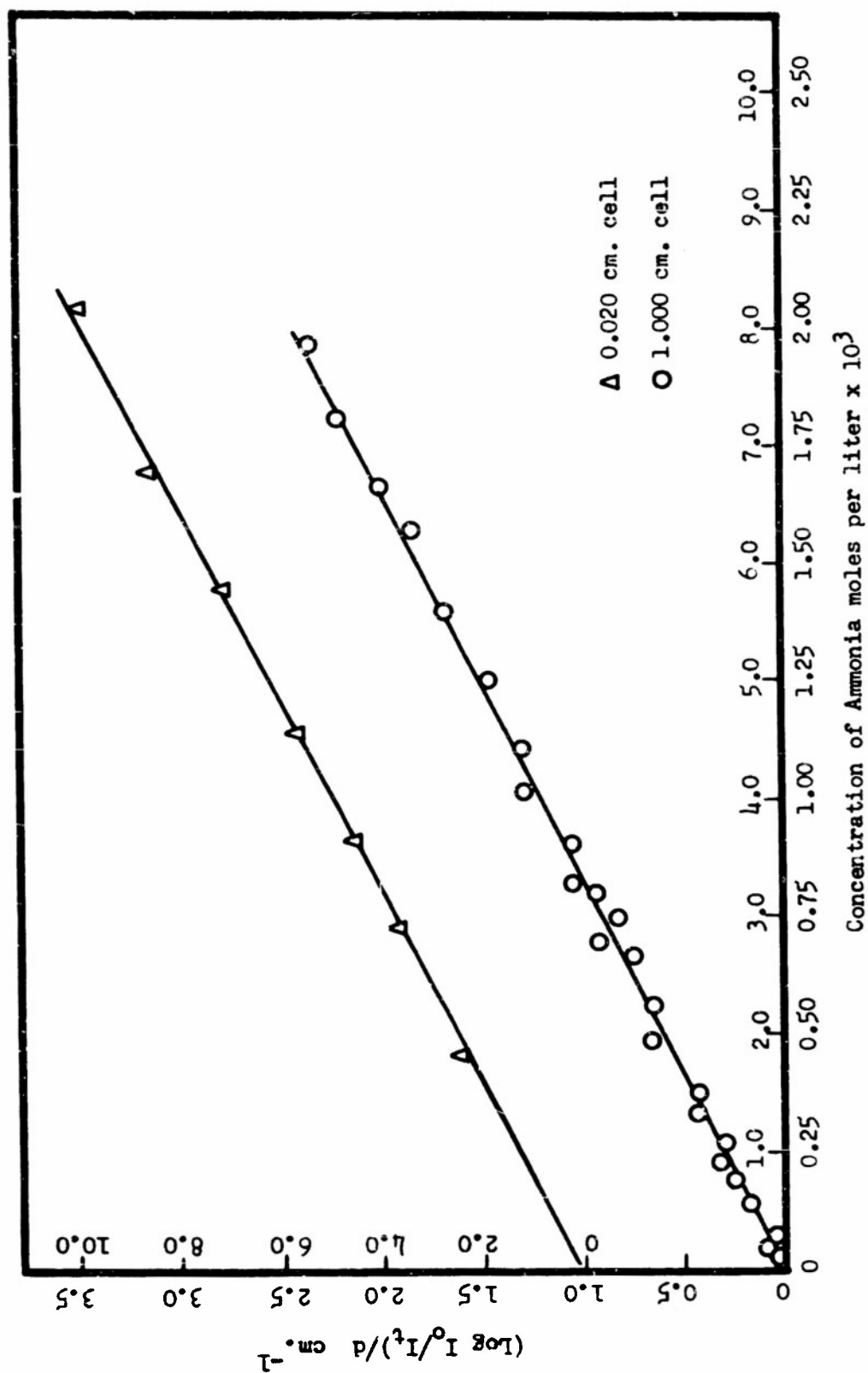
Fig. 4. The Extinction Coefficient of Ammonia at 1849 Å

Similarly, in some experiments the ammonia pressure in the reaction zone was calculated from the mass flow rate and from a linear flow rate established at another pressure for the same orifice size.

The linear flow rates were varied from 7.05 to 11,150 cm. per second. The contact time for the gas in the irradiated zone, obtained by dividing the length of the irradiated zone (26 cm.) by the linear flow rate, varied from 3.69 to 2.33×10^{-3} seconds.

In the analysis of the products, the amounts of the total non-condensable gas, the nitrogen, and the hydrazine produced per unit time were measured. Two quantities of interest were calculated from these data using the stoichiometric reactions

$$2\ NH_3 = N_2 + 3\ H_2 \tag{3}$$

$$2\ NH_3 = N_2H_4 + H_2 \tag{4}$$

1. The apparent amount of ammonia decomposed was given by twice the sum of the hydrazine and the nitrogen produced.

2. The fraction of the ammonia decomposed which was recovered as hydrazine was given by the ratio of the hydrazine to the sum of the hydrazine and nitrogen.

Since the total non-condensable gas minus the nitrogen gave the quantity of hydrogen produced, the hydrazine produced could be calculated from the gas analysis only, because from reactions (3) and (4)

$$N_2H_4 = (N_2 + H_2) - 4N_2 \tag{II}$$

The values for the amount of hydrazine produced which were calculated from Eq. II were more accurate than the values obtained when the hydrazine was recovered and titrated. Both procedures were followed in each run but the value for the hydrazine, which was used in

calculating the amount of ammonia decomposed and the percentage of the decomposed ammonia which was recovered as hydrazine, was the value calculated from the gas analysis by Eq. II.

A summary of the results of the flow photolysis of ammonia is compiled in Table 2. The runs were grouped according to the orifice size (i.e., with the same linear flow rate). Within the groups, the mass flow rate and hence the reaction pressure was varied over the range permitted by the apparatus. In Fig. 5, the percentage of the decomposed ammonia which was recovered as hydrazine* is plotted as a function of the ammonia pressure in the reactor. The legend accompanying Fig. 5 designates the linear flow rate of each point in the figure. The dependence of the rate of decomposition of ammonia on the ammonia pressure in the reactor is shown by the upper curve in Fig. 6. In this figure also, the linear flow rate associated with each point is designated by the legend.

Unfortunately the apparatus did not permit the investigation of the same ammonia pressure range at each linear flow rate. It is evident, however, from Fig. 5, that the per cent hydrazine was essentially independent of the reaction pressure at a given linear flow rate but increased as the linear flow rate was increased. The linear flow rates in the last two experiments reported in Table 2 were much higher than in the other experiments but the per cent hydrazine did not increase. To achieve these high linear flow rates, the runs were performed at such low reaction pressures that there was incomplete absorption of the 1849 Å radiation. Small amounts of non-condensable

---

*The percentage of the decomposed ammonia recovered as hydrazine is, hereinafter, referred to as the per cent hydrazine.

gas were therefore obtained and the error in the analysis was larger than in the other runs. Thus, it was not clear whether the per cent hydrazine would increase to 100 per cent at very high linear flow rates or whether it had a real limit at about 85 per cent. Since the reaction pressure was very low, heterogeneous reaction probably played a much greater role in the last two experiments than it did in the rest of the investigation.

In Fig. 6, the points are all on a smooth curve showing that the rate of ammonia decomposition, which was a measure of the relative quantum yield of ammonia decomposition in the reaction, did not depend on the linear flow rate. The rate had a constant value of about $1 \times 10^{-3} \pm 0.1 \times 10^{-3}$ moles per hour from 100 to 560 mm. pressure of ammonia in the reaction zone (the run at 560 mm. pressure is not shown in Figs. 5 or 7). At lower pressures, the relative quantum yield increased until at 10 mm. pressure the value was about double that at 100 mm. Below 10 mm., the rate of ammonia decomposition decreased because the absorption of the 1849 $\overset{\circ}{A}$ radiation was not complete.

In the experiments reported in Table 3, the surface-to-volume ratio in the zone between the lamp and the orifice was 0.95 cm.$^{-1}$. Two experiments were done in which this zone was packed with Pyrex rods, thereby increasing the surface-to-volume ratio to 8.65 cm.$^{-1}$. The results for these runs are listed in Table 3 together with comparable data for the unpacked system. The examination of the results showed that neither the rate of ammonia decomposition nor the per cent hydrazine was changed when the surface-to-volume ratio was increased in the zone following the lamp. One must conclude therefore either that the reaction was completed before the flowing gas reached the packed zone or that the reaction was not influenced by the increased

Table 2. Results from the Flow Photolysis of Ammonia

Ammonia pressure mm.	Linear flow rate cm./sec.	Total non-condens. gas per hour moles x 10⁴	Nitrogen per hour moles x 10⁴	Measured hydrazine per hour moles x10⁴	Calculated hydrazine per hour moles x 10⁴	Per cent hydrazine	Ammonia decomposed per hour moles x 10⁴
560	7.05	13.15	2.91	1.27	1.50	34.2	8.82
188	21.0	14.07	2.87	2.30	2.59	47.4	10.92
52.2	75.3	15.61	2.90	3.50	4.01	58	13.82
104	76.2	13.23	2.59	3.11	2.87	52.6	10.92
159	76.6	11.62	2.18	2.71	2.90	57.2	10.16
22.5	104	16.00	2.85	4.45	4.60	61.7	14.90
56.8	104	14.62	2.62	4.06	4.14	61.2	13.52
94.0	105	12.85	2.34	3.23	3.49	59.9	11.66
112	106	11.91	2.35	3.00	2.51	51.7	9.72
131	106	11.75	2.33	---	2.43	51.0	9.52
13.8	285	15.12	2.35	4.80	5.85	71.4	16.40
20.3	292	15.21	2.38	4.90	5.69	70.6	16.14
26.9	291	15.35	2.45	5.19	5.55	69.4	16.00
34.5	279	13.99	2.15	4.78	5.39	71.6	15.08
40.6	285	13.46	2.06	5.04	5.22	71.8	14.53
48.2	284	12.88	1.82	4.56	5.60	75.5	14.84
6.91	803	12.80	1.56	5.53	6.82	81.5	16.75
11.6	685	13.97	1.60	6.34	7.57	82.5	18.34
15.7	755	14.35	1.69	6.34	6.66	76.0	16.70
19.2	721	14.42	1.64	7.08	7.18	79.3	17.84

Table 2. (Continued)

Ammonia pressure mm.	Linear flow rate cm./sec.	Total non-condens. gas per hour moles x 10^4	Nitrogen per hour moles x 10^4	Measured hydrazine per hour moles x10^4	Calculated hydrazine per hour moles x 10^4	Per cent hydrazine	Ammonia decomposed per hour moles x 10^4
8.0	1730	15.07	1.59	8.03	8.71	84.7	20.60
7.5	1850	12.82	1.25	7.55	7.82	86.2	18.14
7.5	1870	12.96	1.06	6.96	7.41	82.2	16.94
1.5	5000	4.30	0.48	----	2.38	83.3	5.72
0.8	10000	3.28	0.41	0.66	1.64	80.1	4.10

Table 3. The Effect of Altering the Surface-to-Volume Ratio

Reaction conditions	Ammonia pressure mm.	Linear flow rate cm./sec.	Total non-condens. gas per hour moles x 10^4	Nitrogen per hour moles x 10^4	Calculated hydrazine per hour moles x 10^4	Per cent hydrazine	Ammonia decomposed per hour moles x 10^4
Packed	15.8	495	14.76	1.83	7.32	80.0	18.30
Unpacked	15.8	495	----	---	---	77.0	17.00
Packed	56	159	12.92	2.00	4.92	71.1	13.84
Unpacked	56	159	----	---	---	67.5	13.75
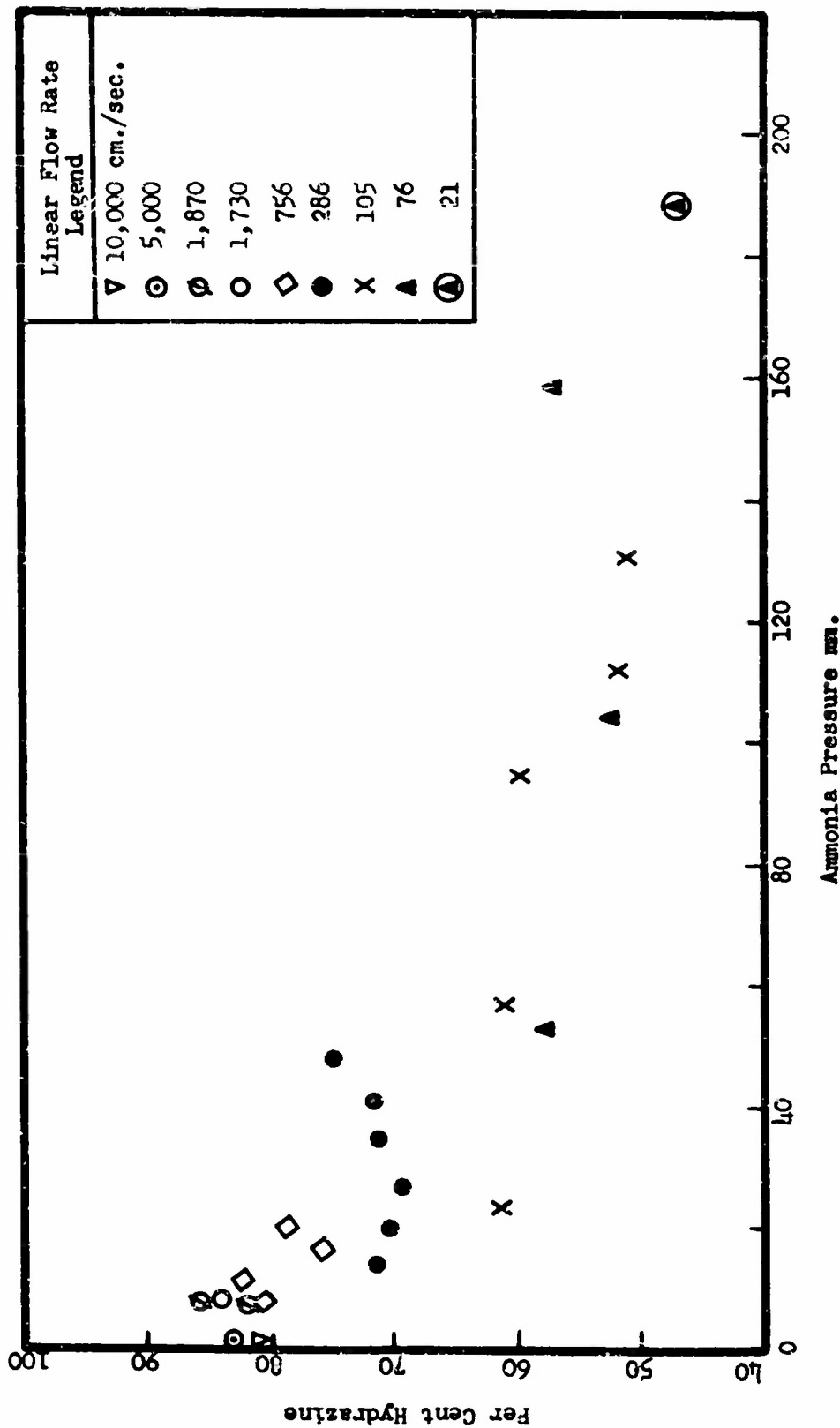
Fig. 5. The Effect of Pressure and Flow Rate on the Conversion of Ammonia to Hydrazine
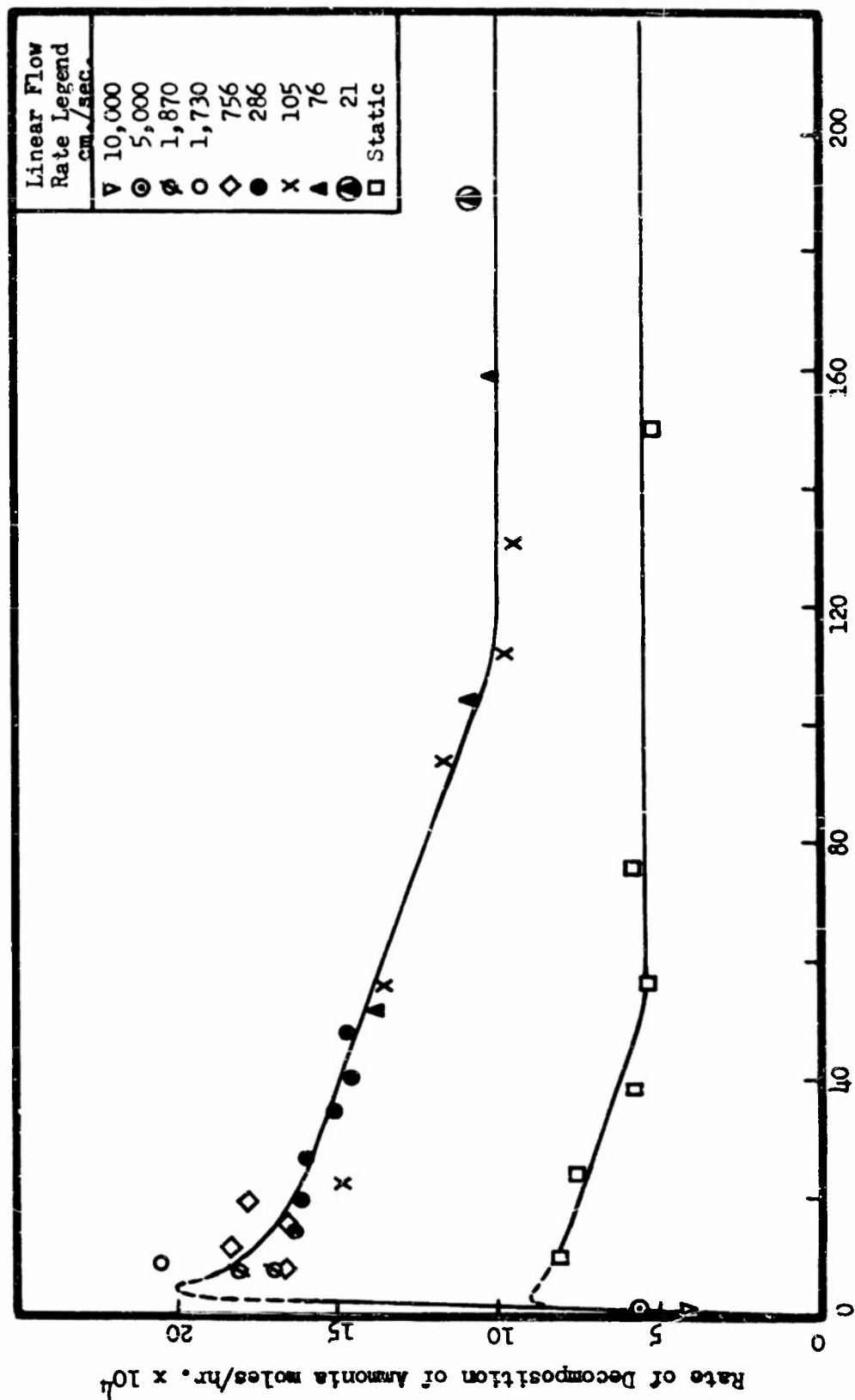
Fig. 6. The Effect of Pressure and Flow Rate on the Rate of Decomposition of Ammonia

opportunity for heterogeneous reaction.

Results from Static Experiments. The summary of the analyses of
the non-condensable products of a series of static experiments on the
photolysis of ammonia is tabulated in Table 4. The analyses of the
condensable residues of these runs indicate that hydrazine is not a
final product of the static reactions.

Table 4. Results from the Static Photolysis of Ammonia

Ammonia pressure mm.	Total gas per hour moles x 10^4	Per cent nitrogen in total gas	Ammonia decomposed per hour moles x 10^4
10	16.14	25.0	8.07
24	15.12	25.0	7.56
38	11.41	25.0	5.71
57	10.60	24.8	5.30
76	11.80	----	5.90
150	10.52	----	5.26
264	11.70	----	5.70

The fact that the nitrogen was almost exactly 25 per cent of the
total non-condensable product showed that the decomposition obeyed the
stoichiometric reaction

$$2 \, NH_3 = N_2 + 3 \, H_2 \tag{3}$$

and also showed that the gas analysis was very reliable.

The rate of ammonia decomposition was plotted as a function of
the ammonia pressure in Fig. 6. The curve obtained was approximately
parallel to the curve which was plotted from the flow experiments.
However, at comparable pressures the static rate was only about one-
half the rate of ammonia decomposition in the flow experiments.

The Photolysis of Hydrazine

When hydrazine at 14 mm. pressure was exposed to 2537 Å radiation for ninety minutes, 2.16×10^{-4} moles of nitrogen, 2.19×10^{-4} moles of hydrogen, and 4.26×10^{-4} moles of ammonia were produced and hence 4.29×10^{-4} moles of hydrazine were decomposed. The products were in exact agreement with the stoichiometric reaction

$$2 \ N_2H_4 = 2 \ NH_3 + H_2 + N_2 \qquad (17)$$
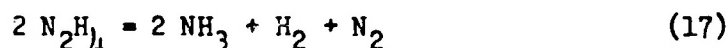
An experiment was also done in which the usual procedure was followed except that the hydrazine was not exposed to 2537 Å radiation. The fact that no products were detected in this experiment showed that all the hydrazine decomposition in the irradiated experiments was due to photolysis.

The intensity of 2537 Å radiation which was incident on the hydrazine was estimated to be about 1×10^{-4} einsteins per minute. This estimate was based on intensity measurements which were made on a similar lamp. The hydrazine decomposed at a rate of 5×10^{-6} moles per minute. If the quantum yield of the hydrazine decomposition was about two, as found by Wenner and Beckman,[44] the 2537 Å radiation was absorbed at a rate of 2.5×10^{-6} einsteins per minute. From the cell geometry, the percentage of the 2537 Å radiation that was absorbed and the pressure of the hydrazine, the extinction coefficient of hydrazine at 2537 Å was calculated, by Eq. I, to be 15 liters moles^{-1} cm.$^{-1}$

Actinometry with n-Propane

The quantum yield, Q, is defined by the equation

$$Q = M/I \qquad \qquad III$$

where M is the number of moles of chemical reaction per minute and

I is the intensity of absorbed light in einsteins per minute. The quantum yield for hydrogen formation in the mercury-photosensitized decomposition of n-propane is known to be 0.46 when the experiment is performed at room temperature with 140 mm. pressure of n-propane.[3] Thus, when the rate of hydrogen formation of this reaction had been measured in the apparatus shown in Fig. 3, the intensity of 2537 Å radiation which was incident on the gas in the system was calculated from Eq. III. The lamp intensity was calculated in this way for a number of values of the lamp current and the results are listed in Table 5.

Table 5. The Lamp Intensity at Various Lamp Currents

Lamp current milliamperes	Calculated lamp intensity einsteins/min. x 10^4
98	1.23
90	1.13
90	1.18
80	1.04
80	1.06
60	0.968
60	0.928
40	0.765
40	0.795
30	0.672
20	0.458
20	0.410
20	0.393

In most of the investigation of the mercury-photosensitized decomposition of ammonia, the lamp current was ninety milliamperes, and therefore in the calculation of the quantum yield of ammonia decomposition for these experiments the light intensity was assumed, from Table 5, to be 1.15×10^{-4} einsteins per minute. The accuracy of the calibrations of the lamp intensity was substantiated by the fact that the same results were obtained with n-propane from two different sources.

The Mercury-Photosensitized Decomposition of Ammonia

Results from Flow Experiments. The experimental observations from the investigation of the mercury-photosensitized decomposition of ammonia were treated in the same manner as has been described for the observations from the photolytic experiments. The linear flow rate of the ammonia through the irradiated zone was calculated from the mass flow rate and the ammonia pressure in this zone. The amounts of hydrogen and hydrazine produced in a run were calculated from the measured amounts of total non-condensable gas and nitrogen. The analysis for hydrazine by titration with potassium iodate was not performed in the mercury-photosensitized experiments because of the difficulty, described in Chapter II, which was encountered in recovering the hydrazine from the condensate of the reaction. The amount of ammonia decomposed and the percentage of the decomposed ammonia which was recovered as hydrazine (per cent hydrazine) was calculated for each experiment, as in the photolytic experiments, from the amounts of hydrogen and nitrogen which were produced. The quantum yield for ammonia decomposition was calculated from Eq. III by using the lamp intensity which was determined in the actinometric experiments with n-propane. All the quantum yields which were reported in this investigation were corrected for incomplete

quenching of the mercury $6(^3P_1)$ atoms as described below.

In the absence of a foreign gas, mercury atoms excited to a $6(^3P_1)$ state by 2537 Å radiation lose their excess energy by fluorescence. When a foreign gas is added, some of the $6(^3P_1)$ atoms transfer their energy to the foreign gas molecules. The extent of the quenching of the resonance radiation from the $6(^3P_1)$ atoms depends on the pressure of the foreign gas. Thus at low ammonia pressures, the excited mercury atoms do not transfer all their energy to ammonia. Incomplete quenching of the $6(^3P_1)$ atoms is equivalent to a decrease in the incident radiation intensity as far as ammonia decomposition is concerned and in the calculation of the quantum yield of ammonia decomposition this pseudo-decrease in the radiation intensity must be considered.

The Stern-Volmer equation was used to correct the quantum yields for the effect of the incomplete quenching of the excited mercury atoms by ammonia.[21] The relationship derived by Stern and Volmer is

$$K = \frac{1}{1 + TZ_k} \qquad \text{IV}$$

where K is the ratio of the intensity of resonance radiation from an irradiated cell containing mercury and a foreign gas to the intensity from the same cell from which the foreign gas has been removed. The lifetime of the excited mercury atoms is represented by T and Z_k designates the number of times per second that an excited mercury atom gives up its energy by collision to one cubic centimeter of foreign gas molecules. The number of quenching collisions, Z_k, was calculated from the kinetic theory equation[23]

$$Z_k = 2\,n\sigma_k^2\,(2\pi RT(1/M_1 + 1/M_2))^{1/2} \qquad \text{V}$$

The number of ammonia molecules per cubic centimeter, n, was calculated to be 3.19×10^{16} times the ammonia pressure in millimeters and the quenching cross-section of ammonia molecules for mercury $6(^3P_1)$ atoms, σ_k^2, was assumed to be 4.20×10^{-16} cm.^{2} [21] In Eq. V, M_1 and M_2 represent the molecular weights of mercury and ammonia; R and T represent the gas constant and the absolute temperature, respectively. When Z_k was evaluated and a value of 1.1×10^{-7} sec.[22] was used for T, Eq. IV reduced to

$$K = \frac{1}{1 + 0.295\,P} \qquad\qquad \text{VI}$$

where P represents the ammonia pressure in millimeters of mercury.

The fraction of the incident 2537 $\overset{o}{A}$ radiation which was transferred to the ammonia by the mercury $6(^3P_1)$ atoms was given by (1-K). Therefore each of the quantum yields, which were calculated assuming that all the incident radiation was transferred to the ammonia, was corrected by dividing by (1-K). The expression (1-K) was calculated for each experiment by substituting the ammonia pressure in the irradiated zone into Eq. VI to obtain K. The quenching correction was important, of course, only at low pressures. At a pressure of 10 mm. only 75 per cent of the 2537 $\overset{o}{A}$ radiation was transferred to the ammonia, as compared to the transfer of 95 per cent of the radiation at 65 mm.

Mitchell and Zemansky[21] have pointed out a number of experimental conditions wherein the assumptions made in the derivation of the Stern-Volmer relationship become invalid. Therefore, this relationship is not the most accurate equation that can be used to calculate the extent of the quenching of the mercury $6(^3P_1)$ atoms in a mercury-photosensitized reaction. However, the more accurate theoretical treatments require a more detailed control and knowledge of the absorption and collision

processes than were available in this investigation. While the accuracy of the Stern-Volmer equation is somewhat questionable, the quantum yields were certainly more accurate after they had been corrected by means of this equation.

A series of experiments was done wherein the exposure time, the total time during which ammonia flowed through the irradiated zone, varied from 15 minutes to 60 minutes. In each run the ammonia pressure was 29 mm. and the linear flow rate of ammonia through the irradiated zone was 270 cm. per second. The results obtained from this investigation are listed in Table 6.

Since neither the quantum yield nor the per cent hydrazine depended on the exposure time, the increase of the non-condensable products with time did not interfere with the reaction. Hydrogen was found to inhibit the static mercury-photosensitized decomposition of ammonia, however, and it was therefore concluded that in the flow runs the non-condensable products were swept into the large condenser flask by the ammonia stream and that they were not able to diffuse back into the reaction zone against the ammonia stream to any appreciable extent.

Since all the controlled reaction parameters were held constant in the runs reported in Table 6 except the exposure time which did not affect the reaction, the data obtained during the experiments were used to estimate the ability of the experimental procedures to give reproducible results. The average deviation from the average per cent hydrazine value was found to be 1.8 and the average deviation from the average quantum yield was 0.012. The fluctuation in room temperature during the investigation was probably the most important uncontrolled reaction parameter since the reaction system was not thermostated. The room temperature was recorded in Table 6 for each of the experiments

Table 6. The Effect of Exposure Time on the Mercury-Photosensitized
Decomposition of Flowing Ammonia

Exposure time min.	Total non-condens. gas per hour moles x 10^4	Nitrogen per hour moles x 10^4	Calculated hydrazine per hour moles x 10^4	Per cent hydrazine	Ammonia decomposed per hour moles x 10^4	Quantum yield	Room temp. °C.
15	16.41	2.08	8.09	79.6	20.34	0.330	28.8
30	15.13	1.71	8.29	82.8	20.00	.324	23.7
30	16.45	2.14	7.91	78.7	20.09	.326	27.0
30	17.75	2.49	7.80	75.8	20.58	.333	31.4
30	16.00	2.06	7.74	79.0	19.60	.317	27.5
45	15.50	1.89	7.56	80.0	18.90	.306	24.5
47	18.28	2.51	8.23	76.6	21.48	.348	31.8
60	15.11	2.04	6.95	77.3	17.98	.292	23.9
60	18.00	2.53	7.88	75.6	20.82	.338	30.5

reported there. The quantum yield appeared to increase and the per cent hydrazine to decrease as the room temperature increased.

A large part of the investigation of the mercury-photosensitized decomposition of flowing ammonia was devoted to a study of the effect on the reaction of a systematic variation of the ammonia pressure and linear flow rate in the irradiated zone. The results from this part of the investigation are compiled in Table 7. In all these runs the lamp current was ninety milliamperes and the exposure time was thirty minutes. The mercury saturator was at room temperature. In Table 7 the experiments which had the same orifice size (i.e., the same linear flow rate) are grouped together and within each group the experiments are listed in the order of increasing ammonia pressure.

The quantum yields for a representative number of the experiments reported in Table 7 are plotted as a function of the ammonia pressure in Fig. 7 and Fig. 8. The experiments in which the ammonia pressure varied from 100 to 700 mm. are plotted in Fig. 7, whereas the experiments with ammonia pressures from zero to 165 mm. are plotted in Fig. 8. Because of the limitations of the apparatus the pressure range which was investigated became narrower as the linear flow rate was increased. The legends accompanying Figs. 7 and 8 designate the linear flow rate associated with each plotted point.

The points plotted in Figs. 7 and 8 fall on a smooth curve within the experimental error, except for experiments at very high linear flow rates where the quantum yields at the highest pressures are much too low. Since more mercury was required to saturate the ammonia stream as the linear flow rate was increased, in the experiments in which the quantum yields appeared to be too low the mercury in the ammonia stream may not have been sufficient to absorb all the incident 2537 Å

Table 7. The Effect of Pressure and Linear Flow Rate on the Mercury-Photosensitized Decomposition of Flowing Ammonia

Ammonia pressure mm.	Linear flow rate cm./sec.	Total non-condens. gas per hour moles x 10^4	Nitrogen per hour moles x 10^4	Calculated hydrazine per hour moles x 10^4	Per cent hydrazine	Ammonia decomposed per hour moles x 10^4	Quantum yield
50	5.8	22.07	5.60	-0.33	0	11.20	0.174
200	5.8	16.40	4.12	0	0	8.24	.121
300	5.8	14.31	3.56	0.07	1.9	7.26	.105
400	5.8	13.10	3.27	0	0	6.54	.095
500	5.8	12.12	3.07	0	0	5.14	.089
590	5.8	11.68	3.13	-0.84	0	6.26	.091
600	5.8	11.61	2.85	0.21	6.8	6.12	.089
8	27.5	24.40	5.98	0.48	7.4	12.92	.268
23	28.0	28.28	6.59	1.92	22.6	17.02	.284
28	27.5	29.10	6.89	1.54	18.2	16.86	.274
45	27.5	25.48	6.00	1.48	19.8	14.96	.234
67	28.0	25.18	5.61	2.74	32.8	16.70	.254
78	27.5	23.68	5.52	1.60	22.5	14.24	.216
85	28.0	23.59	5.11	3.15	38.1	16.52	.250
112	28.0	21.45	4.84	2.09	30.2	13.86	.208
130	26.1	19.98	4.51	1.94	30.1	12.90	.192
139	28.0	19.92	4.47	2.04	31.4	13.02	.194
184	28.5	18.70	4.03	2.58	39.0	13.22	.195
227	27.7	18.02	3.80	2.82	42.6	13.24	.194
286	27.0	15.07	3.42	1.39	28.9	9.62	.140
303	27.3	14.89	3.14	2.33	42.6	10.94	.159
307	27.4	15.69	3.28	2.57	43.9	11.70	.170
374	27.6	13.82	3.02	1.74	36.6	9.52	.138

Table 7. (Continued)

Ammonia pressure mm.	Linear flow rate cm./sec.	Total non-condens. gas per hour moles x 10^4	Nitrogen per hour moles x 10^4	Calculated hydrazine per hour moles x 10^4	Per cent hydrazine	Ammonia decomposed per hour moles x 10^4	Quantum yield
380	27.2	12.05	2.68	1.33	33.2	8.02	0.116
466	28.1	11.43	2.63	0.91	25.8	7.08	.103
475	27.3	12.40	2.68	1.68	38.6	8.72	.126
565	27.7	9.92	2.22	1.04	32.0	6.52	.095
571	27.3	11.22	2.35	1.82	43.2	8.34	.121
664	27.6	8.08	1.81	0.84	31.7	5.30	.077
135	39.1	11.74	2.26	2.69	54.3	9.90	.147
221	47.3	13.02	2.60	2.62	50.2	10.44	.155
282	46.2	11.94	2.22	3.05	57.8	10.54	.153
339	46.4	10.64	2.16	2.02	48.3	8.36	.121
394	45.6	9.47	1.82	2.19	54.8	8.02	.116
9	114	29.87	7.18	1.12	13.6	16.60	.334
17	114	25.43	5.72	3.56	38.4	18.56	.325
26	114	24.17	4.75	5.17	52.2	19.84	.324
46	114	18.90	3.56	4.68	56.8	16.48	.255
93	113	14.28	2.45	4.48	64.7	13.86	.208
142	110	10.93	1.56	4.60	74.4	12.37	.184
165	111	10.25	1.55	4.05	72.3	11.20	.165
23	124	27.77	5.81	4.53	33.8	20.68	.345
23	124	28.58	5.74	5.62	49.5	22.72	.379
42	124	25.19	4.56	6.95	60.4	23.02	.361

Table 7. (Continued)

Ammonia pressure mm.	Linear flow rate cm./sec.	Total non-condens. gas per hour moles x 10⁴	Nitrogen per hour moles x 10⁴	Calculated hydrazine per hour moles x 10⁴	Per cent hydrazine	Ammonia decomposed per hour moles x 10⁴	Quantum yield
43	121	21.82	4.04	5.66	58.4	19.40	0.304
63	125	20.64	3.81	5.40	58.7	18.42	.283
64	122	22.09	3.75	7.09	65.3	21.68	.331
84	123	18.87	2.88	7.35	71.8	20.46	.309
85	123	17.74	2.82	6.46	69.7	18.56	.270
104	124	14.75	2.24	5.79	72.2	16.86	.241
104	126	16.41	2.51	6.37	71.8	17.76	.266
127	123	14.51	2.31	5.27	69.7	15.16	.226
145	126	14.48	2.45	4.68	65.7	14.26	.212
2	270	31.17	7.94	0	0	15.88	.620
4	280	28.50	6.31	3.26	34.0	19.14	.516
6	270	26.47	5.69	3.70	39.4	18.78	.425
10	270	23.06	4.20	5.26	60.0	20.92	.406
10	270	23.58	4.37	6.10	58.3	20.94	.406
11	280	22.40	4.41	4.76	51.9	18.34	.347
18	289	16.76	2.52	6.68	72.6	18.40	.317
28	277	14.07	1.71	7.23	80.9	17.88	.289
28	277	15.11	2.04	6.95	77.3	17.98	.293
29	267	15.13	1.71	8.29	82.8	20.00	.324
29	268	15.50	1.89	7.56	80.0	18.90	.306
29	270	16.45	2.14	7.91	78.7	20.09	.326
29	270	15.41	2.08	8.09	79.6	20.34	.330
29	270	18.00	2.53	7.88	75.6	20.82	.338
29	270	18.28	2.51	8.23	76.6	21.48	.348

Table 7. (Continued)

Ammonia pressure mm.	Linear flow rate cm./sec.	Total non-condens. gas per hour moles x 10⁴	Nitrogen per hour moles x 10⁴	Calculated hydrazine per hour moles x 10⁴	Per cent hydrazine	Ammonia decomposed per hour moles x 10⁴	Quantum yield
29	270	17.75	2.49	7.80	75.3	20.58	0.333
29	270	16.00	2.06	7.74	79.0	19.60	.318
30	270	13.88	1.48	7.96	84.4	18.88	.305
30	270	14.16	1.55	7.96	83.8	19.02	.307
30	270	11.93	1.29	6.78	84	16.14	.261
30	270	10.81	1.11	6.37	85.3	14.96	.242
37	281	11.31	1.24	6.35	83.7	15.18	.239
48	271	10.60	1.07	6.33	85.5	14.80	.231
57	275	9.74	1.00	5.73	85.2	13.47	.206
69	267	9.14	0.83	5.84	87.5	13.33	.203
2	500	28.60	6.69	1.84	21.6	17.06	.667
6	500	21.43	4.00	5.43	57.6	18.86	.428
10	520	16.70	2.58	6.40	71.3	17.95	.260
15	520	13.10	1.46	7.26	83.3	17.14	.253
20	520	10.68	0.89	7.12	88.8	16.02	.232
25	520	10.13	0.73	7.21	90.8	15.88	.262
30	520	9.27	0.62	6.81	91.8	14.85	.242
36	520	7.38	0.41	5.75	93.3	12.32	.198
8	660	15.8	2.36	6.39	73	17.50	.362
1	1000	23.00	5.71	0.16	2.7	11.74	.748
3.5	1050	13.40	3.43	4.68	57.7	16.22	.580
5	1055	14.32	2.18	5.60	72.0	15.56	.380

Table 7. (Continued)

Ammonia pressure mm.	Linear flow rate cm./sec.	Total non-condens. gas per hour moles x 10⁴	Nitrogen per hour moles x 10⁴	Calculated hydrazine per hour moles x 10⁴	Per cent hydrazine	Ammonia decomposed per hour moles x 10⁴	Quantum yield
8	986	12.22	1.40	6.64	82.7	16.07	0.333
10	1045	9.62	0.61	6.18	91.0	13.58	.197
12	1084	7.43	0.50	5.45	91.7	11.89	.222
13.5	1140	5.82	0.27	4.72	94.5	9.99	.185
17	1078	6.97	0.36	5.52	94.0	11.76	.205
2	1520	16.30	3.28	3.18	49.2	12.92	.506
2	1700	17.77	3.35	4.37	56.6	15.44	.603
5	1570	9.62	1.08	5.30	83.2	12.76	.312
6	1740	5.52	0.51	3.49	87.5	7.99	---
8	1630	6.85	0.57	4.56	88.8	10.27	.212
10	1577	5.51	0.38	4.01	91.4	8.77	.178
12	1525	6.29	0.47	4.42	90.4	9.78	.180
0.28	4090	19.80	4.92	0.12	2.4	10.08	1.9
0.87	4090	10.97	2.06	2.74	57.0	9.58	.680
1.28	4090	7.33	0.96	3.48	78.3	8.89	.483
1.82	4300	5.34	0.67	2.64	79.8	6.63	.273
2.56	4090	5.77	0.74	2.81	79.3	7.10	.245
3.21	4090	4.92	0.57	2.64	82.5	6.42	.190
3.84	4090	5.18	0.53	3.05	85	7.17	.196
4.46	4090	3.48	0.35	2.08	85.6	4.86	.124

Table 8. Results from Experiments in which the Mercury Reservoir was Heated

Ammonia pressure mm.	Linear flow rate cm./sec.	Total non-condens. gas per hour moles x 10^4	Nitrogen per hour moles x 10^4	Calculated hydrazine per hour moles x 10^4	Per cent hydrazine	Ammonia decomposed per hour moles x 10^4	Quantum yield
490	5.4	10.71	2.66	0.07	2.5	5.46	0.079
135	39	12.80	2.55	2.58	50.3	10.26	.153
480	39	11.20	2.42	1.52	38.6	7.88	.114
59	51	15.24	3.17	2.56	44.7	11.46	.176
104	51	12.93	2.44	3.16	56.4	11.20	.168
207	52	11.26	2.17	2.58	54.4	9.50	.141
320	51	10.82	2.20	2.02	48.0	8.44	.122
8.5	240	22.52	4.48	4.62	50.7	18.20	.371
12	240	21.55	4.28	4.40	50.7	17.36	.322
33	239	14.22	1.93	6.51	77.4	16.88	.270
57	234	13.32	1.78	6.20	77.8	15.96	.245
83	224	12.60	1.63	6.08	78.8	15.42	.233
4.8	1685	20.23	3.14	7.69	71	21.66	.535
8	1680	17.60	2.21	8.76	80	21.94	.452
11	1690	16.22	1.60	9.84	86	22.88	.435

radiation. A number of experiments were done at high and at low linear
flow rates in which the rate of evaporation of mercury into the ammonia
stream was increased by heating the mercury reservoir. The results
from these runs are listed in Table 8 and the quantum yields are
plotted with encircled symbols in Figs. 7 and 8. As expected, the
quantum yields from experiments at high flow rates, in which the mer-
cury saturator was heated, fell on the same curve in Fig. 8 as the
results from experiments at lower linear flow rates which were plotted
from Table 7. The quantum yields for the experiments at lower linear
flow rates, wherein the mercury saturator was heated, were about the
same as those obtained from similar experiments in which the mercury
saturator was not heated. Therefore, except at high linear flow rates
the ammonia stream contained enough mercury from the unheated mercury
saturator to completely absorb the 2537 $\overset{o}{A}$ radiation.

The results plotted in Figs. 7 and 8 indicate that, if sufficient
mercury was present in the ammonia stream to absorb all the incident
2537 $\overset{o}{A}$ radiation, the quantum yield for ammonia decomposition did not
depend on the linear flow rate of ammonia through the irradiated zone.
The quantum yield did depend, however, on the ammonia pressure in the
irradiated zone. From 700 to 300 mm. ammonia pressure, the quantum
yield was 0.10 $\pm$ 0.05. As the pressure was decreased, the quantum
yield increased slowly to a value of 0.30 $\pm$ 0.05 at 30 mm. At still
lower pressures, the value of the quantum yield increased rapidly
towards one; but in this pressure region the absolute values of the
quantum yields were uncertain because of the large quenching correction
from the Stern-Volmer equation.

Representative data from the values of the per cent hydrazine in
the experiments reported in Tables 7 and 8 are plotted in Figs. 9 and
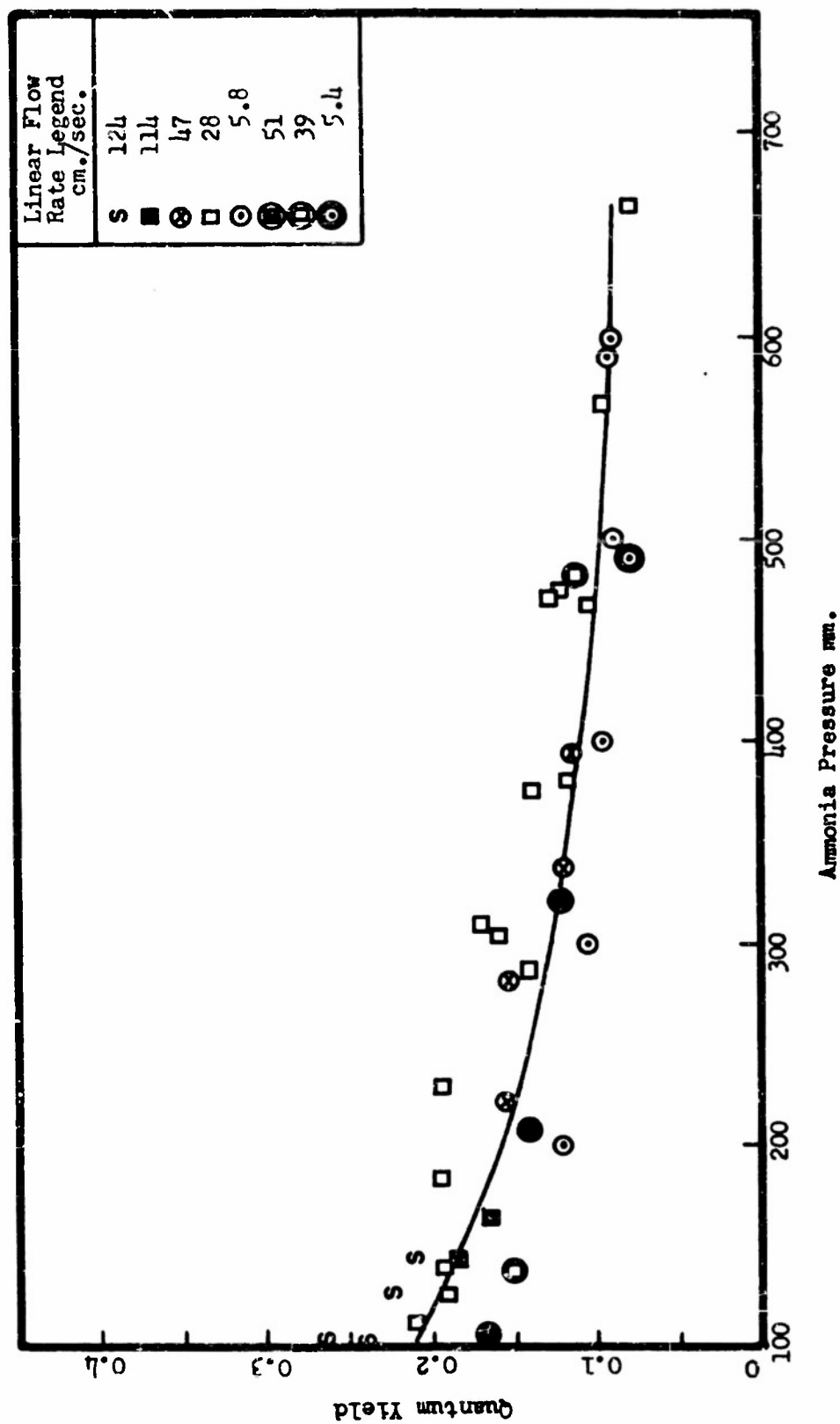
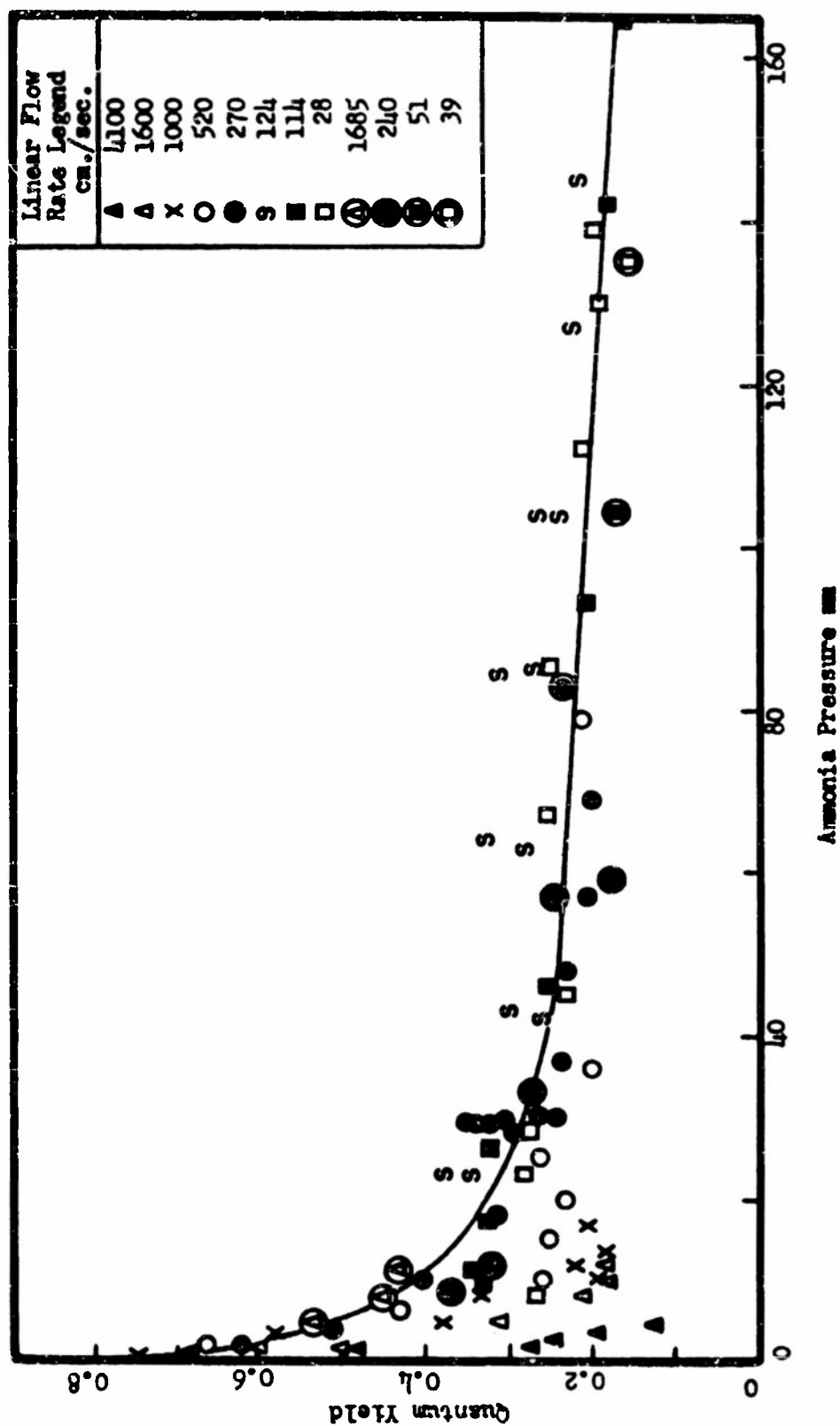Fig. 7. The Effect of Pressure and Flow Rate on the Quantum Yield

Fig. 8. The Effect of Pressure and Flow Rate on the Quantum Yield
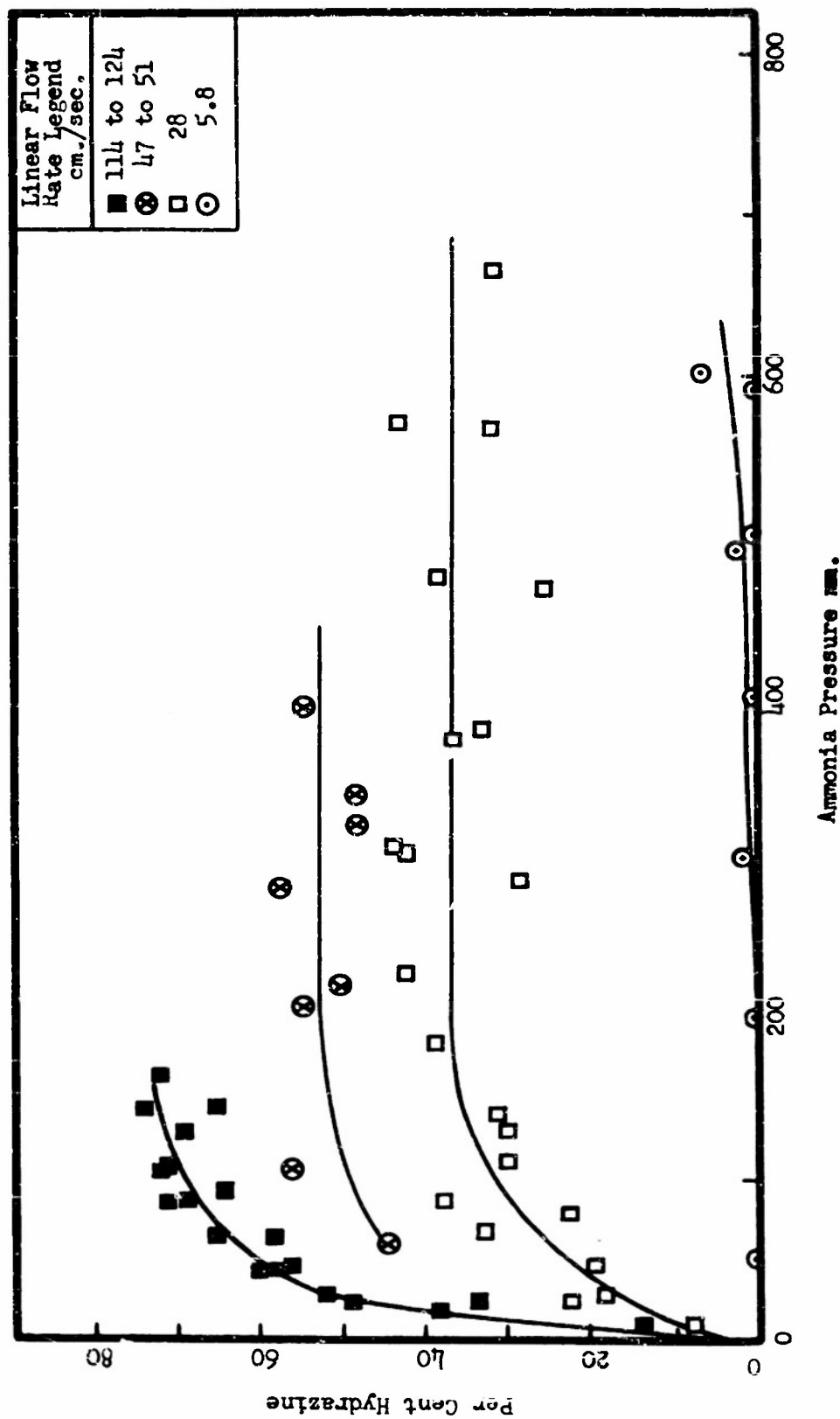
Fig. 9. The Effect of Pressure and Flow Rate on the Per Cent Hydrazine
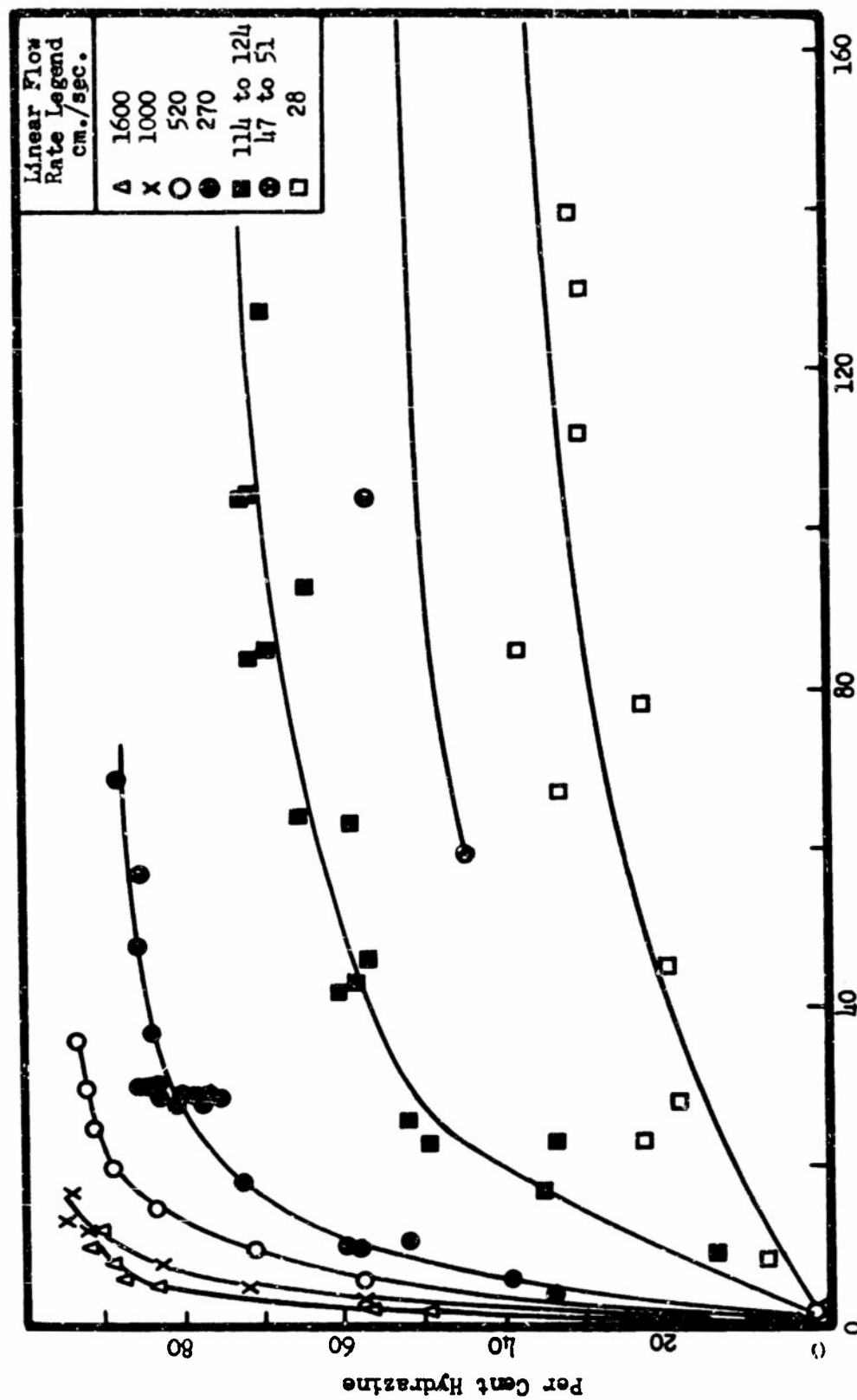
Fig. 10. The Effect of Pressure and Flow Rate on the Per Cent Hydrazine

10. The data plotted in Fig. 9 were restricted to the experiments in which the linear flow rate was 124 cm. per second or less but in which the ammonia pressure varied from zero to about 700 mm. The per cent hydrazine values for experiments in which the ammonia pressure was from zero to 150 mm. are plotted in Fig. 10; in these experiments the linear flow rates varied over the whole range which was studied. The linear flow rates associated with the points in Figs. 9 and 10 are designated by the legends which accompany these figures. Since the per cent hydrazine obtained in an experiment did not change if the mercury vapor pressure was increased by heating the mercury saturator, data from Table 8 were given no special designation when they were plotted in Figs. 9 and 10.

The curves which were obtained from the data plotted in Figs. 9 and 10 show that the per cent hydrazine in the nitrogen-containing products of the ammonia decomposition increased from zero at the lowest linear flow rate (5 cm. per second) to about 95 per cent at very high flow rates. At any particular linear flow rate, the per cent hydrazine also depended on the ammonia pressure. At all linear flow rates, the per cent hydrazine fell to zero at low pressures. At low flow rates the conversion to hydrazine increased slowly with pressure and became pressure independent between 50 and 100 mm. As the linear flow rates became greater the per cent hydrazine increased more rapidly with pressure and appeared to become pressure independent at lower pressures. At very high flow rates, the pressure ranges which were studied did not extend to the pressures at which the per cent hydrazine became pressure independent.

The results from the experiments on the mercury-photosensitized decomposition of ammonia in which the light intensity was varied are

tabulated in Table 9. In all these experiments the ammonia pressure was 29 mm. and the linear flow rate was 270 cm. per second. The light intensities at various lamp currents were determined in the actino-metric experiments with n-propane. The values of the per cent hydra-zine and the quantum yields determined from these experiments are plotted as a function of the light intensity in Figs. 11 and 12, respectively. The per cent hydrazine increased linearly as the light intensity was decreased, and an extrapolation of a straight line through the points plotted in Fig. 11 indicates that the conversion to hydrazine approached one hundred per cent as the light intensity approached zero. The data plotted in Fig. 12 show that the quantum yield for ammonia decomposition increased as the light intensity was increased.

The ammonia pressure, linear flow rate, per cent hydrazine, and quantum yield for experiments in which the ammonia was heated before it passed into the irradiated zone are listed in Table 10. The results for analogous runs in which the ammonia was at room temperature are also given in this table. This part of the investigation was limited to two runs, since the apparatus was not suited for controlling the temperature of the ammonia stream in a systematic manner. The irrad-iated zone could not be heated without changing the lamp intensity. Hence when the hot ammonia stream which was saturated with mercury vapor entered the cool irradiated zone, mercury condensed on the quartz tubing and probably decreased the intensity of 2537 $\overset{o}{A}$ radiation which was incident on the stream of reactants. In general, however, the quantum yield appeared to be higher when the ammonia was heated. If the incident light intensity was decreased in the manner described above, the quantum yields for the experiments in which the ammonia was

Table 9. The Effect of Light Intensity on the Mercury-Photosensitized Decomposition of Flowing Ammonia

Lamp intensity ein./min. x 10⁴	Total non-condens. gas per hour moles x 10⁴	Nitrogen per hour moles x 10⁴	Calculated hydrazine per hour moles x 10⁴	Per cent hydrazine	Ammonia decomposed per hour moles x 10⁴	Quantum yield
1.15	15.13	1.71	8.29	82.8	20.00	0.324
1.15	15.11	2.04	6.95	77.3	17.98	.292
1.15	15.50	1.89	7.56	80.0	18.90	.306
1.15	16.45	2.14	7.91	78.7	20.09	.326
1.15	16.41	2.08	8.09	79.6	20.34	.330
1.15	18.00	2.53	7.88	75.6	20.82	.337
1.15	18.28	2.51	8.23	76.6	21.48	.349
1.15	17.75	2.49	7.80	75.8	20.58	.333
1.15	16.00	2.06	7.74	79.0	19.60	.317
1.08	15.50	1.99	7.52	79.1	19.02	.328
0.95	11.69	1.51	5.65	78.9	14.32	.282
0.95	12.78	1.42	7.12	83.5	17.07	.333
0.78	7.25	0.70	4.40	85	10.25	.240
0.78	7.97	0.87	4.50	83.8	10.74	.257
0.78	8.44	0.90	4.86	84.4	11.51	.273
0.65	5.76	0.50	3.76	88.3	8.52	.244
0.43	2.90	0.20	2.15	90	4.70	.20
0.43	3.20	0.21	2.35	91.6	5.13	.218
0.43	3.68	0.26	2.63	90.8	5.79	.246
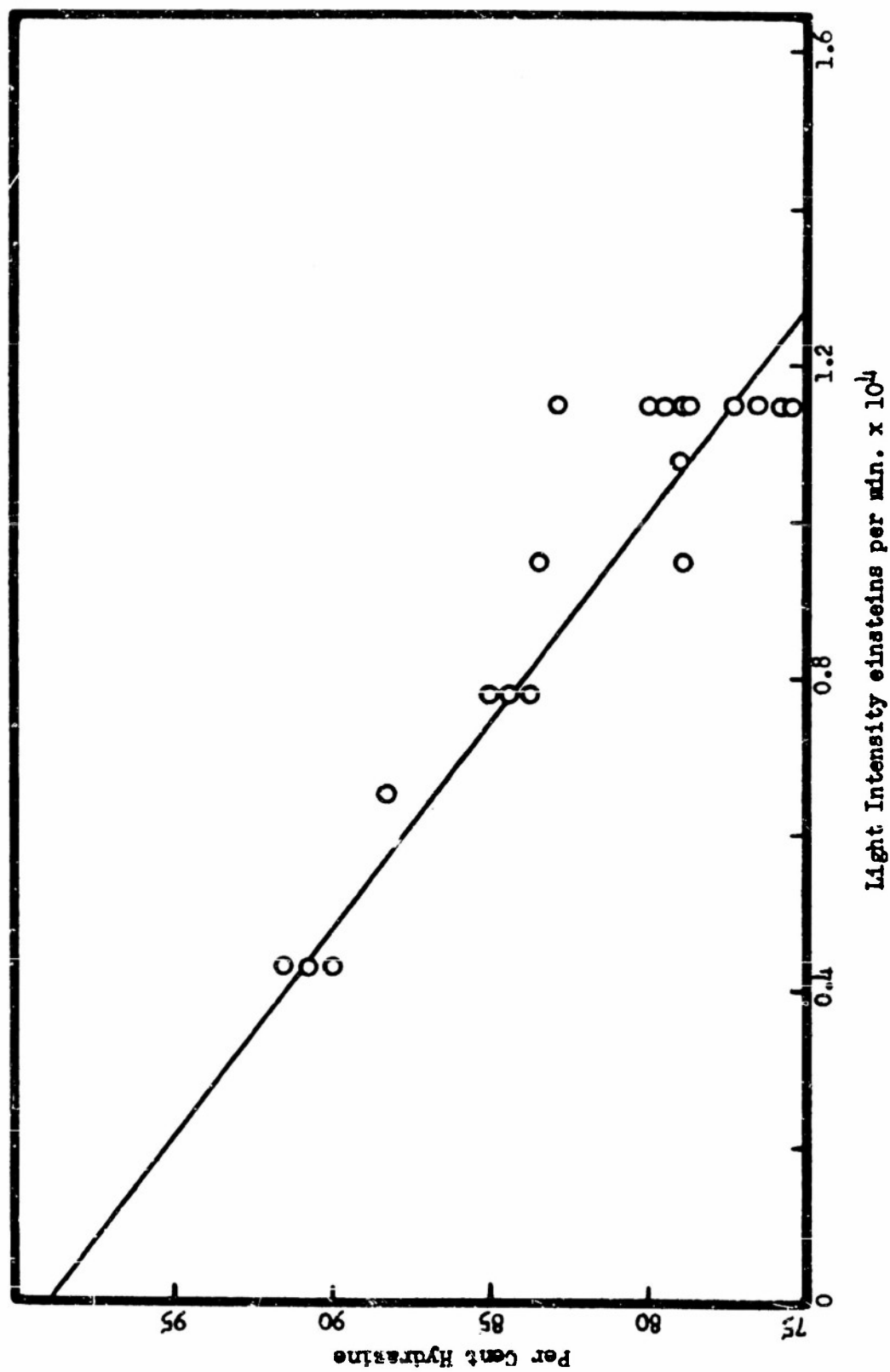
Fig. 11. The Effect of Light Intensity on the Per Cent Hydrazine
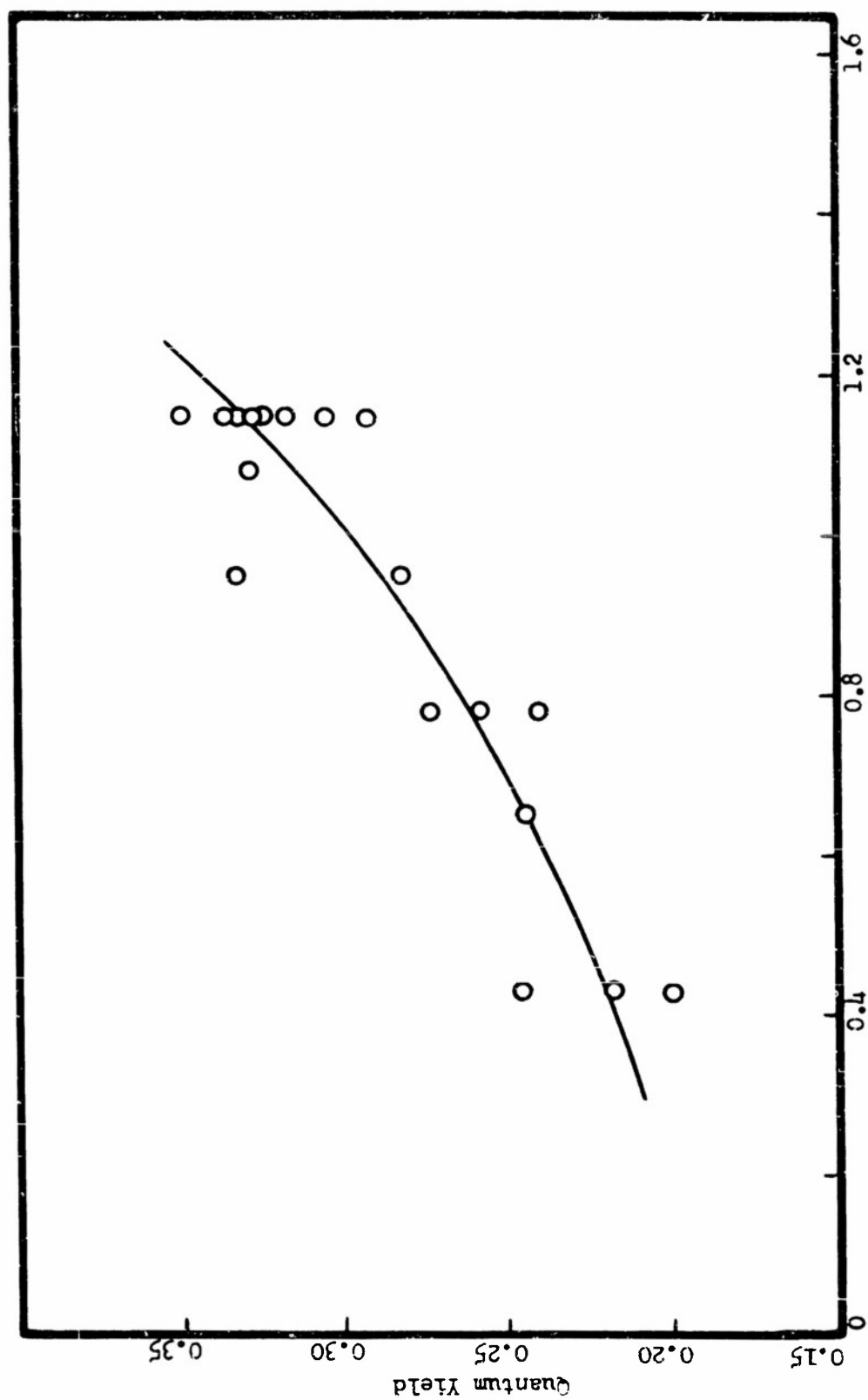
Fig. 12. The Effect of Light Intensity on the Quantum Yield

Table 10. The Effect of Heating the Ammonia Stream

Reaction conditions	Ammonia pressure mm.	Linear flow rate cm./sec.	Per cent hydrazine	Quantum yield
Ammonia at room temp.	135 135	39 39	54.3 50.3	0.147 .153
Ammonia heated	135	39	49.3	.211
Ammonia at room temp.	490	5.4	2.5	.079
Ammonia heated	500	5.4	18.0	.128

heated were even higher than the values reported in Table 10. The per cent hydrazine in the experiment at a linear flow rate of 39 cm. per second was not changed when the ammonia was heated. The change in the conversion to hydrazine which was observed at a flow rate of 5.4 cm. per second, with the ammonia heated, was considered to be within the experimental error which was quite large at very low linear flow rates (as can be seen in the fluctuation of the results plotted in Fig. 10 for the experiments with a linear flow rate of 28 cm. per second).

The per cent hydrazine values and the quantum yields for the experiments in which ethylene was added to the ammonia stream are listed in Table 11. Comparable data from experiments not containing ethylene are also given. The average mass flow rate of ethylene through the system was calculated from the pressure decrease in the ethylene reservoir during a run. By assuming that the linear flow rate of the ethylene was the same as the ammonia linear flow rate,

an approximate value was calculated for the ethylene pressure in each experiment. In the calculation of the quantum yields for the experiments which contained ethylene the usual correction for incomplete quenching was made using the Stern-Volmer relationship and a further correction was made for the competitive quenching of the ethylene. Using Eq. V and values of 48×10^{-16} and 4.20×10^{-16} cm^2 for the quenching cross-sections of ethylene and ammonia,[21,30] the quenching efficiency of ethylene was found to be 9.5 times as great as that of ammonia. To correct the incident light intensity for incomplete quenching, the Stern-Volmer relationship was applied to the pressure of ammonia plus 9.5 times the pressure of ethylene. The incident light that was available to ammonia through collision with $6(^3P_1)$ atoms is given by

$$I = I_{sv}(P_a/(P_a + 9.5P_e)) \qquad VII$$

where I_{sv} is the effective incident intensity calculated from the Stern-Volmer equation, P_a and P_e are the pressures of ammonia and ethylene in millimeters. The per cent hydrazine values in Table 11 were calculated in the usual way from the amounts of hydrazine and nitrogen produced in the experiments. Since the hydrazine was determined by titration, the per cent hydrazine values probably should have been somewhat greater than those reported in Table 11.

At high pressures and low linear flow rates, the per cent hydrazine was greatly increased as the partial pressure of ethylene was increased in the ammonia stream. Also, at high flow rates and low pressures, the per cent hydrazine was increased in proportion to the partial pressure of ethylene. The quantum yield of ammonia decomposition was decreased in the experiments which contained ethylene. This decrease in the quantum yield was partly due to the incomplete recovery

Table 11. Results from Adding Ethylene to the Mercury-Photosensitized Decomposition of Flowing Ammonia

Ammonia pressure	Linear flow rate	Ethylene pressure	Quantum yield	Per cent hydrazine	Per cent hydrazine without C_2H_4	Quantum yield without C_2H_4
mm.	cm./sec.	mm.				
360	16.2	7.9	0.068	93.3	30	0.12
356	16.2	3.1	.075	90.0	30	.12
215	13.6	3 to 4	.103	74	30	.15
330	16.2	2	.095	69.5	30	.12
340	16.2	0.61	.051	76.5	30	.12
23	231	0.69	.055	82.6	72	.30
9	277	0.43	.034	85.1	50	.38
9	277	0.065	.033	79	50	.36
9	277	0.012	.077	67	50	.38

of hydrazine since the hydrazine was determined by the titration analysis.

In experiments with large ammonia pressures where the ethylene did very little quenching of the excited mercury atoms, the amount of hydrogen produced was much less than that to be expected from the amounts of hydrazine and nitrogen which were obtained. The hydrogen, therefore, must have been removed by reaction with ethylene. At low ammonia pressures in experiments in which ethylene quenched a considerable fraction of the mercury $6(^3P_1)$ atoms, much more hydrogen was obtained than was to be expected from the amounts of the hydrazine and nitrogen products. This excess hydrogen was probably a product of the mercury-photosensitized decomposition of ethylene.[34]

The quantitative analysis of the products of the experiments, in which ethylene was added to the ammonia stream, by examination of their infrared spectra was not very satisfactory. The samples always contained ammonia which absorbed infrared radiation in the same regions of the infrared spectrum that were examined for absorption by products such as hydrazine or amines. However, the infrared spectra of the products from experiments which had relatively high ethylene pressures contained absorption peaks in the wave number regions from 2900 to 3150 cm.$^{-1}$, from 1800 to 1950 cm.$^{-1}$, from 1390 to 1485 cm.$^{-1}$, and from 850 to 1050 cm.$^{-1}$ These areas of infrared absorption were found to be characteristic of polyvinyl structures.[5] The infrared spectra of the products of other experiments in which the ethylene pressure was lower showed absorption in the wave number regions from 2800 to 3000 cm.$^{-1}$, from 1350 to 1500 cm.$^{-1}$, and from 700 to 850 cm.$^{-1}$ which was distinct from the absorption of the ammonia in the same sample and was very similar to the absorption spectra of a sample of methylamine. These absorption

peaks were therefore attributed to ethylamine. No evidence for hydrazine was obtained from the infrared spectra but this was not surprising since the ammonia and hydrazine spectra are very similar.

The quantum yields which are reported in Table 11 were calculated from the amounts of hydrazine and nitrogen produced in the reactions. If ethylamine is a product of the mercury-photosensitized decomposition of ammonia in the presence of ethylene, the true quantum yields were larger than the reported values because of the contribution from ethylamine which was not quantitatively analysed.

A series of twenty-three experiments were performed at various ammonia pressures and linear flow rates in which the irradiated zone was packed with fifty feet of platinum wire. The surface area of this wire was calculated to be 7.17 $in.^2$ The per cent hydrazine values and quantum yields were averaged for experiments with the same pressure and linear flow rate and the results were listed in Table 12 with comparable data from experiments which did not contain platinum wire. In general the reaction was unchanged by the addition of the platinum wire although a small increase was noted in the per cent hydrazine at a flow rate of 270 cm. per second and at low ammonia pressures. In some of the experiments, the platinum wire was cleaned before the run was started by heating it until it glowed, but this procedure did not change the results of the experiments.

Results from Static Experiments. The results of the static experiments on the mercury-photosensitized decomposition of ammonia at various pressures and exposure times are compiled in Table 13. The lamp current was ninety milliamperes in these experiments. The amount of the nitrogen product was measured in most of the experiments and was found to be 25 ± 2 per cent of the total non-condensable gas.

Table 12. Results from Experiments Containing Platinum Wire

Ammonia pressure mm.	Linear flow rate cm./sec.	Per cent hydrazine	Quantum yield	Per cent hydrazine without platinum wire	Quantum yield without platinum wire
143	23	30.3	0.146	32	0.17
465	23	37.6	.084	40	.11
31	100	49.2	.217	51	.26
51	100	63.9	.234	61	.24
160	100	74	.162	75	.17
3.5	270	34.0	.587	30	.55
10	270	67.4	.416	61.2	.413
29	270	83.2	.323	80.3	.310
48	270	86.8	.281	84	.26

Thus, the static decomposition obeyed the stoichiometric reaction

$$2\ NH_3 = N_2 + 3H_2 \tag{3}$$

Moreover, no hydrazine was detected when the condensable residues from the experiments were titrated with potassium iodate. The amount of ammonia decomposed in an experiment was assumed from reaction (3) to be one-half of the non-condensable gas produced. The hydrogen pressure in the reaction zone at the end of an experiment was calculated from the amount of hydrogen produced (three-quarters of the non-condensable gas) and the volume of the reaction system.

The quantum yields reported in Table 13 (also in Tables 14 and 15) were corrected for incomplete quenching by the Stern-Volmer equation and for the competitive quenching of the hydrogen produced in the experiments by the same method by which the quantum yields for the flow experiments containing ethylene were corrected for the quenching of ethylene. By using quenching cross-sections of 8.60×10^{-16} cm^2 and 4.20×10^{-16} cm^2 for hydrogen and ammonia in Eq. V, the quenching efficiency of hydrogen was found to be 5.75 times greater than that of ammonia. The average hydrogen pressure in an experiment was assumed to be two-thirds of the final hydrogen pressure. Thus, by the same reasoning used in deriving Eq. VII, the incident light intensity used to calculate the quantum yield of ammonia decomposition is given by

$$I = I_{sv}(P_a/(P_a + 5.75P_h)) \tag{VIII}$$

where I_{sv} is the incident intensity corrected for incomplete quenching and P_a and P_h represent the ammonia pressure and two-thirds of the final hydrogen pressure in millimeters, respectively. The light intensity transferred to ammonia and hydrogen by excited mercury atoms is

given for each experiment in Table 13.

The quantum yields reported in Table 13 are plotted as a function of ammonia pressure in Fig. 13. Curves which were drawn through the points for experiments which had the same exposure time indicate that the quantum yield was pressure independent above about 150 mm. but decreased as the pressure was decreased below 150 mm. At a given ammonia pressure, the quantum yield increased as the exposure time was decreased until, in an experiment of thirty seconds' duration at 505 mm. ammonia pressure, the quantum yield (0.104) was as great as that obtained in the flow experiments at the same pressure.

Since it was suspected that the rate of ammonia decomposition was inhibited when the exposure time was increased by the build-up of the hydrogen concentration, a series of experiments were performed in which hydrogen was added to the ammonia before the reaction was started. The results from these experiments are listed in Table 14. The amount of ammonia decomposed in a run was calculated from the amount of nitrogen produced by assuming the stoichiometry of reaction (3). The quantum yield for ammonia decomposition was observed to decrease as the hydrogen concentration in the reaction was increased.

Finally, a series of experiments were performed in which the lamp intensity was varied. In these experiments the ammonia pressure was about 200 mm. and the exposure time was 45 minutes. The results of these experiments are listed in Table 15. It was observed that the quantum yield was not dependent on the light intensity and hence on the amount of reaction per unit of time. The ratio of hydrogen quenching to ammonia quenching was almost constant in these experiments.

Table 13. Results of the Static Mercury-Photosensitized Decomposition of Ammonia

Exposure time min.	Ammonia pressure mm.	Final hydrogen pressure mm.	Total non-condens. gas per hour moles x 10^4	Per cent nitrogen in non-condens. gas	Quantum yield	Hydrogen light intensity ein./min.x10^4	Ammonia light intensity ein./min.x10^4
45	11.5	1.84	1.23	---	0.017	0.37	0.60
45	12.5	2.11	1.42	---	.020	.39	.60
45	23	2.65	1.75	26.3	.020	.32	.72
47	25	3.61	2.44	26.3	.023	.23	.87
45	46	3.33	2.20	25.7	.022	.24	.85
45	53	3.61	2.44	26.3	.023	.23	.87
45	75	3.92	2.65	25.7	.024	.19	.92
45	103	4.45	3.00	25.3	.026	.16	.96
45	104	4.68	3.16	24.2	.027	.16	.96
45	210	4.94	3.35	23.7	.027	.09	1.04
46	212	5.55	3.64	25.6	.029	.10	1.03
45	287	5.21	3.55	26.6	.028	.07	1.07
45	300	5.14	3.45	22.8	.027	.08	1.06
45	387	5.82	3.91	---	.030	.06	1.08
46	400	5.47	3.64	24.3	.028	.06	1.08
45	500	5.98	4.06	24.3	.031	.05	1.10
46	505	5.62	3.70	28	.028	.05	1.10
45	592	5.93	3.97	25.2	.030	.04	1.11
5	25.5	0.72	4.28	---	.039	.10	0.93
5	52	1.04	6.18	---	.051	.07	1.01
5	81	1.17	7.00	23.3	.056	.06	1.05

Table 13. (Continued)

Exposure time min.	Ammonia pressure mm.	Final hydrogen pressure mm.	Total non-condens. gas per hour moles x 10^4	Per cent nitrogen in non-condens. gas	Quantum yield	Hydrogen light intensity ein./min. x10^4	Ammonia light intensity ein./min. x10^4
5.5	109	1.38	7.48	23.3	0.059	0.05	1.07
5	158	1.36	8.28	24.8	.063	.04	1.09
6	158	1.63	8.08	---	.062	.04	1.09
5	158	1.44	8.60	---	.066	.04	1.09
5	307	1.53	9.16	25.0	.068	.02	1.12
5	381	1.58	9.40	---	.070	.02	1.12
5	505	1.57	9.38	---	.069	.01	1.14
5	660	1.67	9.97	---	.073	.01	1.14
2	25	0.42	6.45	---	.056	.06	0.96
2	49	.54	8.25	---	.066	.04	1.04
2	76	.60	9.15	---	.071	.03	1.07
2	116	.66	10.15	24.6	.077	.03	1.09
2	156	.70	10.58	---	.079	.02	1.11
2	200	.87	13.19	23.2	.099	.02	1.11
2	307	.79	11.95	24.1	.088	.01	1.13
2	380	.89	13.20	---	.097	.01	1.13
2	380	.80	11.92	---	.088	.01	1.13
2	505	.83	12.60	24	.092	.01	1.14
2	660	.86	12.90	24.5	.094	.005	1.145
1	505	.46	13.75	23.8	.100	0	1.15
0.5	505	.24	14.31	---	.104	0	1.15

Table 14. The Static Mercury-Photosensitized Decomposition
of Ammonia with Added Hydrogen

Ammonia pressure mm.	Initial hydrogen pressure mm.	Final hydrogen pressure mm.	Nitrogen per hour moles x 10⁴	Quantum yield	Hydrogen light intensity ein./min.x10⁴	Ammonia light intensity ein./min.x10⁴
206	0	5.24	3.40	0.028	0.10	1.03
205	2.5	5.38	2.50	.021	.12	1.01
210	6.5	8.27	1.53	.0137	.20	0.93
204	13	14.08	0.868	.0089	.32	0.82
200	20	26.63	0.406	.0047	.42	0.72
50	22	22.12	0.085	.0022	.81	0.32
193	27	27.39	0.262	.0035	.51	0.63

Table 15. The Effect of Varying the Light Intensity on the Static Mercury-Photosensitized Decomposition of Ammonia

Ammonia pressure mm.	Final hydrogen pressure mm.	Light intensity ein./min.x10^4	Total non-condens. gas per hour moles x 10^4	Quantum yield	Hydrogen light intensity ein./min.x10^4	Ammonia light intensity ein./min.x10^4
206	5.24	1.13	3.40	0.028	0.10	1.03
200	3.88	0.94	3.34	.032	.07	0.87
200	4.05	0.77	2.04	.024	.06	0.71
204	3.32	0.77	2.25	.026	.05	0.72
205	2.30	0.42	1.49	.031	.02	0.40
200	2.17	0.42	1.38	.029	.02	0.40
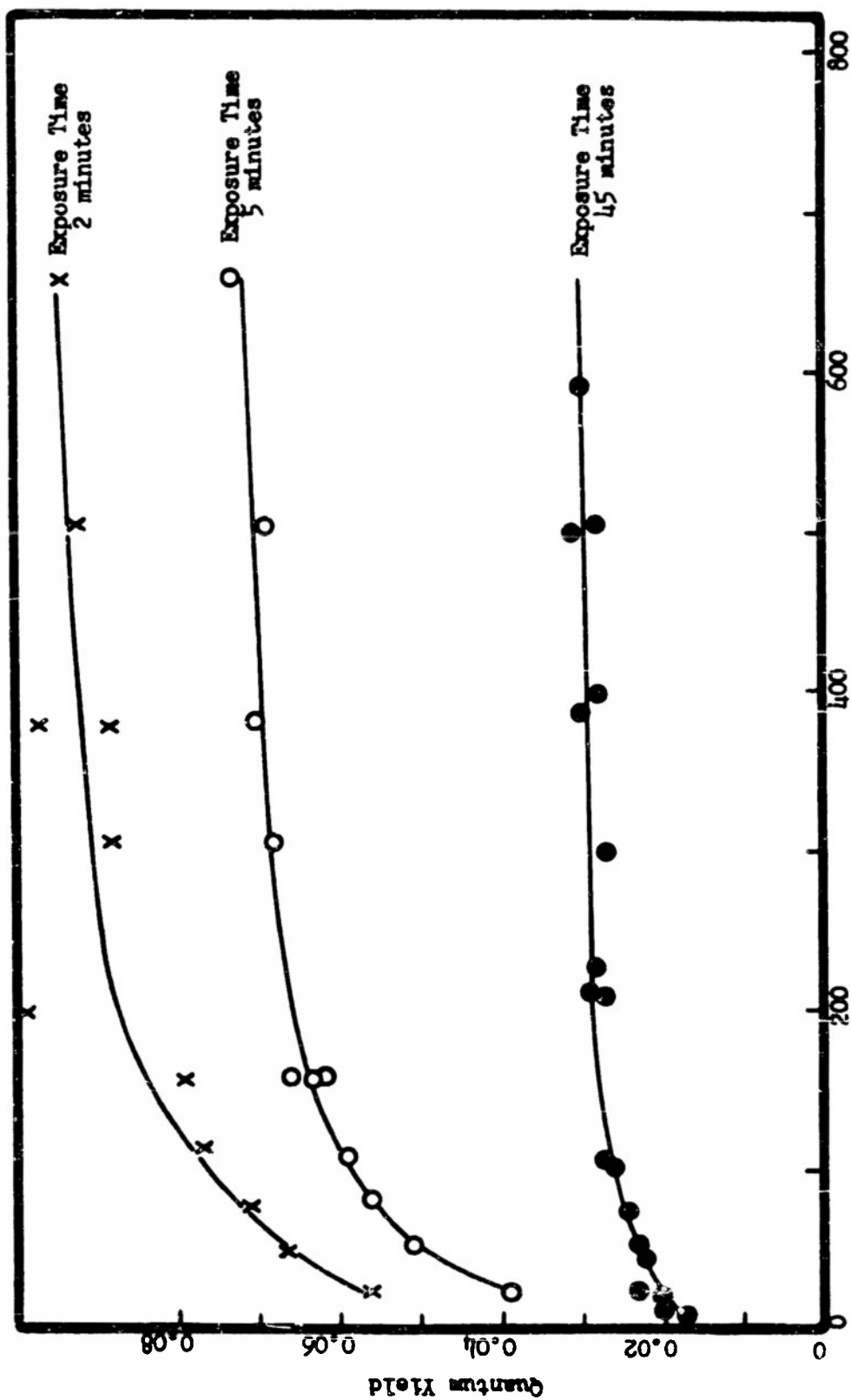
Fig. 13. The Effect of Pressure and Exposure Time on the Quantum Yield

CHAPTER IV

DISCUSSION

Any interpretation of the mechanism of the photodecomposition of ammonia as performed in this research must take cognizance of the experimental results summarized below:

1. The products of the photolysis of flowing ammonia were nitrogen, hydrogen, and hydrazine. The percentage of the hydrazine in the nitrogen-bearing products was independent of the reaction pressure but increased as the linear flow rate of ammonia through the irradiated zone was increased. The rate of decomposition of ammonia did not depend on the ammonia linear flow rate and had a value of $1.0 \times 10^{-3} \pm 0.1 \times 10^{-3}$ moles per hour at ammonia pressures between 100 and 560 mm. At lower pressures the rate of ammonia decomposition increased until at 10 mm. the value of the rate was 2.0×10^{-3} moles per hour.

2. The products of the static photolysis of ammonia were hydrogen and nitrogen. The rate of decomposition of ammonia was $0.5 \times 10^{-3} \pm 0.1 \times 10^{-3}$ moles per hour at ammonia pressures from 40 to 270 mm. The rate increased at lower ammonia pressures until the value at 10 mm. was 0.9×10^{-3} moles per hour.

3. The products of the mercury-photosensitized decomposition of flowing ammonia were nitrogen, hydrogen, and hydrazine. Neither the ratio of these products nor the rate of the reaction depended on the exposure time. The quantum yield of ammonia decomposition did not depend on the linear flow rate of ammonia through the irradiated zone. It increased slowly, as the ammonia pressure was decreased, from a value of 0.09 at 650 mm. to a value of 0.20 at 100 mm. At lower ammonia pressures, the quantum yield increased more rapidly until at a pressure

94

of about one mm. the value of the quantum yield approached unity. The percentage of the decomposed ammonia which was recovered as hydrazine increased when the ammonia linear flow rate was increased. At any particular linear flow rate, the per cent hydrazine approached zero as the ammonia pressure approached zero. As the ammonia pressure was increased, the per cent hydrazine increased and then became independent of the pressure. At low linear flow rates the per cent hydrazine became independent of the pressure at about 100 mm. but as the linear flow rate was increased the per cent hydrazine increased more rapidly with ammonia pressure and became constant at lower ammonia pressures. The per cent hydrazine increased linearly toward one hundred per cent and the quantum yield decreased exponentially as the light intensity was decreased. The addition of ethylene to the reaction caused a large increase in the hydrazine-to-nitrogen ratio both at high flow rates and low ammonia pressures and at low flow rates and high ammonia pressures. Part of the hydrogen from the decomposed ammonia disappeared by reaction with the ethylene, and infrared analyses of the ammonia decomposition products indicated that ethylamine was formed. The addition of 7.17 in.^{2} of platinum surface to the irradiated zone had no effect on the ammonia decomposition. The quantum yield for ammonia decomposition appeared to increase slightly when the ammonia was heated before it passed into the irradiated zone.

4. The products of the static mercury-photosensitized decomposition of ammonia were nitrogen and hydrogen. When the exposure time was very short, the quantum yield for ammonia decomposition at high pressures was about the same as the quantum yield in the flow experiments at the same pressures. The quantum yield decreased rapidly when the exposure time was increased. At high ammonia pressures the quantum yield was almost

constant but it increased rapidly when the ammonia pressure was decreased below 150 mm. The quantum yield also decreased when hydrogen was added to the ammonia. At an ammonia pressure of 200 mm., the quantum yield did not depend on the intensity of the incident radiation.

The similarity of most of the features of the photolysis of ammonia to the features of the mercury-photosensitized decomposition of ammonia indicates that the primary dissociation of ammonia into radicals and the secondary reactions of these radicals are the same in both modes of reaction. In the discussion to follow, therefore, the general term "ammonia decomposition" is used to designate decomposition of ammonia initiated either by 1849 $\overset{o}{A}$ radiation or by collision with mercury $6(^3P_1)$ atoms.

Several investigators[32,42,46] found that the quantum yield was about 0.25 for the static photolysis of ammonia at about 150 mm. ammonia pressure. If this value was assumed for the static photolytic experiments of this investigation, the quantum yield for the flow photolytic experiments approached one at low ammonia pressures.

Ample evidence from other investigations[14,26,37] was presented in the Introduction to show that the primary dissociation of ammonia produced amino radicals and hydrogen atoms. This mode for the primary dissociation was in no way contradicted by the results of this investigation. In the mercury-photosensitized decomposition of flowing ammonia and probably also in the photolysis of flowing ammonia, the quantum yield for ammonia decomposition approached one at low ammonia pressures. The quantum yield for the primary dissociation of ammonia must therefore have been unity. Ammonia regeneration must have occurred, therefore, in the secondary reactions to account for the low quantum yield at high ammonia pressures.

The pressure dependence of the quantum yield might also have been interpreted by an "excited molecule" mechanism. The primary process would then have been described by the following elementary reactions:

$$NH_3 + h\nu_{1849} \longrightarrow NH_3^* \tag{18}$$

$$\text{or } NH_3 + Hg\ 6(^3P_1) \longrightarrow NH_3^* + Hg\ 6(^1S_0) \tag{19}$$

$$NH_3^* + NH_3 \longrightarrow 2NH_3 \tag{20}$$

$$NH_3^* \longrightarrow NH_2 + H \tag{21}$$

In these equations, NH_3^* represents an ammonia molecule containing enough energy to permit it to dissociate. If the excited ammonia molecule could not lose its excess energy by fluorescing, it might have transferred the excess energy to another ammonia molecule by collision as represented in reaction (21), a fraction of the energy being transferred at each collision (thermal degradation). If the excited molecule failed to lose its excess energy in a specific time interval (the average lifetime), it would have dissociated in accordance with reaction (21). Since reaction (21) would be favored at low pressures while reaction (20) would be favored at high pressures, the quantum yield would have decreased from unity as the ammonia pressure was increased. However, a careful investigation by Bonhoeffer,[2] which is reviewed in the Introduction, indicated that if an excited molecule was formed, its lifetime was so short that its only fate was to dissociate. Moreover, if the excited molecule mechanism was operative, the quantum yield should decrease asymptotically to zero at high pressures. In our investigation the quantum yield became almost pressure independent at high pressures but it still had a value greater than zero. One must conclude

therefore that the primary process did not involve an excited ammonia molecule and that the initial reaction of the decomposition was a direct dissociation of ammonia into hydrogen atoms and amino radicals with a quantum yield of unity.

A primary quantum yield of unity requires that ammonia should be one of the reaction products, since in most of the experiments the overall quantum yield for ammonia decomposition was much less than unity. The experimental analyses showed that nitrogen and hydrazine were the other nitrogen-bearing products. Other investigators[19,20,24,27,45] have suggested that ammonia was reformed in the reaction either by the decomposition of part of the hydrazine which was produced or by the recombination of hydrogen atoms and amino radicals. Considerable evidence has been advanced in favor of both mechanisms. In the flow experiments of this investigation the amount of ammonia reformed, as measured by the decrease from unity of the overall quantum yield for ammonia decomposition, did not depend on the linear flow rate of the ammonia. On the other hand, the per cent hydrazine in the nitrogen-hydrazine product varied from 95 per cent at high linear flow rates to zero at low linear flow rates. That is, the hydrazine-to-nitrogen ratio varied greatly when the linear flow rate was changed but the sum of these two products remained constant at a particular ammonia pressure. The constancy of the rate of reformation of ammonia (which follows from a constant rate of formation of the other nitrogen-bearing products and the assumed primary quantum yield of unity) in the experiments in which the hydrazine-to-nitrogen ratio varied so widely indicated that:

1. The ammonia which was reformed in the secondary processes of the ammonia decomposition did not arise from the decomposition of part of the hydrazine which was produced in the reaction.

2. The nitrogen which was observed to be a product of the ammonia decomposition resulted solely from the decomposition of hydrazine, and the decomposition of one mole of hydrazine produced one mole of nitrogen.

These statements are discussed at greater length later in this chapter.

Since ammonia was not reformed by the decomposition of part of the hydrazine produced in the reaction, it was concluded that all of the ammonia reformation was a result of the following reactions:

$$NH_2 + H \longrightarrow NH_3^* \tag{22}$$

$$NH_3^* \longrightarrow NH_2 + H \tag{21}$$

$$NH_3^* + NH_3 \longrightarrow 2NH_3 \tag{20}$$

The symbol, NH_3^*, again represents an ammonia molecule which contains the energy required for dissociation. Earlier in this chapter it was stated that an excited ammonia molecule formed by either reaction (18) or reaction (19) had no detectable existence. If the energy required to break the first nitrogen-to-hydrogen bond of ammonia is 104 kcal. per mole as was reported recently,[35] the excited ammonia molecules from reactions (18) and (19) contain, respectively, 50 kcal. per mole and 8 kcal. per mole more energy than they require to be able to dissociate into amino radicals and hydrogen atoms again. Excited ammonia molecules formed by reaction (22) contain only the energy required for dissociation and it is therefore conceivable that they would have a much longer lifetime than excited ammonia molecules formed by reactions (18) or (19). At high pressures almost all of the excited ammonia molecules produced by reaction (22) were able to lose their excess energy by thermal degradation which proceeded in several stages, one of which is

represented by reaction (20). Therefore, at high pressures the ammonia reformation mechanism was very efficient and the quantum yield was low. The quantum yield did not decrease to zero, however, since some of the amino radicals recombined to form hydrazine. As the reaction pressure decreased, reaction (21) became operative since some of the excited ammonia molecules dissociated before they had an opportunity to lose their excess energy by thermal degradation. Thus ammonia reformation became less efficient as the reaction pressure was decreased. At very low reaction pressures, reaction (20) became negligible compared to reaction (21); and since there was very little ammonia reformed, the quantum yield approached unity.

The quantum yield dependence on pressure required by the above mechanism for ammonia reformation was obeyed by the quantum yields calculated from the experiments on the mercury-photosensitized decomposition of flowing ammonia. A similar pressure dependence for the quantum yields of the static mercury-photosensitized experiments was probably masked by hydrogen quenching effects which are discussed later in this chapter. The quantum yield for the photolysis of flowing ammonia decreased from unity as the ammonia pressure was increased and seemed to become pressure independent at a reaction pressure of about 100 mm. However, only three experiments were done in which the ammonia pressure was greater than 150 mm. More extensive experimentation at high ammonia pressures might show a slight decrease in the quantum yield with increasing ammonia pressure as was the case in the mercury-photosensitized experiments. The pressure dependence of the quantum yield for ammonia decomposition in the static photolysis of ammonia was similar to the dependence observed for the photolysis of flowing ammonia except that it was reduced by a constant factor at all reaction pressures. The

reduction of the static quantum yield was attributed to the reaction

$$NH_2 + H_2 \longrightarrow NH_3 + H \qquad\qquad (7)$$

The hydrazine which was obtained as a product of the photodecomposition of flowing ammonia was undoubtedly formed by the recombination of amino radicals. When two amino radicals combined, the hydrazine molecule formed contained sufficient energy to cause it to dissociate again but apparently the excited hydrazine molecule was able to distribute its excess energy in its vibrational and rotational degrees of freedom so that it had a relatively long lifetime. The lifetime was long enough to permit almost all of the energy-rich hydrazine molecules to lose their excess energy by thermal degradation even at very low reaction pressures since hydrazine was the only major nitrogen-bearing product of several of the flow photodecomposition experiments at 1 or 2 mm. pressure of ammonia. It is stated above that the nitrogen produced in the photodecomposition of ammonia arose from the decomposition of hydrazine formed in the reaction. The decomposition of hydrazine in the ammonia reaction may have been initiated either photochemically or by the attack of hydrogen atoms and amino radicals on hydrazine. The hydrazine-to-nitrogen ratio increased in the ammonia decomposition experiments when the linear flow rate of the ammonia through the irradiated zone was increased. When the linear flow rate was increased, the concentration of the radicals and of hydrazine in the ammonia stream was decreased but the average time that a hydrazine molecule spent in the irradiated zone was also decreased. Thus, either of the suggested mechanisms for the initiation of hydrazine decomposition would have explained the experimental observations. The possibility of photodecomposition of the hydrazine in the irradiated zone was carefully examined by procedures

which are described in the following discussion.

Hydrazine photolysis by 1849 $\overset{o}{A}$ radiation in the flow photolysis of ammonia was examined first. The rate of ammonia decomposition at 100 mm. pressure in the static photolytic experiments (1.5×10^{-7} moles per second) was assumed to represent a quantum yield of 0.25. The 1849 $\overset{o}{A}$ radiation intensity incident on the flowing gas was therefore 6.0×10^{-7} einsteins per second. The maximum partial pressures of hydrazine which were possible in the ammonia stream at various linear flow rates were then calculated. The primary reaction was assumed to be

$$NH_3 + h\nu_{1849} \longrightarrow NH_2 + H \qquad (1)$$

with a quantum yield of one and it was also assumed that all the amino radicals recombined to form hydrazine. The maximum rate of production of hydrazine was, therefore, 3.0×10^{-7} moles per second. From the volume flow rate of the ammonia, the volume in which the above quantity of hydrazine was uniformly distributed was calculated, and hence the partial pressure of hydrazine in the flow stream was obtained. The hydrazine partial pressure varied from 4.8×10^{-2} mm. at a linear flow rate of 7 cm. per second to 2.5×10^{-5} mm. at a flow rate of 10,000 cm. per second.

If the ammonia and hydrazine in the irradiated zone were competing for the 1849 $\overset{o}{A}$ radiation, the absorption equation, Eq. I, is given by

$$I_t = I_o 10^{-\varepsilon_1 c_1 d_1 - \varepsilon_2 c_2 d_2} \qquad IX$$

where the subscripts 1 and 2 refer to ammonia and to hydrazine, respectively. The fraction of the 1849 $\overset{o}{A}$ radiation which was available to the hydrazine was approximately the ratio of $\varepsilon_2 c_2$ to $\varepsilon_1 c_1$. For the experiment with the highest partial pressure of hydrazine in the flow stream, this fraction was 5×10^{-4}.

Thus, 3×10^{-11} einsteins per second of 1849 $\overset{o}{A}$ radiation were available to the hydrazine and, if the quantum yield for hydrazine decomposition is unity, less than 0.01 per cent of the hydrazine was photochemically decomposed.

The mercury-rare gas discharge lamp used as the source of ultra-violet radiation for the photolysis of ammonia emitted about ten times as much radiation at 2537 $\overset{o}{A}$ as at 1849 $\overset{o}{A}$. Moreover, ammonia does not absorb 2537 $\overset{o}{A}$ radiation. The possibility of the photolysis of the hydrazine, produced in the flow photolysis of ammonia, by 2537 $\overset{o}{A}$ radiation was therefore examined. By assuming that the incident intensity of 2537 $\overset{o}{A}$ radiation was 6×10^{-6} einsteins per second and by using the extinction coefficient determined in the experiments on the static photolysis of hydrazine (15 liters moles^{-1} cm.$^{-1}$) and the calculated partial pressure of hydrazine in the experiment with the lowest linear flow rate, it was calculated that less than one per cent of the hydrazine could have been decomposed by 2537 $\overset{o}{A}$ radiation.

The possibility of mercury-photosensitized decomposition of hydrazine in the experiments on the mercury-photosensitized decomposition of flowing ammonia was also examined. The total amount of hydrazine produced in an experiment was considered to be the sum of the amounts of hydrazine and nitrogen obtained from the experiment since nitrogen was considered to arise only from the decomposition of hydrazine. From this calculated value for the total number of moles of hydrazine produced in an experiment and from the total volume of ammonia passing through the reaction system, the concentration of hydrazine in the ammonia stream was calculated for each experiment reported in Tables 7 and 8 by assuming that the hydrazine was uniformly distributed through the ammonia. If, moreover, the assumption was made that the

quenching cross-section of hydrazine for mercury $6(^3P_1)$ atoms was about the same as the ammonia cross-section for the excited mercury atoms, the ratio of the quenching by the hydrazine to the quenching by ammonia was approximately the ratio of the partial pressures of these substances. An experiment from Table 7 was then examined in which the linear flow rate was 5.8 cm. per second and the ammonia pressure was 50 mm. In this experiment the ammonia pressure was low and the hydrazine partial pressure had a higher value (3.0×10^{-2} mm.) than in any of the other experiments. From the ratio of the hydrazine pressure to the ammonia pressure it was deduced that the hydrazine quenched 0.06 per cent of the mercury $6(^3P_1)$ atoms. Thus, the intensity of 2537 Å radiation which was transferred to hydrazine was given by the incident intensity (1.15×10^{-4} einsteins per minute) times 6×10^{-4}, a value of 6.9×10^{-8} einsteins per minute. The rate of production of hydrazine in this experiment was calculated to be 9.3×10^{-6} moles per minute. If the quantum yield for the mercury-photosensitized decomposition of hydrazine is unity, the maximum amount of hydrazine which could have been photochemically decomposed in the experiment was 6.9×10^{-8} moles per minute or less than one per cent of the hydrazine which was produced. Actually, in this experiment only nitrogen was obtained so that all of the hydrazine which was formed must have been subsequently decomposed. Similar calculations were made for many of the other experiments which are reported in Table 7 and in all cases the mercury-photosensitized decomposition of hydrazine accounted for less than one per cent of the hydrazine which was produced.

Since the above calculations precluded the hypothesis that hydrazine formed in the photodecomposition of flowing ammonia was destroyed photochemically, the hydrazine decomposition must have been due to the

reactions of hydrogen atoms and amino radicals with hydrazine. Moreover, since almost all of the hydrazine produced in the flow experiments at low linear flow rates was subsequently destroyed by reaction with radicals, in the static photodecomposition of ammonia the steady state concentration of hydrazine must have been as low as the calculated values in the flow experiments. Therefore, photochemical decomposition of hydrazine could not have been important in the static photodecomposition of ammonia.

According to the mechanism proposed for the primary dissociation of ammonia, a hydrogen atom was produced for each amino radical that was produced. It was assumed that homogeneous hydrogen atom recombination required a three-body collision and that the number of such collisions was negligible at the pressures used in this investigation. Therefore, the hydrogen atoms were considered to have only the following modes of reaction:

1. The hydrogen atoms recombined with amino radicals to reform ammonia.

2. The hydrogen atoms reacted with hydrazine to form new chemical species.

3. Some of the hydrogen atoms diffused to the walls of the reaction vessel and recombined to form hydrogen.

The reaction of hydrogen atoms with hydrazine in the flow investigations was only important in the experiments in which the low values of the hydrazine to nitrogen ratio indicated that much of the hydrazine which was formed was subsequently destroyed.

The amino radicals produced in the initial dissociation of ammonia had modes of reaction similar to those described for the hydrogen atoms and, moreover, could recombine in the gas phase to form hydrazine. Thus, the amino radical steady state concentration in the photodecompo-

sition of ammonia was much smaller than the steady state concentration of hydrogen atoms. The rate of reaction of hydrazine with amino radicals was therefore negligible compared to the rate of reaction of hydrazine with hydrogen atoms.

Hydrogen atoms could react with hydrazine by either of the following reactions:

$$H + N_2H_4 \longrightarrow H_2 + N_2H_3 \tag{11}$$

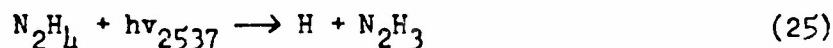$$H + N_2H_4 \longrightarrow NH_3 + NH_2 \tag{16}$$

Arguments have already been introduced in this discussion to show that ammonia was not formed from the decomposition of hydrazine in the photochemical decomposition of flowing ammonia. It was concluded, therefore, that all hydrazine decomposition in the ammonia decomposition experiments proceeded by reaction (11). Since the concentration of hydrogen atoms was much greater than the concentrations of the amino or hydrazyl radicals, the hydrazyl radicals probably disappeared by the reactions

$$H + N_2H_3 \longrightarrow H_2 + N_2H_2 \tag{23}$$

$$N_2H_2 \longrightarrow N_2 + H_2 \tag{24}$$

The above mechanism for the decomposition of hydrazine predicted that one mole of nitrogen would be produced for each mole of hydrazine that was destroyed.
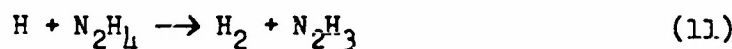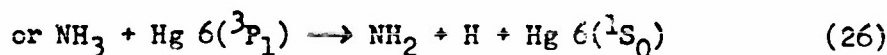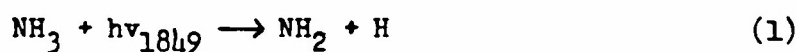
In the photolysis of hydrazine, ammonia was found to be a major product of the decomposition. This observation appeared, at first glance, to contradict the mechanism suggested above for the decomposition of hydrazine in the ammonia decomposition. It seemed likely, however, that in the hydrazine photolysis the reaction proceeded by the

following mechanism:

$$N_2H_4 + h\nu_{2537} \longrightarrow H + N_2H_3 \tag{25}$$

$$H + N_2H_4 \longrightarrow H_2 + N_2H_3 \tag{11}$$

$$2N_2H_3 \longrightarrow 2NH_3 + N_2 \tag{12}$$

Thus ammonia was produced in the photolysis of hydrazine because the hydrogen atom concentration was reduced by reaction (11) so that reaction (23) was negligible compared to reaction (12).

In view of all the foregoing discussion, it was decided that most of the observations made during the investigation of the photodecomposition of ammonia could be interpreted in terms of the following primitive reactions:

$$NH_3 + h\nu_{1849} \longrightarrow NH_2 + H \tag{1}$$

$$\text{or } NH_3 + Hg\ 6(^3P_1) \longrightarrow NH_2 + H + Hg\ 6(^1S_0) \tag{26}$$

$$NH_2 + H \longrightarrow NH_3^* \tag{22}$$

$$NH_3^* \longrightarrow NH_2 + H \tag{21}$$

$$NH_3^* + NH_3 \longrightarrow 2NH_3 \tag{20}$$

$$NH_2 + NH_2 \longrightarrow N_2H_4 \tag{27}$$

$$H + N_2H_4 \longrightarrow H_2 + N_2H_3 \tag{11}$$

$$H + N_2H_3 \longrightarrow H_2 + N_2H_2 \tag{23}$$

$$N_2H_2 \longrightarrow N_2 + H_2 \tag{24}$$

$$H + wall \longrightarrow 1/2 H_2 \tag{28}$$

This mechanism was derived by using some of the experimental observations of the investigation to eliminate other possible mechanisms. The remainder of this chapter is devoted to the discussion of the ability of the above mechanism to interpret the other observations that were made during the investigation.

The effect of varying the linear flow rate at a constant reaction pressure was examined in terms of the reaction mechanism. At a particular linear flow rate a certain volume of gas passed through the irradiated zone each second and the incident radiation produced a certain concentration of radicals and hence of reaction products in the ammonia stream. If the linear flow rate was increased, a larger volume of ammonia passed through the irradiated zone each second but the radiation produced the same amount of reaction as at the lower linear flow rate. Since the same amount of radicals and reaction products were distributed through a larger volume of ammonia when the linear flow rate was increased, the concentrations of the radicals and reaction products were decreased. An increase in the linear flow rate also caused the reaction products to be removed more rapidly from the irradiated zone but this effect was important only when the product concentrations were so large that photochemical decomposition of the reaction products occurred.

The decrease in the hydrazine-to-nitrogen ratio, attributed to the decomposition of hydrazine initiated by hydrogen atoms, as the linear flow rate was decreased, was due to the increase in the concentration of hydrazine in the ammonia stream. To illustrate this point, the data reported in Table 16 were calculated. The hydrazine concentration in the ammonia stream was estimated for each linear flow rate by the procedure which was described above in the discussion of the probability of photochemical decomposition of hydrazine in the ammonia stream.

Table 16. The Dependence of Hydrazine Decomposition on the
Concentration of Hydrazine in the Ammonia Stream

Linear flow rate cm./sec.	Per cent hydrazine decomposed	Estimated hydrazine conc. moles/liter x 10^8
Calculations from the mercury-photosensitized investigation		
4090	---	0.2
1630	---	0.8
1000	---	1.5
500	5	3.2
280	12	5.6
240	21	7.2
125	28	14
51	45	22
46	48	25
39	50	29
28	70	53
5.8	100	160
Calculations from the photolytic investigation		
1730	15	0.48
756	20	1.1
286	29	2.9
105	43	7.9
76	45	11
21	53	40
7.0	66	118

The percentage of the hydrazine which was decomposed was estimated for each flow rate at an ammonia pressure of 100 mm. and is plotted as a function of the hydrazine concentration in the ammonia stream, in Fig. 14. The plot obtained from the photolytic experiments is quite similar to the plot from the mercury-photosensitized experiments. The fraction of the hydrazine which was decomposed also depended on variations in the hydrogen atom concentration. Moreover, the effect of the various parameters of the reaction was undoubtedly complicated by the fact that the reaction was not distributed homogeneously throughout the irradiated tube. The extent of reaction in a unit volume of reactant gas depended on the fraction of the incident radiation which was absorbed therein and therefore the extent of reaction was greatest where the incident radiation entered the reaction system. There existed also a gradient in the product concentration which increased from zero at the entrance of the irradiated zone to some maximum value at the exit of the irradiated zone.

The importance of heterogeneous reaction on the walls of the reaction apparatus was difficult to assess in this investigation. An increase in the surface-to-volume ratio in the zone immediately following the irradiated zone in the flow photolytic experiments had no effect on the reaction. Moreover, when a large surface of platinum wire was added to the irradiated zone in the mercury-photosensitized experiments, the reaction was unchanged although platinum has been shown to be very effective in assisting the recombination of hydrogen atoms. The platinum surface, however, may have been poisoned by ammonia or by mercury in the ammonia stream. Surface reactions may have been important at low reaction pressures, but such reactions were not required to explain any of the experimental observations except to account for the recombination of hydrogen atoms which were not able to react in the gas phase.
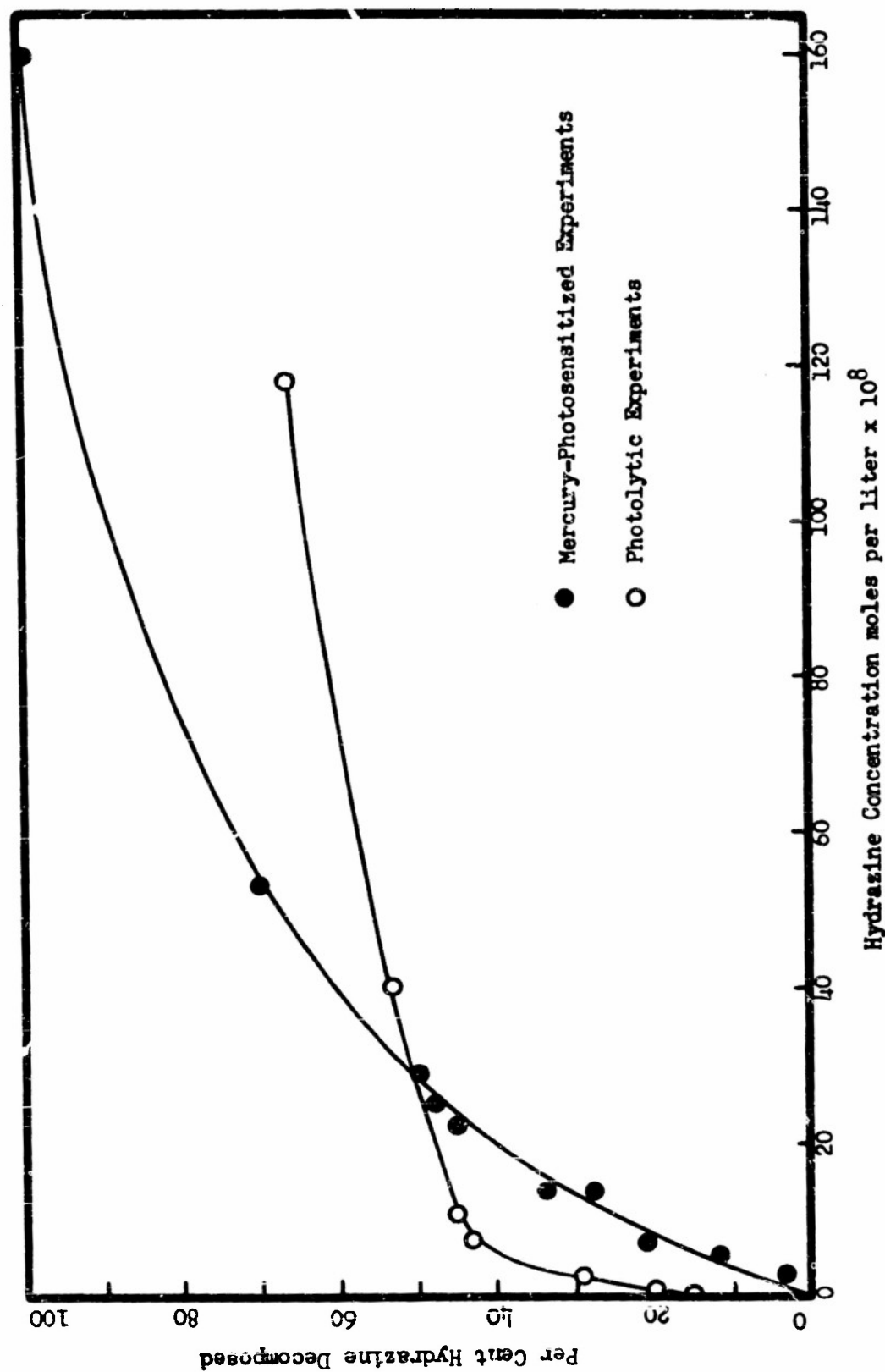
Fig. 14. The Dependence of Hydrazine Decomposition on Hydrazine Concentration

Surface reactions may have been the cause of the contradictory results which have been obtained by different investigators.

The mechanism which was proposed was most easily interpreted if the assumption was made that all of the amino radicals reacted in the gas phase by reactions (22) and (27) before they were able to diffuse to the wall. The number of radicals which were able to diffuse to the walls should have increased when the radical concentration was decreased by an increase in the linear flow rate or when the reaction pressure was decreased. If amino radicals diffused to the walls, ammonia and nitrogen would probably have been formed as well as hydrazine. Thus one would expect that at a given pressure the quantum yield would change as the linear flow rate was varied. Such an effect was not observed. Further evidence that the amino radicals all reacted in the gas phase was provided by the fact that even at very low reaction pressures the quantum yield was high and hydrazine was the major nitrogen-bearing product.

If amino radicals reacted only by reactions (22) and (27), the ratio of these two reactions must have been independent of the linear flow rate since the concentration of hydrogen atoms and amino radicals had the same dependence on linear flow rate. Therefore, the quantum yield did not depend on the linear flow rate.

Several of the experimental observations indicated that the walls of the reaction vessel were very inefficient in removing hydrogen atoms, probably because the walls were saturated with ammonia. The hydrazine-to-nitrogen ratio should have increased at low pressures if hydrogen atoms were readily removed at the walls. It was observed in the photolytic flow experiments that the hydrazine-to-nitrogen ratio did not depend on pressure and in the mercury-photosensitized flow experiments the hydrazine-to-nitrogen ratio decreased at low pressures.

The remarkable increase in the hydrazine-to-nitrogen ratio which was observed when ethylene was added to the mercury-photosensitized decomposition of flowing ammonia was undoubtedly due to the reduction of the hydrogen atom concentration by the rapid reaction of hydrogen atoms with ethylene. The hydrogen production from the experiments which contained ethylene was much lower than the amounts which were to be expected from the amounts of hydrazine and nitrogen produced. The effect of ethylene on the quantum yield of the mercury-photosensitized decomposition of ammonia was not established since ethylamine was qualitatively identified but could not be quantitatively determined.

Ethylene also caused the hydrazine-to-nitrogen ratio to increase at low ammonia pressures where the ratio was decreasing rapidly as the reaction pressure was decreased. It was concluded, therefore, that the decrease in the hydrazine-to-nitrogen ratio at low pressures and a particular linear flow rate in the mercury-photosensitized experiments resulted from an increase in the hydrogen atom concentration arising from photochemical decomposition of hydrogen in the reaction stream. This theory was substantiated by the fact that the hydrazine-to-nitrogen ratio did not decrease at low pressures in the flow photolysis of ammonia where hydrogen could not have been photochemically decomposed. Moreover, the pressure at which the hydrazine-to- nitrogen ratio started to decrease in the mercury-photosensitized experiments was increased when the linear flow rate was increased. The hydrogen concentration in the ammonia stream and hence the importance of hydrogen quenching also increased as the linear flow rate was decreased. Heterogeneous reactions also may have had an important role in the reduction of the hydrazine-to-nitrogen ratio at low ammonia pressures.

It was observed that the hydrazine-to-nitrogen ratio increased as the incident light intensity was decreased. This effect is explained by the fact that the amount of reaction per unit volume was decreased when the light intensity was decreased just as it was when the linear flow rate was increased. Therefore, the per cent hydrazine approached one hundred per cent as the light intensity was decreased toward zero.

The increase in the quantum yield of ammonia decomposition when the lamp current was increased cannot be interpreted in terms of the mechanism which has been proposed. Unfortunately, these experiments were done at an ammonia pressure of 29 mm. and at this pressure heterogeneous reactions may have been important. No change of the quantum yield with light intensity was observed at 200 mm. pressure in the static mercury-photosensitized decomposition of ammonia.

The increase in the quantum yield which was observed when the ammonia was heated may have been due to a decrease of the lifetime of the excited ammonia molecule which was formed by reaction (22).

Hydrogen was shown to inhibit the rate of the static mercury-photosensitized decomposition of ammonia either when hydrogen was added to the reaction or when the concentration of the hydrogen produced in the reaction was allowed to build up by increasing the exposure time. This inhibition can be attributed either to an increase in the number of hydrogen atoms due to the quenching of excited mercury atoms by hydrogen or to some reaction of molecular hydrogen itself. Since the rate in the static photolysis of ammonia was also lower than the rate in the flow photolysis and since hydrogen could not be photochemically decomposed in the photolytic experiments, the reaction rate inhibition was attributed to molecular hydrogen. Hydrogen was considered to react in the following manner:

$$NH_2 + H_2 \longrightarrow NH_3 + H \qquad\qquad (7)$$

However, the increase of the hydrogen atom concentration must have also decreased the overall rate of decomposition of ammonia in the static mercury-photosensitized experiments because when the ratio of hydrogen-to-ammonia quenching became important at low ammonia pressures, the quantum yield for ammonia decomposition decreased instead of increasing as it did at low pressures in the other modes of photochemical decomposition of ammonia. The hydrogen atoms produced by the quenching of hydrogen probably reduced the quantum yield by means of reaction (22).

In all this discussion, it was implicitly assumed that the substrate, ammonia, did not react with the radicals produced in the photodecomposition of ammonia. If an amino radical abstracted a hydrogen atom from an ammonia molecule, another amino radical would have been formed and the species would not have been changed. If a hydrogen atom abstracted a hydrogen atom from ammonia to form molecular hydrogen and an amino radical, the quantum yield would have increased when hydrogen was added to the static mercury-photosensitized decomposition of ammonia. Actually, the quantum yield became very small. The general pressure independence of the ammonia decomposition at ammonia pressures above 150 mm. further substantiated the assumption that ammonia was not involved in the secondary processes of the ammonia decomposition.

The mechanism for the photodecomposition of ammonia which is proposed in this chapter does not purport to be the complete mechanism for the reaction under any experimental conditions. It was advanced because it offers the most simple and the most logical interpretation of the experimental observations at high ammonia pressures and gives a reasonable explanation for many of the observations at low ammonia

pressures. The possible need for the addition of heterogeneous reaction steps to the mechanism at low ammonia pressures is emphasized throughout the discussion. If a substance could be found which would remove hydrogen atoms from the reaction zone but which would not affect the amino radicals, the reaction mechanism could be tested. In such an experiment, the quantum yield for ammonia decomposition should be unity and hydrazine should be the only nitrogen-bearing product of the reaction.

CHAPTER V

SUMMARY

The mercury-photosensitized decomposition of flowing ammonia was studied at room temperature. The products of the decomposition were hydrazine, nitrogen and hydrogen. The quantum yield for ammonia decomposition did not depend on the linear flow rate of ammonia through the irradiated zone. The quantum yield increased in an exponential manner as the ammonia reaction pressure was decreased from a value of 0.09 at 650 mm. pressure to values of almost unity at pressures of a few millimeters. The percentage of the decomposed ammonia which was recovered as hydrazine increased from zero at low ammonia linear flow rates to 95 per cent at high flow rates. At a particular flow rate the percentage of hydrazine in the nitrogen-bearing product increased as the reaction pressure was increased to a maximum value which was pressure independent at high ammonia pressures. The hydrazine-to-nitrogen ratio increased and the quantum yield for ammonia decomposition decreased as the incident light intensity was decreased. When ethylene was added to the reaction, the hydrazine-to-nitrogen ratio was greatly increased and the amount of hydrogen produced was decreased. Evidence was obtained to show that ethylamine was also produced when the reaction contained ethylene. The reaction was not changed when platinum wire was introduced into the irradiated zone.

The products of the static mercury-photosensitized decomposition of ammonia were hydrogen and nitrogen. The quantum yield of ammonia decomposition decreased if the exposure time for an experiment was increased. At very short exposure times and high ammonia pressures, the quantum yield had about the same value as in the flow experiments

117

at comparable pressures. When the exposure time was kept constant, the quantum yield was constant at ammonia pressures from 650 to 150 mm.; at lower pressures the quantum yield decreased. The rate of decomposition of ammonia was greatly decreased when hydrogen was added to the reaction. At an ammonia pressure of 200 mm., the rate did not depend on the intensity of the incident radiation.

The photolysis of flowing ammonia with 1849 Å radiation was also investigated at room temperature. The products of the reaction were hydrazine, hydrogen, and nitrogen. The percentage of the decomposed ammonia which was recovered as hydrazine did not depend on the ammonia pressure in the irradiated zone but it increased from 34 per cent to 85 per cent as the ammonia linear flow rate through the irradiated zone was increased from 7 to 1700 cm. per second. The rate of decomposition of ammonia did not depend on the ammonia flow rate and was almost constant at ammonia pressures from 100 to 560 mm. At lower ammonia pressures the rate increased until at 10 mm. pressure it was twice as great as the rate at 100 mm. The reaction was not changed when the surface-to-volume ratio in the zone immediately following the irradiated zone was increased by a factor of ten.

The products of the static photolysis of ammonia with 1849 Å radiation were hydrogen and nitrogen. The rate of ammonia decomposition was studied at ammonia pressures from 10 to 264 mm. The rate was about one-half as great as the rate in the flow experiments at comparable pressures.

A mechanism was proposed for the photodecomposition of ammonia and was used to interpret the experimental results of the investigation. It was concluded that the quantum yield for the primary dissociation of ammonia into amino radicals and hydrogen atoms was unity and that the

overall quantum yield for ammonia decomposition was decreased, as the ammonia pressure increased, by ammonia reformation from the recombination of hydrogen atoms and amino radicals. Evidence was cited to show that the nitrogen produced in the ammonia decomposition came from the reaction of hydrogen atoms with hydrazine which was produced in the reaction.

The extinction coefficient of ammonia for 1849 $\overset{o}{A}$ radiation was found to be 1.21×10^3 liters moles^{-1}cm.$^{-1}$ at ammonia pressures from 0.45 to 202 mm.

Hydrazine was photolytically decomposed at 14 mm. pressure in a static system by 2537 $\overset{o}{A}$ radiation. The products were two moles of ammonia, one mole of hydrogen, and one mole of nitrogen per mole of hydrazine decomposed.

APPENDIX

An automatic Toepler pump was constructed to transfer gases in the apparatus used for the photodecomposition of ammonia. The design of the pump is shown in Fig. 15 and the electrical circuit which operated the pump is illustrated in Fig. 16.

The Toepler pump was constructed of Pyrex glass and had tungsten wire leads sealed into it at positions 1, 2, and 3. The gas inlet and the gas outlet were sealed to a high vacuum apparatus. The flask F_1 was filled with mercury until contact 2 was just covered. Contacts 1, 2, and 3 were connected to the appropriate positions in the grid circuits of the thyratron tubes as shown in Fig. 16.

The Toepler pump was operated according to the following procedure. Suppose that the flasks F_2 and F_3 had been evacuated and that a low pressure of gas, which was to be pumped into F_3, had been admitted to F_2 through the gas inlet. The flask F_4 was evacuated through the connection to the vacuum pump and air could not enter F_4 through the needle-valve N because the air inlet was blocked by the putty-tipped iron bar R. The thyratron tubes, V_1 and V_2, conducted current except when the grid circuits were closed (i.e., when contact was made between 1 and 2 for V_1 or between 1 and 3 for V_2). Since F_4 was evacuated, the mercury covered the tungsten lead at position 2 and contact was made between 1 and 2 through the mercury in the pump. Thus V_2 conducted current but V_1 did not. Since solenoid S_2 was activated but S_1 was not, the iron bar B was pulled into S_2 and the switch X_1 was closed. After X_1 was closed, current flowed through the solenoid S_3 and through the relay A. The activation of S_3 caused the iron bar R to be raised and air flowed into F_4 at a rate which was controlled by the needle-

valve N. At the same time the activation of the relay A caused the switch X_2 to be opened so that the vacuum pump which was connected to F_4 was shut off. As the pressure increased in F_4, mercury from F_1 flowed into F_2 pushing the gas, which was trapped in F_2 as soon as the gas inlet was sealed by mercury, through the capillary tube into F_3. As soon as the mercury level in F_4 fell below contact 2, the thyratron V_1 conducted once more but the position of the iron bar B was not changed since both S_1 and S_2 were activated. When the mercury from F_1 flowed through the capillary tube into F_3, it closed the contact between the tungsten leads at 1 and 3 and the reverse cycle started. Thyratron V_2 ceased to conduct and S_2 was not activated so that B was pulled into the solenoid S_1. Now the switch X_1 was open and S_3 and A were not activated. The iron rod R dropped down and closed the air inlet to F_4 and the relay A allowed X_2 to close so that the vacuum pump started to evacuate F_4. As F_4 was evacuated, the mercury in F_2 flowed into F_1, but the mercury in the capillary tube remained there and prevented the gas in F_3 from flowing into F_2. When no mercury remained in F_2, gas flowed into F_2 from the gas inlet. When the mercury contact between 1 and 3 was broken both solenoids S_1 and S_2 were activated but the position of B did not change until the mercury covered contact 2. The cycle was then repeated except that the gas in F_2 was pushed through the mercury in the capillary tube into F_3. The pump continued to transfer gas from the gas inlet to the gas outlet as described unless the pressure in F_3 became so high that the mercury from F_1 could not push the gas in F_2 into F_3.

Fig. 15. Automatic Toepler Pump

T = 115 Volt Primary, 5 Volt Secondary
V = Thyratron 5559
R_1 = 100,000 Ohms
R_2 = 500,000 Ohms
R_3 = 100 Ohms
R_4 = 60 Ohms
C_1 = 1 Microfarad
P = Vacuum Pump Motor

S = Solenoid
X = Switch
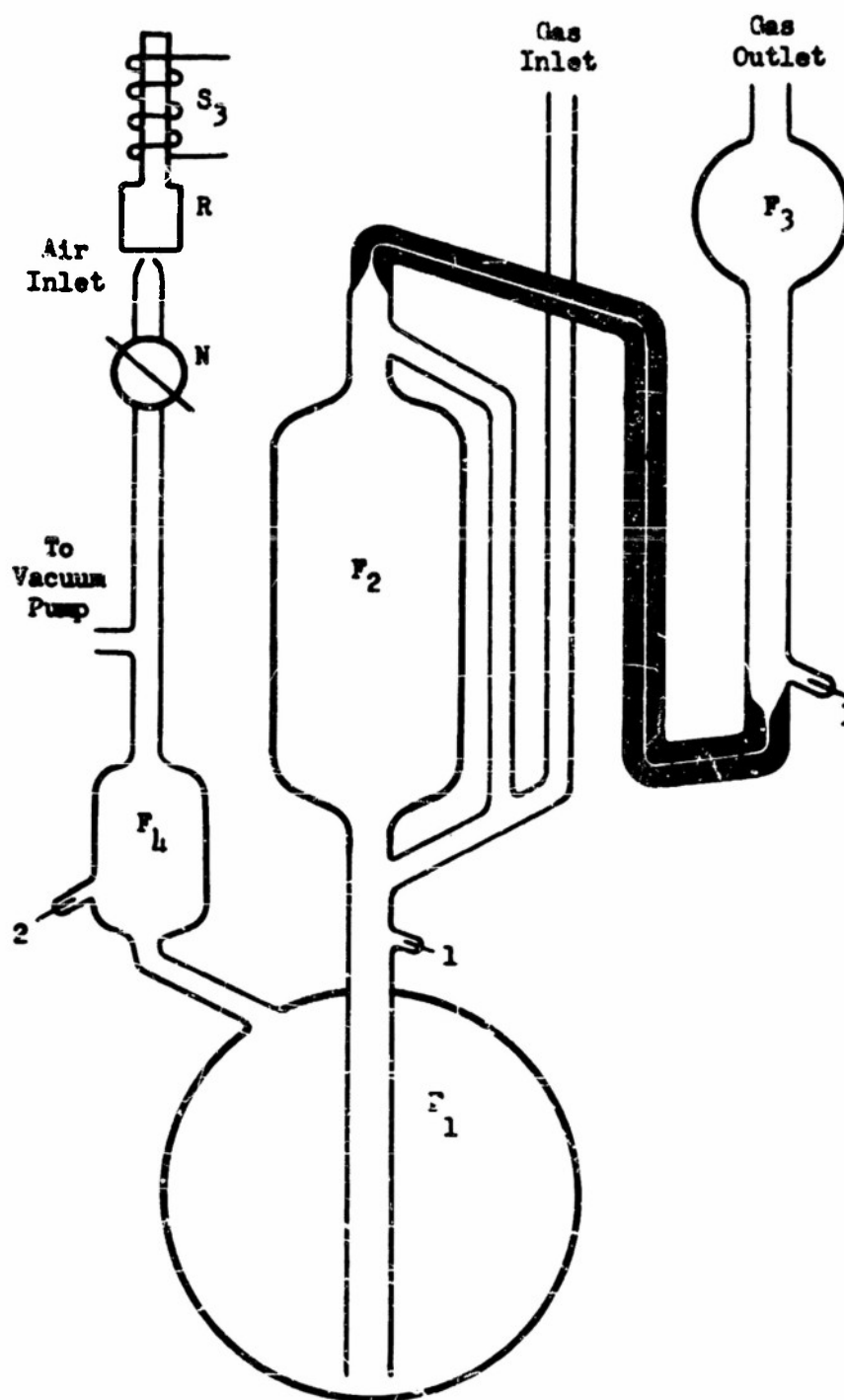A = Relay
B = Iron Bar

Fig. 16. Electrical Circuit for the Automatic Toepler Pump

BIBLIOGRAPHY

1. Audrieth, L. and Ogg, B.: "The Chemistry of Hydrazine," John Wiley and Sons, Inc., New York, 1951, p. 4.

2. Bonhoeffer, K. and Farkas, L.: Z. physik. Chem. 134, 337 (1928).

3. Bywater, S. and Steacie, E.: J. Chem. Phys. 19, 319 (1951).

4. Cario, G. and Franck, J.: Z. Physik. 11, 161 (1922).

5. Colthup, N.: J. Opt. Soc. Am. 40, 397 (1950).

6. Dickinson, R. and Mitchell, A.: Proc. Nat. Acad. Sci. 12, 692 (1926).

7. Dickinson, R. and Mitchell, A.: J. Am. Chem. Soc. 49, 1478 (1927).

8. Dixon, J.: J. Am. Chem. Soc. 54, 4262 (1932).

9. Dixon, J.: Phys. Rev. 43, 711 (1933).

10. Duncan, A.: Phys. Rev. 47, 822, 886 (1935).

11. Emeléus, H.: Trans. Faraday Soc. 28, 89 (1932).

12. Gedye, G. and Rideal, E.: J. Chem. Soc. 129, 1160 (1932).

13. Geib, K. and Harteck, P.: Z. physik. Chem., Bodenstein-Festband, 849 (1931).

14. Herzberg, G. and Ramsay, D.: J. Chem. Phys. 20, 347 (1952).

15. Kahn, A.: Private Communication.

16. Koenig, A. and Brings, T.: Z. physik. Chem., Bodenstein-Festband, 541 (1931).

17. Kuhn, W.: Compt. rend. 178, 708 (1924).

18. Kuhn, W.: J. Chim. Phys. 23, 521 (1926).

19. Melville, H.: Trans. Faraday Soc. 28, 885 (1932).

20. Malville, H. and Birse, E.: Nature 142, 1080 (1938).

21. Mitchell, A. and Zemansky, M.: "Resonance Radiation and Excited Atoms," Cambridge University Press, London, 1934, p. 192 ff.

22. Mitchell, A. and Zemansky, M.: "Resonance Radiation and Excited Atoms," Cambridge University Press, London, 1934, p. 147.

23. Mitchell, A. and Zemansky, M.: "Resonance Radiation and Excited Atoms," Cambridge University Press, London, 1934, p. 155.

24. Mund, W., Brenard, G. and Kaertkemeyer, L.: Bull. Soc. Chim. Belg. 46, 211 (1937).

25. Mund, W. and Van Tiggelen, A.: Bull. Soc. Chim. Belg. 46, 104 (1937).

26. Noyes, W. and Leighton, P.: "The Photochemistry of Gases," Reinhold Publishing Corp., New York, 1941, p. 370.

27. Ogg, R., Leighton, P. and Bergstrom, F.: J. Am. Chem. Soc. 56, 318 (1934).

28. Parts, A.: Annales de e'lluvente d'Ankara. 3:4, (1949-50).

29. Penneman, R. and Audrieth, L.: Anal. Chem. 20, 1058 (1948).

30. Pringsheim, P.: "Fluorescence and Phosphorescence," Interscience Publishers, Inc., New York, 1949, p. 111.

31. Regener, E.: Sitzt. Preuss. Akad., Berlin, 1228 (1904).

32. Shida, S.: Rev. Phys. Chem. Japan 13, 12 (1939).

33. Steacie, E.: J. Chem. Phys. 18, 210 (1950).

34. Steacie, E.: "Atomic and Free Radical Reactions," Reinhold Publishing Corp., New York, 1946, p. 156.

35. Swarc, M.: J. Chem. Phys. 17, 505 (1949).

36. Taylor, H.: J. Phys. Chem. 42, 783 (1938).

37. Taylor, H. and Bates, J.: Proc. Nat. Acad. Sci. 12, 714 (1926).

38. Taylor, H. and Emeléus, H.: J. Am. Chem. Soc. 52, 2150 (1930).

39. Taylor, H. and Bates, J.: Nature 125, 599 (1930).

40. Taylor, H. and Jungers, J.: J. Chem. Phys. 2, 452 (1934).

41. Vanpée, M.: Bull. Soc. Chim. Belg. 53, 179 (1944).

42. Warburg, E.: Sitzt Preuss. Akad. Berlin, 452 (1914).

43. Welge, H. and Beckman, A.: J. Am. Chem. Soc. 58, 2642 (1936).

44. Wenner, R. and Beckman, A.: J. Am. Chem. Soc. 54, 2787 (1932).

45. Wiig, E. and Kistiakowsky, G.: J. Am. Chem. Soc. 54, 1806 (1932).

46. Wiig, E.: J. Am. Chem. Soc. 57, 1559 (1935).

47. Wiig, E.: J. Am. Chem. Soc. 59, 827 (1937).

DISTRIBUTION LIST FOR TECHNICAL AND FINAL REPORTS

Contract N7onr-32912, Project NR 096 162

Studies on Hydrazine
(Revised 7/30/53)

Illinois Institute of Technology

No. of Copies	Addressee	No. of Copies	Addressee
1	Committee on Guided Missiles Office of Secretary of Defense (R and D) Room 3D-125, The Pentagon Washington 25, D. C.	1	Director Office of Naval Research Branch Office 1000 Geary Street San Francisco 9, California
2	Chief of Staff U. S. Air Force The Pentagon Washington 25, D. C. Attn: DCS/D, AFDRD-AC-2 (1) DCS/D, AFOP-00 (1)	2	Officer-in-Charge Office of Naval Research Navy No. 100 Fleet Post Office New York, New York
2	Chief, Bureau of Aeronautics Department of the Navy Washington 25, D. C. Attn: TD-4 (1) SI-532 (1)	2	Commanding Officer Naval Air Rocket Test Station Lake Denmark Dover, New Jersey Attn: Dr. T. Rhinehardt
2	Chief, Bureau of Ordnance Department of the Navy Washington 25, D. C. Attn: Re2d (1) Re9 (1)	1	Central Intelligence Agency 2430 E. Street, NW Washington 25, D. C. Attn: Liaison Division, OCD
2	Chief, Bureau of Ships Department of the Navy Washington 25, D. C. Attn: Code 533 (1) Code 541 (1)	4	Commander U. S. Naval Ordnance Test Station Inyokern P.O. China Lake, California Attn: Reports Unit
3	Chief of Naval Research Department of the Navy Washington 25, D. C. Attn: Code 429	2	Commander U. S. Naval Air Missile Test Center Point Mugu, California
2	Director Office of Naval Research Branch Office Tenth Floor The John Crerar Library Building 86 East Randolph Street Chicago 1, Illinois	2	Director National Advisory Committee for Aeronautics 1724 F Street, NW Washington 25, D. C. Attn: Mr. C. H. Helms
1	Director Office of Naval Research Branch Office 346 Broadway New York 13, New York	7	Director Naval Research Laboratory Washington 25, D. C. Attn: Code 2000 (6) Code 3280 (1)
1	Director Office of Naval Research Branch Office 1030 E. Green Street Pasadena 1, California	1	Superintendent U. S. Naval Postgraduate School Monterey, California
		2	Department of the Army Office, Chief of Ordnance Washington 25, D. C. Attn: ORDTU

No. of Copies	Addressee
2	Commander Naval Ordnance Laboratory White Oak Silver Spring 19, Maryland Attn: The Library, Room 1-333
1.	Chief of Naval Operations Department of the Navy Washington 25, D. C. Attn: OP-51
1	Chief, Research and Engineering Division Office, Chief of Chemical Corps Army Chemical Center, Maryland
1.	Classified Technical Library Atomic Energy Commission 1901 Constitution Avenue Washington 25, D. C.
1	Committee on Fuels and Lubricants Office of Secretary of Defense (R and D) The Pentagon Washington 25, D. C.
1	Flight Research Laboratory Wright Air Development Center Wright Patterson Air Force Base Dayton, Ohio
2	Commanding Officer Office of Ordnance Research Box CM, Duke Station Durham, North Carolina
1	Department of the Interior Bureau of Mines Central Experiment Station 4800 Forbes Street Pittsburgh 13, Pennsylvania
2	Commanding Officer Redstone Arsenal Huntsville, Alabama Attn: ORC, Technical Library
1.	Director National Bureau of Standards 18 Dynamometer Avenue Washington 25, D. C. Attn: Dr. E. F. Fiock
1	Wright Air Development Center Wright Patterson Air Force Base Dayton, Ohio Attn: WCLPF-4

No. of Copies	Addressee
1	Commanding General Air Research and Development Command P.O. Box 1395 Baltimore, Maryland Attn: RDRRC
1	Commanding General Arnold Engineering Development Center Tallahoma, Tennessee Attn: Deputy Chief of Staff, R and D
2	The Atomic Energy Commission 1901 Constitution Avenue Washington 25, D. C. Attn: Mr. J. A. Hayner Engineering Division (1) Dr. C. R. Russell Reactor Division (1)
1	The Brookhaven National Laboratory Upton Long Island, New York Attn: Mr. B. Manowitz
1	Commanding Officer Picatinny Arsenal Dover, New Jersey Attn: Technical Division
1	Applied Physics Laboratory Johns Hopkins University Silver Spring, Maryland Attn: Mr. Arthur Norris
1	Bell Aircraft Corporation Niagara Falls, New York Attn: Mr. R. B. Foster
1	Rand Corporation 1500 4th Street Santa Monica, California Attn: Mr. R. H. Best
1	General Electric Company Project HERMES Schenectady, New York Attn: Mr. C. K. Bauer
1	California Institute of Technology Jet Propulsion Laboratory Pasadena, California
1	North American Aviation, Inc. 12214 Lakewood Blvd. Downey, California Attn: Group 95-17

No. of Copies	Addressee
2	Princeton University Princeton, New Jersey Attn: Project SQUID
1	Massachusetts Institute of Technology Project METEOR Cambridge 39, Massachusetts Attn: Guided Missiles Library
1	Aerojet-General Corporation Azusa, California Attn: Dr. D. Armstrong
1	Battelle Memorial Institute 505 King Avenue Columbus 1, Ohio Attn: Dr. B. D. Thomas
1	Experiment, Incorporated Richmond, Virginia Attn: Dr. J. W. Mullen II
1	Reaction Motors, Inc. Stickle Avenue and Elm Street Rockaway, New Jersey
1	Metalectro Corporation 2900 Kenilworth Avenue Bladensburg, Maryland Attn: Dr. Hans Osborg
1.	Ohio State University Research Foundation Columbus 10, Ohio Attn: Dr. E. L. Johnston
1	Pennsylvania State College State College, Pennsylvania Attn: Dr. W. C. Fernelius Dr. J. G. Aston Dept. of Chemistry
1	University of Illinois Urbana, Illinois Attn: Dr. L. F. Audrieth, Dept. of Chemistry
1	University of Michigan Aeronautical Research Center Willow Run Airport Ypsilanti, Michigan Attn: Mr. L. R. Biasell
1	Mathieson Chemical Company Niagara Falls, New York Attn: Dr. C. C. Clark Research Division

No. of Copies	Addressee
1	Redel Incorporated 7405 Varna Street North Hollywood, California Attn: Mr. T. L. Thompson
1	Detroit Controls Company Research Division Redwood City, California
5	Armed Services Technical Information Agency Document Service Center Knott Building Dayton 2, Ohio
1	Office of Technical Service Department of Commerce Washington 25, D. C.

No. of Copies	Addressee
2	Princeton University Princeton, New Jersey Attn: Project SQUID
1	Massachusetts Institute of Technology Project METEOR Cambridge 39, Massachusetts Attn: Guided Missiles Library
1	Aerojet-General Corporation Azusa, California Attn: Dr. D. Armstrong
1	Battelle Memorial Institute 505 King Avenue Columbus 1, Ohio Attn: Dr. B. D. Thomas
1	Experiment, Incorporated Richmond, Virginia Attn: Dr. J. W. Mullen II
1	Reaction Motors, Inc. Stickle Avenue and Elm Street Rockaway, New Jersey
1	Metalectro Corporation 2900 Kenilworth Avenue Bladensburg, Maryland Attn: Dr. Hans Osborg
1.	Ohio State University Research Foundation Columbus 10, Ohio Attn: Dr. H. L. Johnston
1	Pennsylvania State College State College, Pennsylvania Attn: Dr. W. C. Fernelius Dr. J. G. Aston Dept. of Chemistry
1	University of Illinois Urbana, Illinois Attn: Dr. L. F. Audrieth, Dept. of Chemistry
1	University of Michigan Aeronautical Research Center Willow Run Airport Ypsilanti, Michigan Attn: Mr. L. R. Biasell
1	Mathieson Chemical Company Niagara Falls, New York Attn: Dr. C. C. Clark Research Division

No. of Copies	Addressee
1	Redel Incorporated 7405 Varna Street North Hollywood, California Attn: Mr. T. L. Thompson
1	Detroit Controls Company Research Division Redwood City, California
5	Armed Services Technical Information Agency Document Service Center Knott Building Dayton 2, Ohio
1	Office of Technical Service Department of Commerce Washington 25, D. C.